Periodic driving of a coherent quantum many body system and relaxation to the Floquet diagonal ensemble

Student: Angelo Russomanno
Supervisor: Giuseppe E. Santoro
Academic year: 2013-2014

Contents

Chapter 1

Introduction and overview

1.1 Experimental motivation and main questions

The main experimental motivation for the present Thesis is the large amount of recent experimental works on cold atoms [1]. In these systems it is possible to trap many atoms and keep them well isolated from the environment for a long time. Experimentalists can tailor the dimensionality of the system and control the external fields acting on it [2], and the interactions among its constituents [3] in the desired way. The dynamics is unitary and coherent, and collective phenomena like superfluid-Mott insulator quantum phase transition [4] or BCS-BEC crossover [5] can be observed. Moreover, it is possible to control the external perturbations driving the system: the quantum coherent dynamics of many-body systems becomes a subject of experimental observation [6, 7, 8], and is no longer a purely academic issue.

   A question which has attracted the interest of many experimentalists and theoreticians is what happens to an isolated quantum system when it is prepared in a non-equilibrium state with respect to the Hamiltonian governing the evolution (see Ref. [9] for a review). This is the so-called sudden quantum quench: the system is prepared in the ground state of an Hamiltonian $\hat{H}_0$ and the Hamiltonian is suddenly changed, at $t = 0$, to $\hat{H}$. One of the crucial points of investigation is whether the observables of the system eventually reach a stationary condition, and what are the properties of the stationary regime. In the experiments performed so far, various results have been obtained: in particular, quantum beats persist for long times in a one-dimensional quasi-integrable Tonks-Girardeau gas [6], while there is equilibration to a thermal regime when two one-dimensional Bose condensates are put in contact [10].

   In recent years, important experimental [11, 12, 13, 14, 15, 16] and theoretical [17, 18, 19, 20, 21, 22, 23, 24] works concerning the periodic driving of these systems have appeared. Small amplitude time-periodic fields have been, traditionally, an important instrument to probe equilibrium prop-

erties of systems, but more recently researchers have started considering the effect of larger amplitude periodic drivings on systems which remain quantum coherent for long times [25]. Our main question is if, in isolated periodically driven cold atom systems, observables reach a periodic steady condition analogue to the steady state reached after a quantum quench. To explore relaxation to a periodic regime in the case of periodic driving, it is important to know concepts and results coming from the large amount of theoretical work performed to understand equilibration after a quantum quench. Indeed, we will see that the two phenomena are strictly related and are expected to happen in similar systems. We therefore start by briefly reviewing the theoretical literature concerning quantum quenches and the ensuing equilibration of observables.

1.2 Equilibration in the quantum quench case

The most discussed points in the literature are *i)* the conditions under which the observables of a quenched isolated quantum system can equilibrate and *ii)* the properties that make the system show a thermal behaviour in the equilibrium regime [26, 27, 28, 29, 30, 31, 32, 33, 34, 35, 36, 37, 38, 39]. Independently of the thermal properties, if observables attain an equilibrium condition, their expectation value in the asymptotic regime is always described by the diagonal ensemble [26]. Expanding the state of the system in terms of the eigenstates $|\Phi_n\rangle$ of the Hamiltonian, we can write $|\psi(t)\rangle = \sum_n C_n e^{-iE_n t} |\Phi_n\rangle$, where E_n are the eigen-energies of the system and $C_n = \langle \Phi_n |\psi(0)\rangle$ the overlaps of the initial state with the eigenstates. Because of destructive interference, the expectation value $\langle \psi(t)| \hat{\mathcal{O}} |\psi(t)\rangle$ of an observable $\hat{\mathcal{O}}$ usually relaxes to the diagonal ensemble average $\langle \mathcal{O} \rangle_{\text{diag}} = \sum_n |C_n|^2 \langle \Phi_n| \hat{\mathcal{O}} |\Phi_n\rangle$. As stated in Ref. [26] *"If the system relaxes at all, it must be to this value"*. It is important to stress that the state of the system does not relax, only local observables and the reduced density matrix of localized subsystems [39] do. The asymptotic value shows different properties in different cases: it is interesting to understand when the averages of the observables predicted by the diagonal ensemble are thermal or not.

In many cases the asymptotic regime is not thermal [34, 33, 35, 29, 27, 32, 9] and is described by the so-called Generalized Gibbs Ensemble (GGE). This is the ensemble maximizing the entropy whenever there are conserved quantities in the dynamics [40]. The quantum dynamics conserves all the projectors on the eigenstates of the Hamiltonian $|\Phi_n\rangle \langle \Phi_n|$, which are exponential in the size of the system, and all the powers of the Hamiltonian $\hat{H}^k$, which are infinite; the remarkable thing is that the averages of the observables are obtained by enforcing the conservation of a much smaller number of operators. Nevertheless, not all the observables relax after a quench, so this ensemble does not give a complete description of the system [9]. This

can be clearly seen, for instance, in the case of free-fermion-like Hamiltonians in presence of disorder: the persisting fluctuations of the single-particle correlators make the GGE unable to describe the time-averages of the many-particle observables [41].

The GGE has been demonstrated to hold for "integrable" systems; here the word *integrable* means a system with well-defined quasi-particles retaining their identity upon scattering [9, 42]; the observables whose conservation is enforced by GGE are the occupation numbers of the quasi-particle states. Quantum integrability is a very debated and not completely clear question [43]: integrable are considered also those systems which are solvable by means of Bethe Ansatz; also for them GGE seems to hold [39]. Integrable models are very special but, thanks to the renormalization group (RG) theory [44], they are very important in describing the low-energy behaviour of real systems. These models are, on the contrary, not fully justified when discussing real systems which undergo a non-equilibrium driving and heat up towards high energies; nevertheless discussing them is important because integrable Hamiltonians are closely connected to what is realized in cold atom experiments [1]. One would be tempted to say that we have changed paradigm: we do not try to make theories which describe Nature, but adjust the Nature so that it is described by our theories. Actually this is not completely true: it is possible to experimentally add non-integrable terms to integrable Hamiltonians to see, in the quantum case, at which point there is a crossover from GGE to thermalization; in this way, we can understand the foundations of quantum statistical mechanics.

In the classical Hamiltonian case the situation is quite clear: a system with N degrees of freedom is integrable if it has N constants of motion in involution (i.e., with vanishing Poisson brackets) [45, 46]. Adding an integrability breaking term to the Hamiltonian, KAM theorem [47, 48, 49, 45, 46, 50] states (poorly speaking) that a part of the phase space around resonant orbits becomes chaotic; if the perturbation is strong enough, all the phase space becomes chaotic. In the latter case, the system is ergodic: any trajectory fills uniformly the phase space, and time averages coincide with phase space averages. More precisely, time averages coincide with thermal averages on the microcanonical ensemble [51], with a temperature fixed by the conservation of energy. One instance of that is the Fermi-Pasta-Ulam problem [52]: a chain of harmonic oscillators with a tunable non-linear coupling term. This term breaks integrability and needs to exceed a certain threshold in order to have ergodicity and see all the phase space chaotic [53, 54].

In the quantum case there is no general theorem to guide us. Many works [30, 31, 55, 29, 28, 56], by means of t-DMRG and exact diagonalization, discuss the quench on systems with non-integrable terms and see thermalization or not according to the strength of the integrability-breaking term. These results refer to few dozens of particles and no one knows what

happens in the thermodynamic limit; indeed, the absence of thermalization could be even an effect of finite-size quantum fluctuations [57]. Nevertheless, whenever a quantum system shows thermalization, this is due to the properties of the eigenstates of the Hamiltonian: the expectation value of any physical observable on any eigenstate equals the microcanonical thermal average and depends smoothly on the energy of the eigenstate. This is the so-called Eigenstate Thermalization Hypothesis [58, 59] which has been numerically verified in some cases [26] and we will discuss in some detail in Chapter 5 in connection with the thermalization of the driven Lipkin model.

To conclude, we mention Ref. [60] where it is shown that relaxation (independently of the thermal or non-thermal – GGE – nature of the equilibrium condition) can happen only when the Hamiltonian after the quench has a continuous energy spectrum; this point will be very important in what follows. We will see that convergence to a periodic steady state in a driven system is very similar to the relaxation after a quench; the only difference is the substitution of the eigenstates/eigen-energies of the final Hamiltonian with the Floquet states/quasi-energies.

1.3   Overview of the results

Besides the studies about quantum quenches, there is a community of people who studies what happens when a quantum phase transition (QPT) [61] is crossed by varying a parameter of the Hamiltonian linearly in time (see Refs. [62, 9] for a review). The question is how the universality properties of the static QPT reflect in those of the dynamical case, in the limit of a vanishing crossing rate. Indeed, since the spectral gap closes at the QPT, there is never perfect adiabaticity, and there is always a non-vanishing density of excitations, which happens to show a universal scaling with the rate.

Recently, the question has been posed concerning a similar issue when the system evolves coherently under a periodic sequence of these QPT-crossings, especially when the adiabatic limit is approached. With this question in mind, we started studying the dynamics of a uniform quantum Ising chain model periodically driven by changing the transverse field across the quantum critical point. [1] What struck us was that all the considered local observables approached asymptotically a steady periodic regime, analogue to the stationary limit reached in quench problems. We understood that this regime is described by a diagonal Floquet ensemble, analogue to the diagonal ensemble we have discussed in the quantum quench case. Floquet states, which we discuss in Chapt. 2, are a basis of solutions of the Schrödinger

---

[1]Before us, the question has been discussed by means of the Landau-Zener approximation [21]. Technically, we have preferred to evaluate numerically the exact evolution over a single driving period (which is possible due to integrability of the model and the Bogoliubov-de Gennes equations) and then propagate it, by applying the Floquet theory [63, 64, 65].

equation, periodic "up to a phase" $\mathrm{e}^{-i\overline{\mu}_\alpha t}\,|\Phi_\alpha(t)\rangle$, in terms of which the state can be expanded: $|\psi(t)\rangle = \sum_\alpha R_\alpha \mathrm{e}^{-i\overline{\mu}_\alpha t}\,|\Phi_\alpha(t)\rangle$; destructive interference can make the expectation values of the observables converge to the Floquet-diagonal ensemble average $\langle\mathcal{O}\rangle_{\mathrm{diag}}(t) = \sum_\alpha |R_\alpha|^2\,\langle\Phi_\alpha(t)|\,\hat{\mathcal{O}}\,|\Phi_\alpha(t)\rangle$. The situation is very similar to the sudden quench: in both cases we have an isolated system and convergence towards a steady regime follows from destructive interference among the typical frequencies of the system. In the quantum quench case they are the eigen-energies of the Hamiltonian, in the periodically driven one they are the Floquet quasi-energies; in both cases continuity of the spectrum is essential [66, 60]. Concerning the Ising model, we verify that observables converge towards a periodic steady regime also when we break translational invariance (making the quasi-particle modes time-dependent) in a way that most of the Floquet spectrum is still a continuum. Although we verify explicitly the convergence to the Floquet diagonal ensemble for the Ising model (integrable and reducible to quasi-particles), this is expected to be a very general result: the only requirement is the continuity of the bulk of the Floquet spectrum (which is possible in the thermodynamic limit, in absence of disorder). Moreover, only observables coupled with an extensive amount of Floquet states in the continuum attain this asymptotic regime. We will show that these are very general conditions which are met, for instance, in all systems showing relaxation after a sudden quench; we have seen in the previous section that there is plenty of examples in literature [9]. Also in this case only continuity of the final Hamiltonian spectrum is important [60], and this property is inherited by the Floquet spectrum if the system is driven. We argue that integrability breaking does not affect the convergence to a periodic steady regime in itself, but modifies the asymptotic value attained, exactly as it happens in the sudden quench case. Indeed, because of integrability, in the Ising model the stationary value reached by observables does not show a thermal value.We cannot introduce an effective temperature T valid for all the observables and the stationary value attained has a strong dependence on the details of the external driving. In the case we address, this dependence reflects the universal behaviour of the quantum phase transition around which we perturb: at low frequencies the number of excitations scales with the frequency as it does with the rate in the case of linear crossing protocol. These results have been published in Ref. [66] and are discussed in Chapts. 2 and 3 of the present Thesis.

The question about integrability and thermal properties of the asymptotic regime deserves special attention. If there is thermalization after a quantum quench, it happens at a temperature fixed by the conserved energy of the system. In the driven case, instead, there is no energy conservation and, in ergodic systems, the energy increases until the $T = \infty$ value. In the classical case thermalization happens as a consequence of the ergodic dynamics; in the quantum case instead the eigenstates have thermal properties so that the diagonal ensemble coincides with the thermal one.

The dynamics has only the auxiliary role of destroying coherence through dephasing and making explicit the thermal properties of the diagonal ensemble. This is the Eigenstate Thermalization Hypothesis (ETH) which has been conjectured [58, 59, 67, 68] and verified in many systems thermalizing after a quantum quench [26, 55, 31, 9, 69, 30, 56]. About periodic driving, a recent paper has shown the case of an ergodic driven quantum spin chain heating up until $T = \infty$ [70] and another one has verified that its eigenstates obey ETH [71].

In the present Thesis we consider the case of thermalization in the driven Lipkin model. This is the fully-connected version of the Ising model and in it we can see very clearly the connection among classical chaos and ETH. Indeed, in the limit $N \to \infty$ (N is the number of spins) it is described by a classical Hamiltonian with a single degree of freedom. In the quantum quench case, this Hamiltonian is time-independent and the dynamics is regular; when there is driving it can show chaos and even ergodicity. We will see how, correspondingly to an ergodic classical dynamics, quasi-energies and Floquet states obey ETH and induce thermalization to $T = \infty$. This problem is discussed in Chapt. 5 of the present Thesis.

Once we have understood the existence of a stationary periodic regime, it is interesting to study the properties of the system in this condition using the same tools employed to discuss the asymptotic regime attained after a quench. Apart from the distinction between regular and ergodic, it is interesting to understand the existence of long-range-order [72] and entanglement [73, 74], aiming at the application to quantum information problems [75, 76, 77]. There are many objects which can be considered: entanglement entropy [73, 74], correlators [78, 36, 37], statistics of the observables [79]. We will focus on the last one. Because of quantum fluctuations, measuring an observable gives a different result in each realization of a process; the possibility to have a statistics of these measurements, to compare with theoretical predictions, is nowadays an experimental reality [80]. Among the many interesting quantities, we will consider the work performed on a system. Although, strictly speaking, it is not an observable [81], its statistics can give a lot of information on the system. Indeed, quench and driving are irreversible thermodynamical transformations whose study is interesting from the point of view of theory and applications. The remarkable Jarzynski equality [82, 81, 83] links the average over this distribution of a function of the non-equilibrium work to the variation in free-energy of the corresponding quasi-static transformation. Moreover, the work statistics shows, for small values of the work, universal properties independent of the details of the system and the driving protocol [84, 85, 86, 87, 88, 89]. Power-laws in the work distribution have been observed when there is a quantum phase transition, this distribution becomes indeed a tool to detect such a phenomenon [84, 86, 87, 88, 89]. In the case of the driven uniform quantum Ising model in transverse field, we will show how this distribution

becomes periodic for long times in the thermodynamic limit. In this limit, it becomes also a δ function; nevertheless for L finite but large, there is a finite probability density out of the δ, it approximately attains the periodic regime before finite-size revivals arise. We will show that the work probability distribution becomes "universal" at small W, *i.e.* dependent only on the initial and final values attained by the driving field. Moreover, we will see a peculiar behaviour in correspondence of the quantum phase transition. We discuss these questions in Chapt. 3; a partial account of these results has been published in Ref. [90] where we consider only the stroboscopic dynamical fidelity which is the probability of performing a vanishing work.

The question of energy absorption is very interesting also if we consider its behaviour in the linear response limit. Linear Response Theory (LRT) predicts a steady energy absorption, which is impossible if the energy-per-site spectrum is bounded. In the quantum Ising chain in transverse field, we are able to compare the results of LRT with the exact evolution. When the driving couples to an extensive portion of the chain, LRT holds for a finite time, independent of L and increasing if we consider a smaller perturbation amplitude; after this time, energy absorption saturates. This reflects in the response of the observable coupled to the driving field: the term which is out-of-phase with respect to the driving, predicted by LRT and responsible for energy absorption, vanishes after a transient. Nevertheless, LRT works for long times in predicting the part of the response (the one in phase with the driving) which has no relation with energy absorption: here LRT and Floquet-diagonal ensemble predictions do agree. The situation is different when the driving is localized and couples to few sites whose number is constant when L increases. In this case LRT is obeyed for a time scaling as $\sim L$ which becomes infinite in the thermodynamic limit. There are no problems connected with energy absorption: the energy increment per site is infinitesimal with respect to the total energy. In both cases, the persisting out-of-phase term is a consequence of a degeneracy in the Floquet spectrum: terms oscillating with approximately the same phase do not cancel by destructive interference. In the case of extensive driving, the degeneracy arises when the driving amplitude goes to 0; when the driving is localized the degeneracy appears also when $L \to \infty$. These results have been published in Ref. [91].

We conclude this overview with a list of the works where part of the results of this Thesis have been published

- A. Russomanno, A. Silva, and G. E. Santoro. Periodic steady regime and interference in a periodically driven quantum system. *Phys. Rev. Lett*, 109:257201, 2012.

- A. Russomanno, A. Silva, and G. E. Santoro. Linear response as a singular limit for a periodically driven closed quantum system. *J. Stat. Mech.*, page P09012, 2013.

- S. Sharma, A. Russomanno, G. E. Santoro, and A. Dutta. Loschmidt echo and dynamical fidelity in periodically driven quantum systems. *EPL*, 106:67003, 2014.

Chapter 2

Steady state of observables in quenched and driven systems

In this Chapter we will discuss the general formalism to describe systems undergoing a periodic driving and the conditions under which the observables converge to an asymptotic periodic regime. In particular, we show that there is a very strict analogy with the case of quantum quench. In the last case, the observables can attain an asymptotic steady state represented by the diagonal ensemble introduced in the previous Chapter; this happens whenever the eigen-energies and the eigenstates of the Hamiltonian leading the evolution obey some special conditions, which we review in Sec. 2.1. In Sec. 2.3 we will see that something very similar happens for periodically driven systems, provided we substitute eigen-energies and eigenstates with their analogue for the periodically driven systems: Floquet quasi-energies and Floquet states. The stationary diagonal ensemble is replaced by the time-periodic Floquet-diagonal ensemble; observables relax to it under conditions very similar to those valid for the quantum quench. Floquet theory is a cornerstone of this Thesis; we review it in Sec. 2.2. We conclude this Chapter with Sec. 2.4, where we discuss how general is our result concerning the convergence to the Floquet-diagonal ensemble.

2.1   Results for the case of a quantum quench

In the foregoing Chapter we have provided a brief review of the large amount of experimental and theoretical results concerning the relaxation of observables after a quantum quench. In particular, we have underlined how, if the observables relax to some limit, this limit has to be represented by the diagonal ensemble. Here we discuss in more detail this relaxation and the conditions that the Hamiltonian governing the evolution has to satisfy to make it possible. We will apply our arguments to a bounded many body system with N "particles" which is the kind of system considered in exper-

iments on quenches.

In a quantum quench problem, one considers the coherent evolution under a Hamiltonian $\hat{H}$ of a state $|\psi_0\rangle$ which is a non-equilibrium state with respect to $\hat{H}$, hence it differs from every energy eigenstate [1]. Denoting by E_n the eigen-energies of $\hat{H}$ and by $|\Phi_n\rangle$ the corresponding eigenstates, the state of the system at time t can be written in the form $|\psi(t)\rangle = \sum_n C_n e^{-iE_n t} |\Phi_n\rangle$, where $C_n \equiv \langle \Phi_n | \psi_0 \rangle$ are the overlaps of the initial state with the eigenstates. Considering a generic observable $\hat{\mathcal{O}}$, we can write its expectation value $\langle \mathcal{O} \rangle_t \equiv \langle \psi(t) | \hat{\mathcal{O}} | \psi(t) \rangle$ at time t as

$$\langle \hat{\mathcal{O}} \rangle_t = \underbrace{\sum_n |C_n|^2 \mathcal{O}_{nn}}_{\mathcal{O}_{\text{diag}}} + \underbrace{\sum_{n \neq m} C_n^* C_m \mathcal{O}_{nm} e^{i(E_n - E_m)t}}_{\mathcal{O}_{\text{off-diag}}(t)}, \qquad (2.1)$$

where we have defined the matrix elements $\mathcal{O}_{nm} \equiv \langle \Phi_n | \hat{\mathcal{O}} | \Phi_m \rangle$. The term labeled $\mathcal{O}_{\text{diag}}$ is the time-independent part of the expectation, while the off-diagonal component $\mathcal{O}_{\text{off-diag}}(t)$ collects all the fluctuations around it, if there are no degeneracies. If this is the case, and we average $\langle \hat{\mathcal{O}} \rangle_t$ over an infinite time, the fluctuating off-diagonal component vanishes and only the diagonal time-independent term will persist:

$$\overline{\langle \hat{\mathcal{O}} \rangle_t} \equiv \lim_{t_f \to \infty} \frac{1}{t_f} \int_0^{t_f} dt \, \langle \hat{\mathcal{O}} \rangle_t = \mathcal{O}_{\text{diag}} . \qquad (2.2)$$

$\mathcal{O}_{\text{diag}}$ can be seen as the expectation value of $\hat{\mathcal{O}}$ over a density matrix $\hat{\rho}_{\text{diag}}$, i.e., $\mathcal{O}_{\text{diag}} = \text{Tr} \left[\hat{\mathcal{O}} \, \hat{\rho}_{\text{diag}} \right]$, defined as the "diagonal ensemble":

$$\hat{\rho}_{\text{diag}} = \sum_n |C_n|^2 |\Phi_n\rangle \langle \Phi_n| . \qquad (2.3)$$

It is immediate to see that, if the observables converge to a stationary limit, this is represented by the average on the diagonal ensemble. In Chapter 5 we will discuss what are the properties of the eigenstates so that such diagonal ensemble average equals the microcanonical average providing thermalization of the observables.

We can ask what are the properties of the Hamiltonian $\hat{H}$ such that the fluctuating part $\mathcal{O}_{\text{off-diag}}(t)$ vanishes asymptotically, and the observables actually tend to a stationary limit. Our argument is based on the properties of the eigen-energies of $\hat{H}$ and leads to the conclusion that in the relaxation process, up to very pathological cases, only the properties of $\hat{H}$ matter [60]. Indeed, one can introduce a kind of weighted joint density of states

$$f_{\mathcal{O}}(\omega) = \pi \sum_{n \neq m} C_n^* C_m \, \mathcal{O}_{nm} \, \delta(\omega - (E_m - E_n)) \qquad (2.4)$$

---

[1] All the following arguments are very easy to generalize to the case where the initial condition is not a pure state $|\psi_0\rangle$ but a density matrix $\hat{\rho}_0$. We will give an explicit instance of this in the case of periodic driving, discussed in Sec. 2.3.

in such a way that the fluctuating part can be written as the Fourier transform of $f_{\mathcal{O}}(\omega)$:

$$\mathcal{O}_{\text{off}-\text{diag}}(t) = \frac{1}{\pi} \int_{-\infty}^{\infty} d\omega f_{\mathcal{O}}(\omega) e^{-i\omega t} . \qquad (2.5)$$

We clearly see that, for the long-time behaviour of $\mathcal{O}_{\text{off}-\text{diag}}(t)$, the spectral properties of the Hamiltonian are crucial. Indeed, if $\hat{H}$ has a discrete spectrum, then $f_{\mathcal{O}}(\omega)$ is a discrete sum of Dirac's deltas, a very singular object which gives rise to persisting time fluctuations once Fourier transformed. We would observe this behaviour if $\hat{H}$ is a disordered Hamiltonian which, even in the thermodynamic limit, can show localization and a pure point spectrum. Only if the spectrum is a continuum, the Dirac's deltas can merge to give a regular function. Whenever this happens, the Fourier transform of $f_{\mathcal{O}}(\omega)$ (the fluctuating part) tends to 0 for infinite time. Mathematically, this is the essence of the Riemann-Lebesgue lemma [92] (a Lebesgue integrable $|f_{\mathcal{O}}(\omega)|$ is regular enough for its application); physically, it results from the destructive interference among infinitely many, close frequencies. Even if the spectrum of $\hat{H}$ has a discrete component, we can see relaxation to the diagonal ensemble for those observables with non-vanishing matrix elements mainly between eigenstates in the continuum. Since we deal with bounded systems, a continuous spectrum can be found if the system is "not disordered" and the thermodynamic limit is performed. It is remarkable that, for the convergence to stationariety, only the continuity properties of the spectrum matter. Indeed, convergence occurs even if the initial state $|\psi_0\rangle$ is the ground state of a different disordered Hamiltonian $\hat{H}_0$ [60]. It is true that, if we choose an observable $\hat{\mathcal{O}}$ which couples to a finite number of eigenstates, or a state $|\psi_0\rangle$ which is a superposition of just few eigenstates, we see persisting time fluctuations; but these are pathological cases. In particular, because of the time-energy uncertainty relation [93], to prepare the system in an eigenstate, we have to apply a perturbation to it for a time longer than the inverse gap with nearby levels, the so-called Heisenberg time. This time is exponentially large in the number N of particles, because in many-body systems the gap between nearby levels is proportional to [94, 58, 95] $e^{-S(E)}$ — where $S(E)$ is the entropy at energy E — and is therefore exponentially small. These considerations could not apply to the ground state [94] and its immediate neighborhood, but this is not a problem because, even if we can prepare the system in its ground state, it is impossible to make a discrete superposition of it and few other many-body eigenstates. Indeed, the issue comes from these superpositions, not from the single eigenstates. The same argument shows that it is very difficult to measure an observable coupling only to few eigenstates: we need to make the system interact with a measuring apparatus for a time which is exponentially large in N.

We stress that the previous discussion applies only in the thermodynamic limit. Practically, we can do simulations only for finite N; even if the system

we consider has a continuous spectrum for $N \to \infty$, it will show discrete eigenvalues for any finite N, and we will therefore observe finite-size revivals. Moreover, if we take $|\psi_0\rangle$ to be a disordered state, it is not immediate to see relaxation of observables by inspection [60]. An object which, evaluated for N finite, gives information on the relaxation in the thermodynamic limit are the quadratic infinite-time-fluctuations [2] of the expectation value:

$$(\delta \mathcal{O}_{\text{time}})^2 = \overline{\left(\langle \hat{\mathcal{O}} \rangle_t - \overline{\langle \hat{\mathcal{O}} \rangle_t} \right)^2} \tag{2.6}$$

Under the hypothesis of non-degenerate spectrum, they are easily evaluated as [95, 60]

$$(\delta \mathcal{O}_{\text{time}})^2 = \sum_{n \neq m} |\mathcal{O}_{nm}|^2 |C_n|^2 |C_m|^2 . \tag{2.7}$$

The physical meaning of $(\delta \mathcal{O}_{\text{time}})^2$ is rather clear: If it is small, this means that the system stays close to its average for most of the time, and relaxation to the diagonal ensemble is attained. In numerical applications, one evaluates this quantity for N finite and looks for a scaling with N, marking the vanishing of fluctuations in the thermodynamic limit. In the case of semiclassical chaotic systems [67], or, more generally, in quantum systems whose observables relax to a thermal value [96], due to the Eigenstate Thermalization Hypothesis, this object can be shown to vanish in the thermodynamic limit. We will discuss better this point in Chapt. 5. We now move to generalizing this discussion to periodically driven systems; to that purpose we need to introduce the reader to the Floquet theory which we will have many opportunities to apply in the rest of this Thesis.

2.2 Floquet theory

To discuss the dynamics under time-periodic Hamiltonians, the Floquet theory is of utmost importance. A wide literature on the topic exists (see for instance [64, 97, 66, 98, 99]). For a time periodic Hamiltonian $\hat{H}(t) = \hat{H}(t + \tau)$, with $\tau = 2\pi/\omega_0$, in analogy with Bloch theorem in the standard band theory of crystalline solids [100] [3], it is possible to construct

---

[2]Like the time average in Eq. (2.2), the finite-time fluctuations approach this value if one averages on a time longer than the Heisenberg time. As we have pointed out, this is exponentially large in N, so this quantity would seem to have no physical meaning. Nevertheless this is an useful quantity: whenever $\langle \hat{\mathcal{O}} \rangle_t$ relaxes this object is vanishingly small in the thermodynamic limit [95].

[3]One finds the Bloch states by diagonalizing simultaneously the Hamiltonian and the discrete translation operator which in crystalline space-periodic solids commute. One can do the same in time-periodic Hamiltonians provided that one extends the ordinary Hilbert space considering time as a coordinate. In this extended space, the discrete time-translation operator commutes with the extended Floquet Hamiltonian [99].

a complete set of solutions of the Schrödinger equation (the Floquet states) which are periodic in time "up to a phase factor"

$$|\Psi_\alpha(t)\rangle = \mathrm{e}^{-i\bar{\mu}_\alpha t}\,|\Phi_\alpha(t)\rangle \ . \tag{2.8}$$

The states $|\Phi_\alpha(t)\rangle$, the so-called Floquet modes, are periodic, $|\Phi_\alpha(t+\tau)\rangle = |\Phi_\alpha(t)\rangle$ while the real quantities $\bar{\mu}_\alpha$ are called Floquet quasi-energies. Notice that the Floquet modes and quasi-energies are not univocally defined. Indeed, if we multiply the Floquet modes by a phase factor $\mathrm{e}^{-in\omega_0 t}$, they are still periodic; in doing that we need to shift the quasi-energies by $n\omega_0$. Therefore the quasi-energies are defined up to translations of an integer number of ω_0, an ambiguity analogous to the one affecting the quasi-momentum of Bloch states in crystalline solids [100]. One can define Brillouin zones also in the Floquet case, and we will always work in the first Brillouin zone, i.e., we translate all the quasi-energies by an integer number of ω_0 so that they fall in the interval $[-\omega_0/2, \omega_0/2]$.

There are many useful methods to evaluate the Floquet modes, which are based on some of their properties. One possibility [64] is to extend the Hilbert space by considering time as a coordinate living in the interval $[0,\tau]$; the extended Hilbert space is the tensor product of the original one and the Hilbert space generated by the basis functions $\{\mathrm{e}^{-in\omega_0 t}\}$. In this extended space, we can introduce an effective static Hamiltonian: its eigen-energies are the quasi-energies in the different Brillouin zones and the eigenstates give the Fourier coefficients of the periodic Floquet modes. In practice, this method is difficult to implement because it forces us to work with infinite matrices, whose eigenvalues are unbounded from below. In the practice of the present work, we have found more useful to exploit the fact that Floquet modes are eigenstates of the time evolution operator over one period, with eigenvalues given by the quasi-energy phase factors. Indeed, Floquet states obey the Schrödinger equation, and they satisfy the condition

$$\hat{U}(t+\tau,t)\,|\Psi_\alpha(t)\rangle = |\Psi_\alpha(t+\tau)\rangle$$

where $\hat{U}(t+\tau,t)$ is the time-evolution operator over one period, starting from time t. Using Eq. (2.8) and the periodicity of the Floquet modes, we find the eigenvalue equation

$$\hat{U}(t+\tau,t)\,|\Phi_\alpha(t)\rangle = \mathrm{e}^{-i\bar{\mu}_\alpha\tau}\,|\Phi_\alpha(t)\rangle \ .$$

Actually, in our numerical implementation, we diagonalize $\hat{U}(\tau,0)$ [4] to find the $|\Phi_\alpha(0)\rangle$, and then evolve these states up to the desired time.

---

[4]Because computer routines usually diagonalize Hermitian operators, we do not diagonalize $\hat{U}(\tau,0)$ directly, but rather consider an Hermitian operator associated to it

$$\hat{A} = -i\left(\mathbf{1} - \hat{U}(\tau,0)\right)\left(\mathbf{1} + \hat{U}(\tau,0)\right)^{-1} \ ;$$

if we denote by a_α its eigenvalues, the Floquet quasi-energies will be $\mu_\alpha = \frac{\omega_0}{\pi}\,\mathrm{atan}(a_\alpha)$, a number falling inside the first Brillouin zone.

From the Floquet operator $\hat{U}(\tau, 0)$, we can introduce the so-called Floquet Hamiltonian $\hat{H}_F$ such that

$$\hat{U}(\tau, 0) = e^{-i\hat{H}_F \tau} . \tag{2.9}$$

The Floquet states at time 0, $|\Phi_\alpha(0)\rangle$, and quasi-energies can be seen as the eigenstates and eigen-energies of this Hermitian operator.

Remarkably, thanks to Floquet theory, the knowledge of the time evolution operator $\hat{U}(t, 0)$ for times $0 \leq t < \tau$ allows us to reconstruct the state of the system at all times, whatever is the initial state. To see how this is possible, we exploit the fact that the Floquet states are solutions of the Schrödinger equation. Therefore, the time evolution operator from 0 to t can be written in terms of the Floquet modes and quasi-energies as:

$$\hat{U}(t, 0) = \sum_\alpha e^{-i\overline{\mu}_\alpha t} |\Phi_\alpha(t)\rangle \langle\Phi_\alpha(0)| . \tag{2.10}$$

In particular, thanks to the periodicity of the Floquet modes, we find:

$$\hat{U}(\tau, 0) = \sum_\alpha e^{-i\overline{\mu}_\alpha \tau} |\Phi_\alpha(0)\rangle \langle\Phi_\alpha(0)| .$$

If $t = n\tau + \delta t$ with $0 < \delta t < \tau$, we use n times the resolution of identity $\mathbf{1} = \sum_\alpha |\Phi_\alpha(0)\rangle \langle\Phi_\alpha(0)|$ in Eq. (2.10) and we exploit that, for periodicity, $|\Phi_\alpha(t)\rangle = |\Phi_\alpha(\delta t)\rangle$; we end up with the remarkable result that:

$$\hat{U}(t, 0) = \hat{U}(\delta t, 0) [\hat{U}(\tau, 0)]^n . \tag{2.11}$$

If $t = n\tau$, this formula reduces to $\hat{U}(n\tau, 0) = [\hat{U}(\tau, 0)]^n$, showing that, for a stroboscopic dynamics probing the system at times $t_n = n\tau$, it is enough to know one single operator, the Floquet operator $\hat{U}(\tau, 0)$. [5]

We conclude this section showing how the state of the system at all times can be explicitly written in terms of Floquet modes and quasi-energies. If we assume that the system starts in the density matrix $\hat{\rho}_0$, we can expand the density matrix at time t in the Floquet basis. Exploiting the fact that the Floquet states are solutions of the Schrödinger equation we see that $\langle\Psi_\alpha(t)| \hat{\rho}(t) |\Psi_\beta(t)\rangle = \langle\Phi_\alpha(0)| \hat{\rho}_0 |\Phi_\beta(0)\rangle$. Defining $\rho_{\alpha\beta} \equiv \langle\Phi_\alpha(0)| \hat{\rho}_0 |\Phi_\beta(0)\rangle$ we can write

$$\hat{\rho}(t) = \sum_{\alpha\beta} e^{-i(\overline{\mu}_\alpha - \overline{\mu}_\beta)t} \rho_{\alpha\beta} |\Phi_\alpha(t)\rangle \langle\Phi_\beta(t)| . \tag{2.12}$$

---

[5]Eq. (2.11) is very useful in numerical work: we can just restrict to integrate the Schrödinger equation over the first period, and we will find the dynamics at all times for free. We need to do that as many times as the dimension of the Hilbert space: taking as initial condition each of the components of a basis, we obtain the time evolution operator $\hat{U}(t, 0)$ at the times t we desire, within the first period. Obviously in numerical work we restrict times to a mesh; if we are interested in the stroboscopic dynamics, we can evaluate just $\hat{U}(\tau, 0)$.

We will have the opportunity to exploit this formula in the next section, to show when we expect relaxation to the Floquet diagonal ensemble of the observables.

2.3 Convergence to the periodic Floquet diagonal ensemble

In this section we discuss, in the case of periodically driven closed quantum systems, a phenomenon strictly analogous to the relaxation in the diagonal ensemble observed after a quantum quench which we discuss in Sec. 2.1. We will see that, under appropriate conditions on the Floquet spectrum, most observables attain a stationary condition in which they are periodic with the same period of the driving; we define this condition "periodic steady regime". In this stationary limit the observables are given by the average over a periodic Floquet diagonal ensemble which is strictly analogous to the static diagonal ensemble of the quenched case. To see how this works, we consider a closed quantum system starting at time 0 in the density matrix $\hat{\rho}_0$, and evolving coherently under a time-periodic Hamiltonian $\hat{H}(t) = \hat{H}(t+\tau)$. We discuss the dynamics of an observable $\hat{\mathcal{O}}(t)$, which can be either time-independent or τ-periodic. By means of Eq. (2.12) we can write its quantum expectation value at time t in a form strictly reminiscent of Eq. (2.1)

$$
\begin{aligned}
\langle \hat{\mathcal{O}} \rangle_t &\equiv \mathrm{Tr}[\hat{\rho}(t)\hat{\mathcal{O}}(t)] \\
&= \underbrace{\sum_{\alpha} \rho_{\alpha\alpha}\mathcal{O}_{\alpha\alpha}(t)}_{\langle\mathcal{O}\rangle_t^{\mathrm{diag}}} + \underbrace{\sum_{\alpha\neq\beta} \mathrm{e}^{-i\left(\overline{\mu}_\alpha-\overline{\mu}_\beta\right)t}\rho_{\alpha\beta}\mathcal{O}_{\beta\alpha}(t)}_{\langle\mathcal{O}\rangle_t^{\mathrm{off-diag}}} ,
\end{aligned}
\tag{2.13}
$$

where τ-periodic matrix elements $\mathcal{O}_{\beta\alpha}(t) \equiv \langle\Phi_\beta(t)| \hat{\mathcal{O}}(t) |\Phi_\alpha(t)\rangle$ appear. We can see that, in absence of degeneracies in the Floquet spectrum, the diagonal part $\langle\mathcal{O}\rangle_t^{\mathrm{diag}}$ collects all the τ-periodic terms of the response of the observable, while $\langle\mathcal{O}\rangle_t^{\mathrm{off-diag}}$ gives the fluctuations around this periodic behaviour. Indeed, we can define what we will call the *Floquet diagonal ensemble* density matrix $\hat{\rho}_{\mathrm{diag}}(t)$,

$$
\hat{\rho}_{\mathrm{diag}}(t) = \sum_{\alpha} \rho_{\alpha\alpha} |\Phi_\alpha(t)\rangle \langle\Phi_\alpha(t)| ,
\tag{2.14}
$$

such that the periodic part of the average can be expressed as

$$
\langle\mathcal{O}\rangle_t^{\mathrm{diag}} = \mathrm{Tr}\left[\hat{\mathcal{O}}\hat{\rho}_{\mathrm{diag}}(t)\right] .
\tag{2.15}
$$

This formula resembles that for the diagonal ensemble in the quantum quench case (Eq. (2.3)): the difference is that this is not a static object, but depends periodically on time with the same period of the driving. As

we have done for the relaxation to the diagonal ensemble in Sec. 2.1, we can discuss the conditions under which the fluctuations $\langle \mathcal{O} \rangle_t^{\text{off-diag}}$ vanish for large times and the observables tend to the Floquet diagonal ensemble value.

To study the behaviour of off-diagonal fluctuations, we again introduce a time-dependent weighted joint density of states, similar to that in Eq. (2.4), defined as

$$F_{\mathcal{O},t}(\omega) \equiv \pi \sum_{\alpha \neq \beta} \rho_{\alpha\beta}\, \mathcal{O}_{\beta\alpha}(t)\, \delta\left(\omega - \overline{\mu}_\alpha + \overline{\mu}_\beta\right)\ . \qquad (2.16)$$

We can see that this object is τ-periodic in time. This definition allows us to write the fluctuating term as

$$\langle \mathcal{O} \rangle_t^{\text{off-diag}} = \int_{-\infty}^{+\infty} \frac{\mathrm{d}\omega}{\pi}\ F_{\mathcal{O},t}(\omega)\, \mathrm{e}^{-i\omega t}\ . \qquad (2.17)$$

It is easy to show that $\langle \mathcal{O} \rangle_t^{\text{off-diag}}$ vanishes after a transient if, whatever is the value of t, $F_{\mathcal{O},t}(\omega)$ is a regular function [6] of ω. To that purpose, choosing any $0 \leq t_0 < \tau$, we exploit the τ-periodicity in t of $F_{\mathcal{O},t}(\omega)$, and consider

$$\langle \mathcal{O} \rangle_{t_0+n\tau}^{\text{off-diag}} = \int_{-\infty}^{+\infty} \frac{\mathrm{d}\omega}{\pi}\ F_{\mathcal{O},t_0}(\omega)\, \mathrm{e}^{-i\omega(t_0+n\tau)}\ .$$

This expression vanishes for $n \to \infty$ due to the Riemann-Lebesgue lemma [92]; the argument is exactly the same as that following Eq. (2.5).

As in the quantum quench case, if the Floquet spectrum is discrete then $F_{\mathcal{O},t}(\omega)$ is singular: a discrete sum of Dirac's deltas giving rise to persisting fluctuations. Hence, to have vanishing fluctuations, it is necessary that the Floquet spectrum is a continuum; in bounded many-body systems, this can happen only in the thermodynamic limit. If there is a discrete component in the spectrum, we can have also convergence to the Floquet diagonal ensemble, provided we take an initial state $|\psi_0\rangle$ having overlap mainly with Floquet states in the continuum. This is true also if we take observables coupled to Floquet states in different components of the spectrum, but the number of relevant Floquet levels in the continuum has to be extensive with respect to the discrete ones. We can have a pure point spectrum in the thermodynamic limit (and persisting fluctuations) also in the thermodynamic limit when the Hamiltonian is disordered. Noteworthy is the case in which, in a static disordered Hamiltonian, the discrete and the continuous parts of the spectrum are both extensive and are separated by a mobility edge [101, 102]. A periodic external perturbation can couple levels in the two regions of the spectrum by means of multi-photon resonances. The resulting Floquet states, which are superpositions of eigenstates in the continuum and discrete part of the spectrum, will show a continuous Floquet

---

[6]It is enough that $|F_{\mathcal{O},t}(\omega)|$ is Lebesgue-integrable.

spectrum. This phenomenon has been predicted for hydrogen atoms under an ac electric field [103]; we are not aware of genuinely many-body cases in which it occurs.

As for the case of a quantum quench, the relaxation to the Floquet diagonal ensemble depends almost exclusively on the properties of the Floquet spectrum of the Hamiltonian which drives the evolution. If the spectrum is continuous, we can have persisting fluctuations only in very pathological cases: whenever the initial state is a discrete superposition of few Floquet states or the observable considered couples only to few of them. As in the quantum quench, these superpositions are practically impossible to realize and the observables are practically impossible to measure. Indeed, Floquet states are obtained from eigenstates through an adiabatic switching on of the periodic driving [104]. Even if one assumes to have succeeded in preparing a discrete superposition of few many-body states, it is impossible to switch on adiabatically the external perturbation. Indeed, if the system is non-integrable, the Floquet quasi-energies are exponentially close and the switching-on time has to be exponential large in the system size. Here, as in the quantum quench case, integrable models [9, 96] could be the exception. [7]

For the bounded quantum many body systems we consider, a continuous Floquet spectrum and exact convergence to the Floquet diagonal ensemble can exist only in the thermodynamic limit. Practically, however, we can numerically integrate the Schrödinger equation only for systems with finite N. To see if, in the limit $N \to \infty$, the observables tend to the periodic regime, we can consider the scaling with N of the stroboscopic time-fluctuations. Here, the definitions are very similar to those of Eqs. (2.2), (2.7), except that we consider discrete times. (Indeed, we are probing the convergence of the observables to a steady periodic regime where the observables appear as constants if they are probed stroboscopically.) To define the stroboscopic fluctuations, we need first to define the stroboscopic average of an observable

$$\overline{\langle \mathcal{O} \rangle_{k\tau}} = \lim_{n \to \infty} \frac{1}{n} \sum_{k=0}^{n-1} \langle \hat{\mathcal{O}} \rangle_{k\tau} = \sum_\alpha \rho_{\alpha\alpha}(0) \mathcal{O}_{\alpha\alpha}(0) \ . \qquad (2.18)$$

In absence of degeneracies in the Floquet spectrum, the stroboscopic time-fluctuations are [8]

$$(\delta \mathcal{O}_{\text{strobo}})^2 = \overline{\left(\langle \mathcal{O} \rangle_{k\tau} - \overline{\langle \mathcal{O} \rangle_{k\tau}} \right)^2} = \sum_{\alpha \neq \beta} |\rho_{\alpha\beta}|^2 \, |\mathcal{O}_{\alpha\beta}(0)|^2 \ . \qquad (2.19)$$

---

[7]Thanks to the extensive number of conserved local operators [96], there are selection rules dividing the Hamiltonian in not interacting blocks, in each of the blocks the separation between levels can be not exponentially small in the size of the system.

[8]As in the quantum quench case, in generic non-integrable systems, the finite-time stroboscopic average and fluctuations approach the infinite-time values for times exponentially large in N; nevertheless if an observable relaxes, then its expectation stays, for most of the time, near the Floquet diagonal value [95].

When there is relaxation to the Floquet diagonal ensemble in the thermo-dynamic limit, this object scales to zero as N is increased, and we can check this numerically.

2.4 Discussion on the generality of the convergence to the Floquet-diagonal ensemble

The relation among continuity of the spectrum and convergence of the observables we have discussed above is very powerful. Indeed, if a quenched system has a continuous spectrum, the same happens to the Floquet spectrum of the same system if the perturbation is no more sudden but is periodic. Therefore, from the foregoing discussion, we expect convergence to the Floquet diagonal ensemble in all the systems which relax to the diagonal ensemble after a quench. In literature there is plenty of examples, integrable or not, enjoying this property [39, 26, 27, 28, 29, 30, 31, 60, 41, 32, 33, 34, 35, 36, 37, 105, 106, 107, 38, 39], so relaxation to the Floquet diagonal ensemble seems to be a pretty general phenomenon. Indeed, as far as we know, this convergence to the Floquet diagonal ensemble has been observed numerically in literature at least in one case. In Fig. 1 of Ref. [20] we observe that the energy becomes periodic after a transient in a one-dimensional Hubbard model undergoing uniform driving. This model is special being Bethe-Ansatz integrable, but — as we have observed before — our effect seems to be as general as the relaxation to the diagonal ensemble.

In this Thesis we will show numerically the convergence to the Floquet diagonal ensemble in two cases of integrable models: the quantum Ising chain in transverse field (Chapt. 3) and the Lipkin model (Chapt. 5). The first one will be an opportunity to discuss the limits of applicability of the Floquet diagonal ensemble in predicting the spectrum of quantum fluctuations of the work performed on the system. We will see in some detail how the convergence is independent of the translational invariance and factoriz-ability of the model by means of a quantum Ising model with a localized inhomogeneity, which will give us the opportunity to reply to some criticism addressed to our result [108, 109]. Using the quantum Ising chain, we will show also (Chapt. 4) how, in the limit of small driving, linear response the-ory (LRT) fails to correctly predict the relaxation to the diagonal ensemble, because of some gaps in the Floquet spectrum which close only in the limit of vanishing amplitude.

While the Ising model shows always a perfectly regular dynamics, the Lipkin model, instead, under appropriate conditions on the driving can show an ergodic behaviour. In this case the system heats up until the observables converge to their $T = \infty$ value. Indeed, because of quantum chaos, the Eigenstate Thermalization Hypothesis is valid and the averages over the Floquet ensemble equal the $T = \infty$-thermal ones. Moreover, in the ergodic

case, the Floquet spectrum is that of a random matrix which we know to be a continuum in the thermodynamic limit, in agreement with the convergence to the Floquet-diagonal ensemble. As for the thermalization after a quantum quench [67, 95, 110], these results, shown in this specific example, are likely true whenever a periodically driven quantum system is ergodic.

Chapter 3

Ising model with time-periodic driving

3.1 Introduction: the translationally invariant case

Having discussed the general theory of relaxation to the Floquet diagonal ensemble, we are ready to show it in a specific example. We consider, for that purpose, the Quantum Ising chain in a transverse field, which has been the subject of many studies concerning the equilibration after a quantum quench [36, 37, 111]. The model is a linear chain of 1/2-spins interacting by means of the Hamiltonian

$$\hat{H}(t) = -\frac{1}{2} \sum_{j=1}^{L} \left[J_j \hat{\sigma}_j^z \hat{\sigma}_{j+1}^z + h_j(t)\hat{\sigma}_j^x \right] \ . \tag{3.1}$$

Here the $\hat{\sigma}_j^{x,z}$ are Pauli matrices at site j, L is the chain length, and we impose periodic boundary conditions (PBC). The couplings J_j act longitudinally along the z spin direction, while the external field $h_j(t)$ acts transversally. This Hamiltonian can always be mapped onto a quadratic Fermionic Hamiltonian, via a Jordan-Wigner transformation [112] (see Appendix B). The quadratic Fermionic problem to which we map the model can be easily diagonalized, and even its quantum dynamics can be easily computed numerically, since the Heisenberg's equations for the Fermionic operators are linear.

This applies whatever the J_j and the h_j are. We will consider a non-translationally invariant example in Sec. 3.3. Now, for the sake of a clearer exposition, we focus on the case of a uniform chain with $J_j \equiv J = 1$ and $h_j \equiv h$. In this case, the system shows a quantum phase transition (QPT) at $|h_c| = 1$ [61]: if $|h| < 1$ the longitudinal coupling wins and the system is ferromagnetic; for $|h| > 1$ the transverse coupling dominates and the system is a quantum paramagnet. Applying the Jordan-Wigner transformation and

a Fourier transform (which is possible due to translational invariance) the Hamiltonian becomes a sum of decoupled two-level systems

$$
\hat{H}(t) = \sum_{k>0}^{\text{ABC}} \hat{H}_k(t) = \sum_{k>0}^{\text{ABC}} \left(\begin{array}{cc} \hat{c}_k^\dagger & \hat{c}_{-k} \end{array} \right) \left(\begin{array}{cc} E_k(t) & -i\Delta_k \\ i\Delta_k & -E_k(t) \end{array} \right) \left(\begin{array}{c} \hat{c}_k \\ \hat{c}_{-k}^\dagger \end{array} \right) ,
$$
(3.2)

where $E_k(t) = h(t) - \cos k$, $\Delta_k = \sin k$ and $\hat{c}_k$ are Fermionic operators in Fourier space. The superscript on the sum symbol means that we consider states with an even number of fermions. This implies anti-periodic boundary conditions (ABC) on the real-space fermions $\hat{c}_j$ [112] (see Appendix B) and makes the sum over k restricted to positive k of the form $k = (2n+1)\pi/L$ with $n = 0, \ldots, L/2 - 1$. Because of the conservation of fermion parity and momentum, each $\hat{H}_k(t)$ acts on a 2-dim Hilbert space generated by $\{\hat{c}_k^\dagger \hat{c}_{-k}^\dagger |0\rangle, |0\rangle\}$; we can represent the operator $\hat{H}_k$ in this basis, which we define the *standard basis*, by a 2×2 matrix

$$
H_k(t) = E_k(t)\sigma^z + \Delta_k \sigma^y ,
$$
(3.3)

with instantaneous eigenvalues

$$
\pm \epsilon_k(t) = \pm\sqrt{E_k^2(t) + \Delta_k^2} .
$$
(3.4)

At the critical point $h = 1$, the eigenvalues are $\pm \epsilon_k = \pm 2\sin(k/2)$; so, if we drive the system taking for instance $h(t) = 1 + A\cos(\omega_0 t)$, the driving frequency ω_0 will be resonant to the proper excitations of the system whenever $-4 < \omega_0 < 4$. This will be important in what follows, where we will see that Floquet quasi-degeneracies emerge from multi-photon resonances. In Chapt. 4 we will see how the gap at the quasi-degeneracies alters the energy absorption behaviour at resonant driving frequency in the linear response regime.

The eigenstates of the instantaneous Hamiltonian can be expanded in the standard basis and acquire a BCS-like form. For instance, the ground state at time t is given by

$$
\left| \Psi_{\text{GS}}^t \right\rangle = \prod_{k>0}^{\text{ABC}} \left| \psi_{k\,\text{GS}}^t \right\rangle = \prod_{k>0}^{\text{ABC}} \left(u_{k\,0}^t + v_{k\,0}^t \hat{c}_k^\dagger \hat{c}_{-k}^\dagger \right) |0\rangle .
$$
(3.5)

Here $v_{k\,0}^t = i\sin(\theta_k^t/2)$ and $u_{k\,0}^t = \cos(\theta_k^t/2)$, with θ_k^t given by $\tan\theta_k^t = (\sin k)/(h(t) - \cos k)$. These coefficients result from the diagonalization of the Hamiltonian in Eq. (3.2). Indeed, by means of a unitary rotation of angle θ_k^t around σ_x, one can define new Fermionic operators $\hat{\gamma}_k(t)$ in terms of the old ones $\hat{c}_k$

$$
\left(\begin{array}{c} \hat{\gamma}_k(t) \\ \hat{\gamma}_{-k}^\dagger(t) \end{array} \right) = \mathrm{e}^{i\sigma_x \theta_k^t/2} \left(\begin{array}{c} \hat{c}_k \\ \hat{c}_{-k}^\dagger \end{array} \right)
$$
(3.6)

such that the k-component of the Hamiltonian Eq. (3.2) acquires a diagonal form $\hat{H}_k(t) = \epsilon_k(t) \left(\hat{\gamma}_k^\dagger(t)\hat{\gamma}_k(t) - \hat{\gamma}_k(t)\hat{\gamma}_k^\dagger(t) \right)$, with the $\epsilon_k(t)$ defined in Eq. (3.4). The ground state Eq. (3.5) is the vacuum for these new Fermionic operators: $\hat{\gamma}_k(t) \left| \Psi_{\mathrm{GS}}^t \right\rangle = 0 \ \forall \ k$. If we initialize the system in the ground state and study its dynamics under a uniform driving we see that, because of the factorization in 2×2 spaces, also the solution of the Schrödinger equation acquires a factorized BCS-like form

$$| \Psi(t) \rangle = \prod_{k>0}^{\mathrm{ABC}} | \psi_k(t) \rangle = \prod_{k>0}^{\mathrm{ABC}} \left(u_k(t) + v_k(t)\hat{c}_k^\dagger \hat{c}_{-k}^\dagger \right) |0\rangle \ , \qquad (3.7)$$

where $u_k(t)$, $v_k(t)$ obey the Bogoliubov-de Gennes equations (Schrödinger equation in the $\{\hat{c}_k^\dagger \hat{c}_{-k}^\dagger |0\rangle, |0\rangle\}$ basis)

$$i\hbar\frac{d}{dt} \left(\begin{array}{c} v_k(t) \\ u_k(t) \end{array} \right) = \left(\begin{array}{cc} E_k(t) & -i\Delta_k \\ i\Delta_k & -E_k(t) \end{array} \right) \left(\begin{array}{c} v_k(t) \\ u_k(t) \end{array} \right) \ . \qquad (3.8)$$

Initializing the system in the ground state at $t = 0$ we impose, as initial conditions, $v_k(t = 0) = v_{k\,0}^{t=0}$ and $u_k(t = 0) = u_{k\,0}^{t=0}$. We will focus on local observables (possibly τ-periodic) whose expectation value can be written in a k-space factorized form

$$b(t) = \frac{1}{L} \sum_{k>0} \langle \psi_k(t)| \, \hat{B}_k \, |\psi_k(t)\rangle \ . \qquad (3.9)$$

This obviously happens when the operator itself can be factorized: examples are the energy-per-site $\hat{e}(t) = \hat{H}(t)/L$ and the transverse magnetization-per-site $\hat{m} = \frac{1}{L} \sum_j \hat{\sigma}_j^x = \frac{2}{L} \sum_{k>0} (\hat{c}_{-k}\hat{c}_{-k}^\dagger - \hat{c}_k^\dagger \hat{c}_k)$. Even if less straightforwardly, also the single particle Green's functions $\langle \hat{c}_i^\dagger \hat{c}_j \rangle$ and $\langle \hat{c}_i \hat{c}_j \rangle$ can be written in this factorized form ($\hat{c}_j$ are the real space Fermionic operators defined in Appendix B). The single particle Green's functions are very important objects because, thanks to the Gaussian nature of states Eqs. (3.5) and (3.7) and to Wick's theorem [113], all the correlators and the many-particle operators can be written in terms of them [112, 114].

3.2 Convergence to the periodic regime in the translationally-invariant case

As introduced in the previous section, let us consider the case of a uniform periodic driving of a uniform Quantum Ising chain in transverse field [1]. In each k-subspace we solve numerically the Bogoliubov-de Gennes equations

---

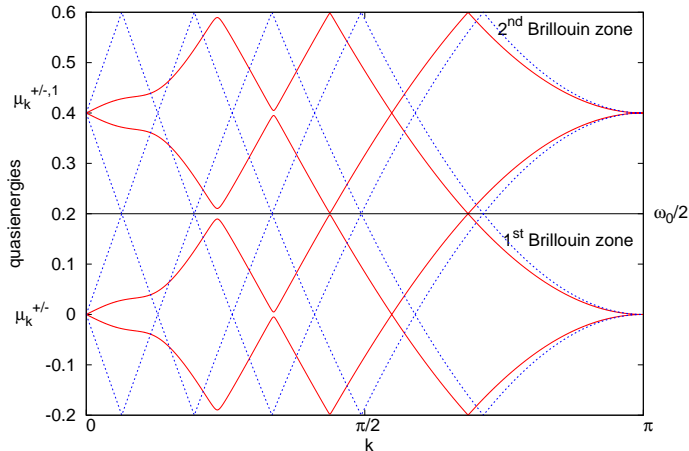[1]The results presented in this Section have been published in Ref. [66].

Figure 3.1: Single-mode Floquet quasi-energies vs k for a driving around the critical point with $A = 1$ and frequency $\omega_0 = 0.4$ (red solid line). We plot for comparison the unperturbed single-mode eigen-energies, folded and replicated in the different Brillouin zones.

Eq. (3.8) and apply the methods described in Chapter 2 to evaluate the Floquet quasi-energies $\mu_k^+ = -\mu_k^- = \mu_k$ (they are opposite because of the vanishing trace of the Hamiltonian $\hat{H}_k$) and the associated Floquet modes $\left|\phi_k^{\pm}(t)\right\rangle$. In terms of these objects, the k-component of the state at time t can be written as

$$|\psi_k(t)\rangle = r_k^+ \, \mathrm{e}^{-i\mu_k t} \left|\phi_k^+(t)\right\rangle + r_k^- \, \mathrm{e}^{i\mu_k t} \left|\phi_k^-(t)\right\rangle , \qquad (3.10)$$

where the overlap factors are defined as $r_k^{\pm} = \left\langle\phi_k^{\pm}(0)\right| \psi_k(0)\rangle$. We periodically drive the system across its quantum critical point

$$h(t) = 1 + A\cos(\omega_0 t + \varphi_0) . \qquad (3.11)$$

We do so to fix ideas and because we would like to explore the dynamics around a quantum phase transition; different periodic time-dependences would give similar results in terms of continuity of the Floquet spectrum and convergence to the periodic steady regime. The results which follow are obtained for a driving amplitude $A = 1$ and $\varphi_0 = 0$. In the thermodynamic limit the Floquet spectrum is a continuum: an instance of that can be seen in Fig. 3.1. We note the periodical repetition of the Floquet-spectrum in the different Brillouin zones and the presence of quasi-degeneracies in the form of avoided crossings. For comparison, we plot the spectrum of the unperturbed Hamiltonian folded and replicated in the different Brillouin zones. We see how the multi-photon resonances (crossings of replicas of the single-mode spectrum in different Brillouin zones) become quasi-degeneracies of
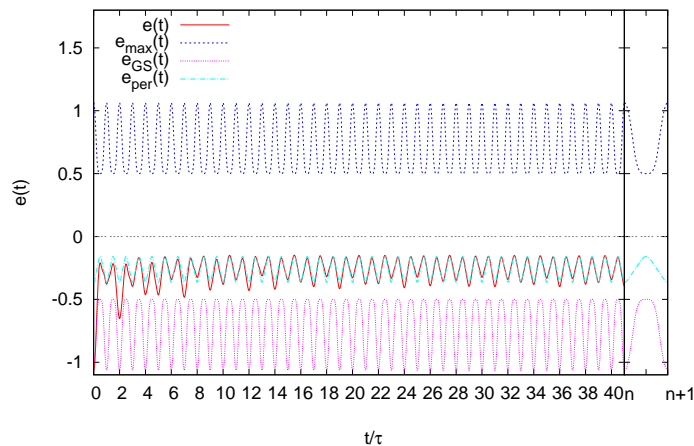
25

Figure 3.2: Convergence of the energy-per-site to its periodic regime when $A = 1$ and the driving frequency is $\omega_0 = 2$. We see how the asymptotic periodic value of the energy is well below its $T = \infty$ value $\langle e \rangle_{T=\infty} = 0$.

the Floquet spectrum: the driving leads to the opening of small gaps. The continuity of the Floquet spectrum leads to the asymptotic decay of fluctuations of the observables of type Eq. (3.9) around the periodic steady regime. The behaviour of different observables is pretty much the same; from now on we will focus our numerical analyses mainly on the energy-per-site $\hat{e}(t) = \hat{H}(t)/L$. We can see in Fig. 3.2 an instance of convergence to the periodic steady regime. The fluctuations decay polynomially in time, as $t^{-3/2}$ when $\omega_0 < 4$ and $t^{-1/2}$ otherwise. As we discussed before, $\omega_0 = 4$ is a special frequency: it marks the border of the resonances in case of driving of infinitesimal amplitude; in the finite amplitude case when $\omega_0 \leq 4$ the first Floquet quasi-resonance appears. The general argument on convergence to the periodic regime (explained in Section 2.3) in this case acquires a quite transparent form. Indeed, using the expansion Eq. (3.10) in Eq. (3.9) and going into the thermodynamic limit $L \to \infty$ which implies $\frac{1}{L} \sum_{k>0}^{\text{ABC}} \to \frac{1}{2\pi} \int_0^\pi \mathrm{d}k$, we find (in analogy with Eq. (2.13))

$$b(t) = b^{\text{diag}}(t) + b^{\text{off}-\text{diag}}(t) \tag{3.12}$$

where we have defined

$$b^{\text{diag}}(t) \equiv \sum_{\alpha=\pm} \int_0^\pi \frac{\mathrm{d}k}{2\pi} |r_k^\alpha|^2 \langle \phi_k^\alpha(t)| \hat{B}_k |\phi_k^\alpha(t)\rangle \tag{3.13}$$

$$b^{\text{off}-\text{diag}}(t) \equiv \int_0^\pi \frac{\mathrm{d}k}{\pi} \Re \left[r_k^{-*} r_k^+ \langle \phi_k^-(t)| \hat{B}_k |\phi_k^+(t)\rangle \, \mathrm{e}^{-2i\mu_k t} \right] . \tag{3.14}$$

The first term is τ-periodic; the second one gives rise to fluctuations which vanish for $t \to \infty$. This is easy to see: up to a change of variables (made

26

possible by the smoothness of the μ_k), this term is already in the form of Eq. (2.16) to which Riemann-Lebesgue lemma applies. The mapping of the problem to an assembly of two-level systems allows an interesting physical interpretation of the decay of the fluctuating part in the present case: it is a dephasing among spins with different characteristic frequencies akin to the inhomogeneous broadening in NMR [115].

We can see this decay of fluctuations from another perspective; we can evaluate – for finite L – the stroboscopic fluctuations of $b(t)$ as in Eq. (2.19). We find, up to terms of order $1/L^2$

$$(\delta b_{\mathrm{strobo}})^2 = \frac{1}{L} \int_0^\pi \frac{\mathrm{d}k}{2\pi} \left| r_k^{-*} r_k^+ \left\langle \phi_k^-(0) \right| \hat{H}_k(0) \left| \phi_k^+(0) \right\rangle \right|^2 + O\left(\frac{1}{L^2}\right) . \quad (3.15)$$

So, if the integral is finite and independent of L, stroboscopic fluctuations vanish in the thermodynamic limit $L \to \infty$. The integral stays finite even if we take as initial state a state of the BCS form (3.5) with u_k and v_k initialized in a random fashion: thanks to the continuity of the Floquet spectrum, the Riemann-Lebesgue lemma still applies to Eq. (3.14). So, as discussed before, for the sake of convergence to the periodic regime, only the regularity of the evolution Hamiltonian (embodied in the Floquet spectrum) is important [60].

Once established that observables become periodic after a transient, it is interesting to look in more detail at the properties of their periodic steady regime. We focus on the excitation energy per site defined as

$$e_{\mathrm{ex}}(t) = e(t) - e_{\mathrm{GS}}(t) , \quad (3.16)$$

where $e_{\mathrm{GS}}(t)$ is the instantaneous ground state energy at time t. After an integer number of periods (whenever $t = t_{2n} = 2n/\omega_0$), the $e_{\mathrm{ex}}(t)$ so defined has the physical meaning of the work done on the system by the external driving. Moreover, for $A = 1$, when $t = t_{2n+1} = (2n+1)\pi/\omega_0$ we have $h(t) = 0$, and it is easy to see that the excitation energy $e_{\mathrm{ex}}(t)$ equals the density of defects (kinks) ν_d of the classical Ising chain

$$\nu_d(\omega_0, n) = \langle \Psi(t_{2n+1})| \sum_{j=1}^L \left[1 - \hat{\sigma}_j^z \hat{\sigma}_{j+1}^z\right] |\Psi(t_{2n+1})\rangle /(2L) = e_{\mathrm{ex}}(t_{2n+1}) .$$
$$(3.17)$$

Studying this quantity allows us to understand the relationship among integrability and energy absorption, and see how the adiabatic limit is reached for $\omega_0 \to 0$. If the system was exactly adiabatic [116], the excitation energy would vanish. This cannot happen, for any finite frequency: we are sweeping the field around the critical point, where the gap in the instantaneous spectrum closes up. The interpretation of the excitation energy as defect density is important. For a single sweep at rate v, the Kibble-Zurek mechanism [117] gives rise to a scaling of the defect density with $v^{1/2}$. We can
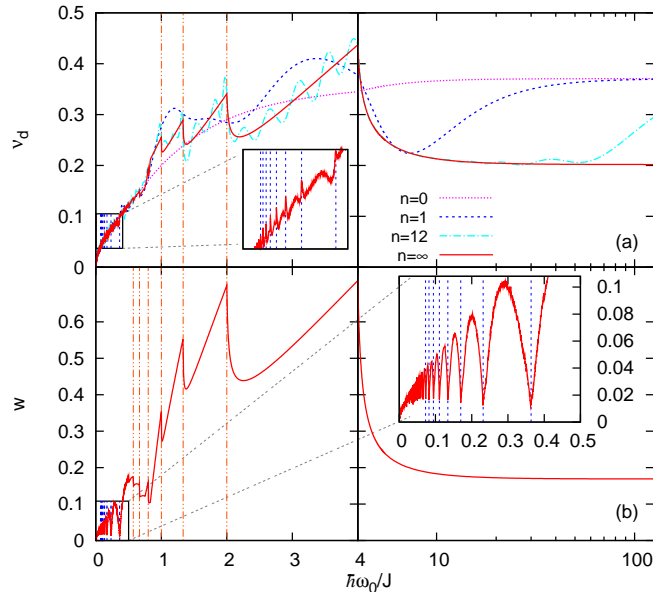
Figure 3.3: The density of defects for a driving field $h(t) = 1 + \cos(\omega_0 t)$ at the end of half-periods, i.e., at times $t = t_{2n+1} = (2n + 1)\pi/\omega_0$ when the transverse field vanishes; $n = 0$ is the result of a single LZ crossing. (b) The asymptotic total work (per spin) done on the system $w = \lim_{n\to\infty} e(t_{2n}) - e(0)$, where $t_{2n} = 2n\pi/\omega_0$, versus the frequency ω_0 of the transverse field.

interpret the process in each two dimensional k-subspace as a single Landau-Zener (LZ) [118] event; however slow is the crossing, there are always modes of low k undergoing tunneling from the ground to the excited state of the corresponding 2×2 problem. In the case of a periodic driving, there is a sequence of LZ crossings and the system keeps coherence among one and the next. The interference among different modes gives rise to a periodic steady value of the absorbed work; it is nevertheless interesting to discuss the effect of interference among subsequent LZ events and how it manifests in the properties of the stationary energy.

Our conclusions can be summarized in Fig. 3.3. In the upper panel we plot the density of defects, at $t = t_{2n+1}$, for different n. We see that, after the first sweep ($n = 0$), the number of defects scales like $\omega_0^{1/2}$ for small ω_0 and settles to a plateau for large ω_0: The small ω_0 scaling is just the Kibble-Zurek one [117] and the large ω_0 plateau gives precisely the density of defects one obtains if the system remains frozen in the initial state. As n increases, we see the appearance of interference effects until, for $n = \infty$, we settle to the asymptotic value. First of all we notice that, even after infinite sweepings, there is an overall scaling as $\sqrt{\omega_0}$ at moderate frequencies of the asymptotic periodic value; upon that overall behaviour, we observe some

features. We see: *i)* a plateau for large ω_0, *ii)* some peaks at intermediate frequencies $\omega_0 = 4/p$ (for some p integer) and *iii)*, in the small frequency region, some small spikes at the values ω_0 obeying $J_0(2/\omega_0) = 0$ (J_0 is the zeroth-order Bessel function [119]). The feature *i)* comes from the fact that the Floquet states, for high frequency, are — up to corrections $O(1/\omega_0^2)$ — constantly equal to the eigenstates of the unperturbed Hamiltonian.

About features *ii)* and *iii)*, we can discuss them better if we probe stroboscopically the excitation energy at times equal to an integer number of periods ($t_{2n} = 2\pi n/\omega_0$) and consider its asymptotic value, which we plot versus ω_0 in the lower panel of Fig. 3.3. At the times considered, the Hamiltonian equals its initial value $\hat{H}(t_{2n}) = \hat{H}(0)$, the excitation energy acquires the physical value of stroboscopic work-per-spin $w_n = e(t_{2n}) - e_0$ performed on the system; we define its asymptotic value for $n \to \infty$ as w_∞. Here, feature *ii)* can be seen in the form of marked peaks at the frequencies $\omega_0 = 4/p$, feature *iii)* as dips in the absorbed energy for those ω_0 such that $J_0(2/\omega_0) = 0$.

To understand the peaks at $\omega_0 = 4/p$, we can see that w_∞ is an integral in k involving only terms diagonal in the Floquet basis (like Eq. (3.13)); the integrand (which we define w_k) shows marked spikes in correspondence to those values of k where there are anti-crossings in the Floquet quasi-energies (see the left panel of Fig. 3.4). If we increase the frequency across $\omega_0 = 4/p$ (for some p), the value of k where there is one of the anti-crossings (and the corresponding maximum) goes beyond the upper integration limit at π, hence there is a sudden decrease of the integral. We can see an instance of this for $p = 5$ in the right panel of Fig. 3.4. Concerning feature *iii)*, we see sudden drops of the asymptotic absorbed energy w_∞ at the frequencies satisfying $J_0(2/\omega_0) = 0$ (lower panel of Fig. 3.3), because there the small-k modes undergo coherent destruction of tunneling (CDT) [120] from the ground to the excited state. This can be easily seen by applying to the single k-mode Hamiltonian matrix Eq. (3.3) a time-dependent unitary rotation around σ_x, and then first order perturbation theory (for details, see Appendix A). This approximation is valid only for the small k non-adiabatic modes: there are large dips because CDT affects precisely these modes which would be the only ones giving a non-vanishing contribution to the absorbed energy at low frequency.

Nevertheless, the most interesting thing we can notice in Fig. 3.3 is that the asymptotic absorbed energy depends on ω_0, and is definitely smaller than the value 1, corresponding to the maximum entropy (and then to a thermal state with $T = \infty$). Moreover, it is easy to verify that, starting from another initial state, the asymptotic energy would be different.

These features are a consequence of integrability: consistently with the results for sudden quenches in integrable systems [9, 42, 39, 121], the asymptotic periodic condition of the local observables can be described in terms of a GGE ensemble. To this aim, we define L time-periodic Fermionic op-
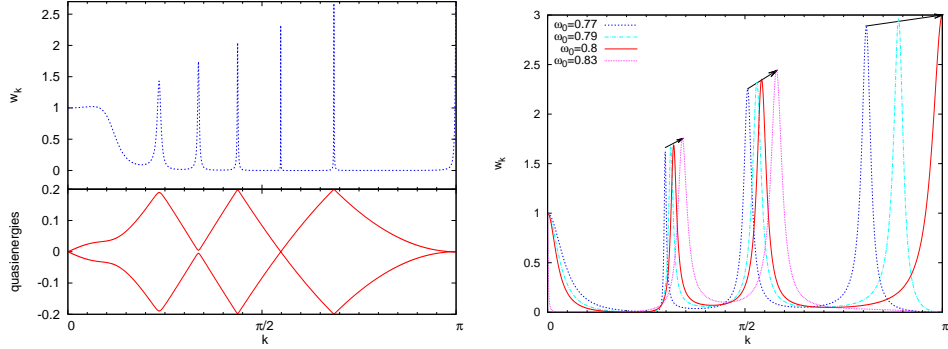
Figure 3.4: (Upper left panel) The integrand w_k of the asymptotic total work per spin w for $\omega_0 = 0.4$. Notice the peaks occurring at the values of k for which the quasi-energies are quasi-resonant (lower panel). (Right panel) The integrand w_k for some frequencies around $\omega_0 = 0.8$ ($\omega_0 = 4/p$ with $p = 5$). The black arrows mark the direction of increasing frequency. Notice the uppermost right peak whose top is at $k = \pi$ for $\omega_0 = 0.8$ and then disappears.

erators $\hat{\gamma}_{Pk}(t)$ by applying a unitary transformation to the operators $\hat{c}_k$

$$\begin{pmatrix} \hat{\gamma}_{Pk}(t) \\ \hat{\gamma}^\dagger_{P-k}(t) \end{pmatrix} = \begin{pmatrix} \xi_k(t) & \eta_k(t) \\ -\eta_k^*(t) & \xi_k^*(t) \end{pmatrix} \begin{pmatrix} \hat{c}_k \\ \hat{c}^\dagger_{-k} \end{pmatrix} \tag{3.18}$$

where we have defined the periodic coefficients $\xi_k(t) = \langle 0 | \phi_k^-(t) \rangle$ and $\eta_k(t) = \langle 0 | \hat{c}_{-k}\hat{c}_k | \phi_k^-(t) \rangle$ as the components of one of the Floquet modes in the standard basis. (The Floquet mode $|\phi_k^-(t)\rangle$ is the vacuum of $\hat{\gamma}_{Pk}(t)$ – $\hat{\gamma}_{Pk}(t)|\phi_k^-(t)\rangle = 0$ and $|\phi_k^+(t)\rangle = \hat{\gamma}^\dagger_{Pk}(t)|\phi_k^-(t)\rangle$.) It is easy to show that, once the convergence to the periodic regime has been attained, the expectation values of any object of the type Eq. (3.9) which has relaxed is given by

$$b^{\text{diag}}(t) = \int \frac{dk}{2\pi} \text{Tr}\left[\hat{B}_k(t)\hat{\rho}_{Gk}(t)\right] , \tag{3.19}$$

where the density matrix $\hat{\rho}_{Gk}$ is given by:

$$\hat{\rho}_{Gk}(t) = \frac{1}{1 + \lambda_k^2} e^{-\lambda_k \hat{\gamma}^\dagger_{Pk}(t)\hat{\gamma}_{Pk}(t)} . \tag{3.20}$$

The density matrix $\hat{\rho}_G(t) = \prod_k \hat{\rho}_{Gk}(t)$ is the generalization to the present time-periodic case of the so-called Generalized Gibbs Ensemble [9, 27]. Following Ref. [40], we can show that this is the ensemble which maximizes the

entropy under the constraint of constant occupations [2] $\langle \hat{\gamma}^{\dagger}_{P\,k}(t)\hat{\gamma}_{P\,k}(t)\rangle_t \equiv |r^+_k|^2$. The Lagrange multipliers λ_k enforce these constraints; their value depends on the initial conditions as $\lambda_k = \log\left(|r^-_k|^2/|r^+_k|^2\right)$. So we can see how strict is the analogy between the GGE form of the diagonal ensemble attained by the quantum Ising model in the case of quantum quench [36, 37, 9] and that of the Floquet diagonal ensemble in the case of periodic driving.

The GGE form is a consequence of the integrability of the model: the asymptotic condition of the local observables is determined by as many parameters as the number of spins. We will see in Chapt. 5 an example of an ergodic system where the Floquet states obey the Eigenstate Thermalization Hypothesis [59, 58] with $T = \infty$. In that case, the system will heat up until infinite temperature and any memory of the initial state is lost: the random properties of the Floquet states make the averages on the Floquet diagonal ensemble independent of the initial state considered. In this way the asymptotic condition is fixed *a priori* without previous knowledge of any parameter.

It is important to stress that the GGE ensemble does not give a complete description of the asymptotic condition. We will show in Sec. 3.4 that the work statistics of the system tends to an asymptotically periodic regime which is not described by the GGE ensemble Eq. 3.19. This is a point which can be verified experimentally thanks to the recent development of techniques [10, 80] which allow to probe the quantum probability distribution of observables. Before moving to this very interesting point, we discuss the robustness of the convergence to the diagonal Floquet ensemble towards breaking translational invariance by means of the application of inhomogeneous fields.

3.3 Breaking of translational invariance

The case we have discussed above is very special: not only it is translationally invariant and integrable, but also reducible to an assembly of independent 2-level systems. This was just an example of a far more general class of systems undergoing relaxation to the Floquet diagonal ensemble. Relaxation depends only on spectral properties: in Sec. 2.4 we have argued that, if a system relaxes after a quantum quench because of a continuous energy spectrum, then, most likely it will attain the asymptotic periodic regime under a corresponding periodic driving, due to a continuous Floquet spectrum. Therefore, our results seem to be quite general: there are many examples in literature of relaxation to the diagonal ensemble, both in integrable and

---

[2]It is easy to see that $\langle \hat{\gamma}^{\dagger}_{P\,k}(t)\hat{\gamma}_{P\,k}(t)\rangle_t$ is a constant; it is enough to write each k-component of the state in the form Eq. (3.10) and then use the properties $\hat{\gamma}_{P\,k}(t)\left|\phi^-_k(t)\right\rangle = 0$ and $\left|\phi^+_k(t)\right\rangle = \hat{\gamma}^{\dagger}_{P\,k}(t)\left|\phi^-_k(t)\right\rangle$.

non-integrable systems. In this section we show, for the quantum Ising chain in transverse field, that translational invariance and related factorizability in decoupled 2×2 problems are not crucial for the relaxation to the Floquet diagonal ensemble: as usual, the important point is the "bulk" of the Floquet spectrum being a continuum. In doing so, we will have the opportunity of replying to some criticism and deceptive citations addressed to our work [108, 109]. The claim of these authors, indeed, is that convergence to the Floquet diagonal ensemble follows from decoupling, and even applying a time-dependent change of basis to the system we would destroy it. We will show that it is not so by considering a Quantum Ising chain in a transverse field without translational invariance: this is a quadratic Fermionic model but its dynamics under a driving cannot be reduced to an assembly of decoupled 2-level systems. In the next Subsection we will discuss briefly the dynamics of this model to set the notation, help the reader to understand our numerical analysis and the reason why there is no decoupling. Then, in Subsection 3.3.2 we will move to discuss how the Floquet theory applies to this system, giving an explicit form of the single and many-particle Floquet states and quasi-energies. Finally, in Subsection 3.3.3, we will show numerically, for a specific example, how the relation among relaxation to the periodic Floquet-diagonal ensemble and continuity of the single-particle Floquet spectrum works in the non-uniform Ising chain.

3.3.1   The dynamics of the non-uniform Quantum Ising Model

In this subsection we make a summary on the diagonalization and the dynamics of the system when there is no translational invariance; the interested reader can find details of the calculations in Refs. [122, 123] or in Appendix B. The main point is that the Hamiltonian Eq. (3.1) (through the Jordan-Wigner transformation Eq. (B.1)) can be reduced to a quadratic fermion form expressed in terms of fermionic operators $\hat{c}_j$ localized on sites j (see Eq. (B.2)). If $\hat{\mathbf{c}}$ is a vector collecting these L operators we can write

$$\hat{H}(t) = \begin{pmatrix} \hat{\mathbf{c}}^\dagger & \hat{\mathbf{c}} \end{pmatrix} \mathbb{H}(t) \begin{pmatrix} \hat{\mathbf{c}} \\ \hat{\mathbf{c}}^\dagger \end{pmatrix} \tag{3.21}$$

where $\mathbb{H}(t)$ is a $2L \times 2L$ Hermitian matrix. We show in Appendix B that both the many-body instantaneous ground state of the system $|\text{GS}\rangle_t$ and the solution of the Schrödinger equation $i\hbar\partial_t |\Psi(t)\rangle = \hat{H}(t) |\Psi(t)\rangle$ with $|\Psi(0)\rangle = |\text{GS}\rangle_0$ are Gaussian states of the form

$$|\Phi\rangle = \sqrt{|\det[\mathbf{U}]|}\, e^{\frac{1}{2}(\hat{\mathbf{c}}^\dagger)^{\text{T}} \cdot \mathbf{Z} \cdot (\hat{\mathbf{c}}^\dagger)}|0\rangle \quad \text{where} \quad \mathbf{Z} \equiv -(\mathbf{U}^\dagger)^{-1} \cdot \mathbf{V}^\dagger; \tag{3.22}$$

where $\mathbf{U}$ and $\mathbf{V}$ are $L \times L$ matrices which, like Japanese robots, join to compose a $2L \times 2L$ unitary matrix

$$\mathbb{U} = \begin{pmatrix} \mathbf{U} & \mathbf{V}^* \\ \mathbf{V} & \mathbf{U}^* \end{pmatrix}.$$

If we take $|\Phi\rangle = |\text{GS}\rangle_t$, the ground state at time t, we need to choose the matrix $\mathbb{U} = \mathbb{U}_t$ as the one which diagonalizes the matrix $\mathbb{H}(t)$

$$\mathbb{U}_t^\dagger \cdot \mathbb{H}(t) \cdot \mathbb{U}_t = \mathbb{E}_D(t) \ , \qquad (3.23)$$

with $\mathbb{E}_D(t) = \text{diag}\,(\epsilon_\mu(t), -\epsilon_\mu(t))$. The L positive eigenvalues $\epsilon_\mu(t)$ give the energies of the elementary excitations above the ground state at time t. Instead, if we take $|\Phi\rangle = |\Psi(t)\rangle$, a solution of the Schrödinger equation, the matrix $\mathbb{U} = \mathbb{U}(t)$ we have to consider must obey the Bogoliubov-de Gennes (BdG) equations:

$$i\hbar\frac{d}{dt}\mathbb{U}(t) = 2\mathbb{H}(t) \cdot \mathbb{U}(t)\,. \qquad (3.24)$$

If we take as initial state the ground state, the initial conditions are given by $\mathbb{U}(0) = \mathbb{U}_0$ where $\mathbb{U}_0$ diagonalizes $\mathbb{H}(0)$. The BdG equations are a system of $2L \times 2L$ Schrödinger-like first order linear differential equations; by solving it we know everything about the 2^L-dimensional many-body state of the system. In this way, for instance, we obtain the quantum expectation values of all many-body observables. Indeed, the state of the system is Gaussian at all times, therefore Wick's theorem [113] applies and each expectation value can be written as a sum of products of the single-particle Green functions $G_{ij}(t) = \langle \hat{c}_i^\dagger \hat{c}_j \rangle_t$ and $F_{ij}(t) = \langle \hat{c}_i \hat{c}_j \rangle_t$. In terms of the components $\mathbf{U}(t)$ and $\mathbf{V}(t)$ of the matrix $\mathbb{U}(t)$ they can be written as

$$\begin{aligned}
G_{ij}(t) &= \left[\mathbf{V}(t) \cdot \mathbf{V}^\dagger(t)\right]_{ij} \\
F_{ij}(t) &= \left[\mathbf{U}(t) \cdot \mathbf{V}^\dagger(t)\right]_{ij} \ .
\end{aligned} \qquad (3.25)$$

Therefore, thanks to the Gaussian form of the state, both the statics and the dynamics of the system are reduced to the statics and the dynamics of pairs of elementary excitations, given respectively by Eqs. (3.23) and (3.24). This is a great advantage: although the Hilbert space is 2^L dimensional, the dynamics is given by the solution of a system of $2L \times 2L$ first order differential equations which can be easily implemented numerically. By exploiting the block form of the matrix $\mathbb{U}(t)$ we can further restrict to a system of $2L \times L$ equations. Nevertheless, we cannot map the problem to independent 2×2 blocks as in the translationally invariant case. Indeed, although the state of the system can be written in a factorized BCS form like in Eq. (3.7), the basis in which this can be done is time-dependent and in general different from the time-dependent basis in which the Hamiltonian is block-diagonal (we show this in some detail in Appendix B). Physically, in the non-uniform generic case, the subspaces corresponding to elementary excitations change in time; the dynamics mixes pairs of different excitations and creates superpositions of them; in this way, any 2×2 factorization is destroyed. In the uniform case, on the contrary, those subspaces are constant — being imposed by the

k-space structure — and the dynamics can at most create superpositions of the vacuum and a pair of excitations with some k, but the different k remain independent. The strong constraint of translational symmetry forbids mixing of excitations with different values of k.

3.3.2 Single and many particle Floquet dynamics

Consider a uniform value of the longitudinal couplings $J_j = J = 1$, but a site dependent time-periodic field $h_j(t) = h_j(t+\tau)$ ($\tau = 2\pi/\omega_0$): the Hamiltonian Eq. (3.1) is τ-periodic and so is the $2L \times 2L$ matrix $\mathbb{H}(t)$ appearing in its fermionized version Eq. (3.21) (see also Eq. (B.2)). This matrix is the effective Hamiltonian driving the evolution in the Bogoliubov-de Gennes equations Eq. (3.24). Indeed their structure is that of $2L$ copies (one for each column) with different initial data of the same Schrödinger-type equation in a $2L$-dimensional Hilbert space with the periodic Hamiltonian $\mathbb{H}(t)$. We can apply to this equation the Floquet theory discussed in Chapter 2. Indeed, we introduce the time evolution operator $\mathbb{U}_\mathbf{1}(t,0)$ associated to this unitary evolution; it is the solution of the Bogoliubov-de Gennes equations Eq. (3.24) when we take as initial condition the $2L \times 2L$ identity matrix $\mathbf{1}_{2L}$. It is a very useful object, if we choose generic initial conditions $\mathbb{U}_0$, we can exploit it to construct the solution to Eq. (3.24) as

$$\mathbb{U}(t) = \mathbb{U}_\mathbf{1}(t,0)\mathbb{U}_0 \ .$$

Moreover, thanks to Eq. (2.11), the knowledge of $\mathbb{U}_\mathbf{1}(t,0)$ on the first period of the driving allows to reconstruct it at all subsequent times and we have all the information on the dynamics.

In particular, by diagonalizing $\mathbb{U}_\mathbf{1}(\tau,0)$, we can find explicitly a basis of $2L$ Floquet solutions of the Bogoliubov-de Gennes equations. These solutions are $2L$-tall time-dependent column vectors; L of them are

$$\mathbf{w}_{F\alpha}(t) = e^{-i\mu_\alpha t/\hbar} \begin{pmatrix} \mathbf{u}_{P\alpha}(t) \\ \mathbf{v}_{P\alpha}(t) \end{pmatrix} \quad \text{for } \alpha = 1 \cdots L \ , \qquad (3.26)$$

with

$$\begin{cases} \mathbf{u}_{P\alpha}(t+\tau) = \mathbf{u}_{P\alpha}(t) \\ \mathbf{v}_{P\alpha}(t+\tau) = \mathbf{v}_{P\alpha}(t) \end{cases} \ . \qquad (3.27)$$

To find the remaining L, we exploit the particle-hole symmetry embodied in the block form of $\mathbb{H}(t)$ (see Eq. (B.4)): if $\mathbf{w}_{F\alpha}(t)$ is a solution, so is $\widetilde{\mathbf{w}}_{F\alpha}(t) = e^{i\mu_\alpha t/\hbar} \begin{pmatrix} \mathbf{v}_{P\alpha}^*(t) & \mathbf{u}_{P\alpha}^*(t) \end{pmatrix}^T$. These objects can be interpreted as single-particle Floquet states, similarly to those in Eq. (3.10). We can collect all these single-particle quasi-energies μ_α into a diagonal matrix $\boldsymbol{\mu} = \text{diag}(\mu_\alpha)$, and the various τ-periodic column vectors into $L \times L$ matrices $\mathbf{U}_P(t)$ and $\mathbf{V}_P(t)$, obtaining a very pleasant-looking solution of the BdG

equations Eq. (3.24)

$$\mathbb{U}_F(t) = \left(\begin{array}{c|c} \mathbf{U}_F(t) & \mathbf{V}_F^*(t) \\ \hline \mathbf{V}_F(t) & \mathbf{U}_F^*(t) \end{array} \right) = \left(\begin{array}{c|c} \mathbf{U}_P(t) \cdot \mathrm{e}^{-i\boldsymbol{\mu}t/\hbar} & \mathbf{V}_P^*(t) \cdot \mathrm{e}^{i\boldsymbol{\mu}t/\hbar} \\ \hline \mathbf{V}_P(t) \cdot \mathrm{e}^{-i\boldsymbol{\mu}t/\hbar} & \mathbf{U}_P^*(t) \cdot \mathrm{e}^{i\boldsymbol{\mu}t/\hbar} \end{array} \right) .$$

(3.28)

This is an important object: in terms of it we can construct the Many-Body Floquet states of the Hamiltonian Eq. (3.21). They are Gaussian states of the form Eq. (3.22), as far as we know, we are the first to find their form. The state with vanishing Floquet quasi-energy is

$$|\Psi_0(t)\rangle_F = \sqrt{|\det[\mathbf{U}_F(t)]|}\, \mathrm{e}^{\frac{1}{2}(\hat{\mathbf{c}}^\dagger)^T \cdot \mathbf{Z}_F(t) \cdot (\hat{\mathbf{c}}^\dagger)}|0\rangle \quad \text{where}$$

$$\mathbf{Z}_F(t) \equiv -(\mathbf{U}_F^\dagger(t))^{-1} \cdot \mathbf{V}_F^\dagger(t) ;$$

(3.29)

indeed it is not difficult to show that this state is periodic by using the very definition Eq. (3.28). To make the other Floquet states, one constructs L Fermionic Bogoliubov operators $\hat{\gamma}_{F\alpha}(t)$ (we can find a similar formula in Eq (B.7))

$$\left(\begin{array}{c} \hat{\boldsymbol{\gamma}}_F(t) \\ \hat{\boldsymbol{\gamma}}_F^\dagger(t) \end{array} \right) = \mathbb{U}_F^\dagger(t) \cdot \left(\begin{array}{c} \hat{\mathbf{c}} \\ \hat{\mathbf{c}}^\dagger \end{array} \right) .$$

(3.30)

These operators enjoy the Floquet property $\hat{\gamma}_{F\alpha}(t+\tau) = \mathrm{e}^{i\mu_\alpha \tau}\hat{\gamma}_{F\alpha}(t)$ for all times. All the 2^L different many-body Floquet states can be obtained by applying an appropriate number of different $\hat{\gamma}_{F\alpha}^\dagger(t)$ operators to the state $|\Psi_0(t)\rangle_F$

$$|\Psi_{\boldsymbol{\alpha}}(t)\rangle_F = \prod_{j=1}^n \hat{\gamma}_{F\alpha_j}^\dagger(t)|\Psi_0(t)\rangle_F \quad \text{where} \quad n \leq L \quad \text{and} \quad \alpha_j \neq \alpha_i \quad \text{for} \quad j \neq i .$$

To find the corresponding periodic Floquet modes one defines some periodic operators $\hat{\gamma}_{P\alpha}^\dagger(t)$ such that $\hat{\gamma}_{F\alpha}^\dagger(t) = \mathrm{e}^{-i\mu_\alpha t}\hat{\gamma}_{P\alpha}^\dagger(t)$

$$\left(\begin{array}{c} \hat{\boldsymbol{\gamma}}_P(t) \\ \hat{\boldsymbol{\gamma}}_P^\dagger(t) \end{array} \right) = \left(\begin{array}{c|c} \mathbf{U}_P(t) & \mathbf{V}_P^*(t) \\ \hline \mathbf{V}_P(t) & \mathbf{U}_P^*(t) \end{array} \right) \cdot \left(\begin{array}{c} \hat{\mathbf{c}} \\ \hat{\mathbf{c}}^\dagger \end{array} \right) ;$$

(3.31)

similarly to the Floquet states, the Floquet modes are

$$|\Phi_{\boldsymbol{\alpha}}(t)\rangle_P = \prod_{j=1}^n \hat{\gamma}_{P\alpha_j}^\dagger(t)|\Psi_0(t)\rangle_F \quad \text{where} \quad n \leq L \quad \text{and} \quad \alpha_j \neq \alpha_i \quad \text{for} \quad j \neq i .$$

(3.32)

We can easily see that the many body Floquet quasi-energies are sums of the single particle quasi-energies μ_α. Marking them with an over-line as in

Sec. 2.2 we have[3]

$$\overline{\mu}_{\boldsymbol{\alpha}} = \sum_{j=1}^{n} \mu_{\alpha_j} \quad \text{where} \quad n \leq L \quad \text{and} \quad \alpha_j \neq \alpha_i \quad \text{for} \quad j \neq i \,.$$

The matrix in Eq. (3.28), moreover, allows us to write explicitly a generic solution of the Bogoliubov-de Gennes equations in terms of single particle Floquet modes and quasienergies

$$\mathbb{U}(t) = \mathbb{U}_F(t) \cdot \mathbb{R} \tag{3.33}$$

where we have defined $\mathbb{R} \equiv \mathbb{U}_F^\dagger(0)\mathbb{U}(0)$ with the block decomposition $\mathbb{R} = \left(\begin{array}{c|c} \mathbf{R} & \mathbf{S}^* \\ \hline \mathbf{S} & \mathbf{R}^* \end{array} \right)$. This implies

$$\mathbb{U}_{\mathbf{1}}(t,0) = \mathbb{U}_F(t)\mathbb{U}_F^\dagger(0) \,;$$

exploiting the unitarity of $\mathbb{U}_F(t)$ we can verify explicitly that $\mathbb{U}_{\mathbf{1}}(n\tau,0) = [\mathbb{U}_{\mathbf{1}}(\tau,0)]^n$.

3.3.3 Broken translational invariance and relaxation to the Floquet-diagonal ensemble

Thanks to the analysis we have just done, we can write, for any operator quadratic in the Fermionic operators $\hat{c}_j$, the Floquet-diagonal component and the off-diagonal part (see Eq. (2.13)) in terms of the single-particle Floquet modes and quasienergies. This applies to observables, like the energy or the tranverse magnetization, and to other objects like the single-particle Green functions Eq. (3.25). In the latter case the Floquet-diagonal component is explicitly

$$
\begin{aligned}
G_{ij}^{\text{diag}}(t) &= R_{\alpha i}^* V_{P\nu\alpha}(t) V_{P\nu\alpha}^*(t) R_{\alpha j} + S_{\alpha i}^* U_{P\nu\alpha}(t) U_{P\nu\alpha}^*(t) S_{\alpha j} \\
F_{ij}^{\text{diag}}(t) &= R_{\alpha i}^* U_{P\nu\alpha}(t) V_{P\nu\alpha}^*(t) R_{\alpha j} + S_{\alpha i}^* V_{P\nu\alpha}(t) U_{P\nu\alpha}^*(t) S_{\alpha j}
\end{aligned}
\tag{3.34}
$$

and the off-diagonal component is a much more involved formula we report in Appendix B. Although the Green functions are expectations of non-Hermitian operators, they are very important. The state of the system is indeed Gaussian and we can apply the Wick's theorem [113] to any observable $\hat{\mathcal{O}}$ which is many-particle in the Fermionic operators [4]; in this way its expectation value can be written as the sum of products of single-particle

---

[3] All these considerations, of course, apply also to the translationally invariant case; here the Floquet Fermionic operators are $\hat{\gamma}_{Fk}(t) = \mathrm{e}^{i\mu_k t}\hat{\gamma}_{Pk}(t)$, where $\hat{\gamma}_{Pk}(t)$ are defined in Eq. (3.18).

[4] One important example are the spin correlators [112] $\langle \hat{\sigma}_i^z \hat{\sigma}_j^z \rangle_t$.

Green functions. Indeed, it depends in a definite way on the various Green functions

$$\langle \hat{\mathcal{O}} \rangle_t = \mathcal{F}_{\mathcal{O}} \left(\{ G_{ij}(t), F_{ij}(t) \}_{i,j=1,\ldots,L} \right) . \qquad (3.35)$$

If all the Green functions relax to the single-particle Floquet diagonal ensemble, then the expectations of all the many-particle observables $\hat{\mathcal{O}}$ relax to an asymptotically periodic condition which, by means of Eq. (3.34), depends on the relaxed Green's functions as

$$\langle \hat{\mathcal{O}} \rangle_t \xrightarrow{t \to \infty} \mathcal{F}_{\mathcal{O}} \left(\left\{ G_{ij}^{\text{diag}}(t), F_{ij}^{\text{diag}}(t) \right\}_{i,j=1,\ldots,L} \right) .$$

By necessity, this asymptotic limit has to coincide with the many body Floquet diagonal ensemble average [5]

$$\langle \mathcal{O} \rangle_t^{\text{diag}} = \sum_{\boldsymbol{\alpha}} |_0 \langle \text{GS} | \Phi_{\boldsymbol{\alpha}}(0) \rangle |^2 \, _P \langle \Phi_{\boldsymbol{\alpha}}(t) | \hat{\mathcal{O}} | \Phi_{\boldsymbol{\alpha}}(t) \rangle_P \, ,$$

where the many-body Floquet modes are given by Eq. (3.32). This discussion shows us that, for the relaxation of the observables in this integrable model, only the continuity of the single particle Floquet spectrum matters. Moreover, observables relax to the diagonal Floquet ensemble in the thermodynamic limit if this happens for the Green functions. Therefore, to explore relaxation, we can restrict to inquire if the time-fluctuations for finite L $\delta |G_{ij}|_{\text{strobo}}$ and $\delta |F_{ij}|_{\text{strobo}}$ (see Eq. (2.19)) scale to zero for increasing L. Matter of fact, the formulae are extremely awful, therefore we limit ourselves to show to the reader, for different values of L, the time dependence of an operator whose expectation is strictly related to the Green function $G_{jj}(t)$, the transverse magnetization on the site j. It is defined as $\hat{m}_j = \hat{\sigma}_j^x$ and, after the Jordan-Wigner transformation, it acquires the form

$$\hat{m}_j = 2 \hat{c}_j^\dagger \hat{c}_j - 1 . \qquad (3.36)$$

We break translational invariance by means of a Gaussian inhomogeneity in the driving field localized on the centre of the chain

$$h_j(t) = 1 + h_G \, \mathrm{e}^{-(j-j_c)^2/2l^2} + A \cos(\omega_0 t) .$$

Thanks to periodic boundary conditions in the spins, this mimics confinement in experiments. The length l on which the inhomogeneity is localized remains finite in the thermodynamic limit. The inhomogeneity gives rise to some discrete levels in the single-particle Floquet spectrum whose number remains finite in the thermodynamic limit; on the contrary, the number of the levels in the continuum (corresponding to extended Floquet states) scales

---

[5]In principle, one could directly show that the two formulae agree using the explicit expression Eq. (3.32), but it is not an easy computation.

with the size L of the system; we can see this in the left panel of Fig. 3.5. The discrete levels correspond to single-particle Floquet modes localized inside the inhomogeneity, while those in the continuum correspond to modes extended to the whole chain. This property allows us to find single-particle operators and Green functions (for instance, of the form Eq. (3.36)) coupling mainly to modes in one part of the spectrum or in the other; this gives rise to markedly different behaviours of the fluctuations around the Floquet diagonal ensemble (see discussion in Sec. 2.3). Thanks to Eq. (3.35), we will later generalize our discussion to many-particle objects.

Whenever an operator couples mainly to the continuous part of the single-particle Floquet spectrum, its expectation relaxes to the Floquet diagonal ensemble in the thermodynamic limit; indeed the fluctuating terms coming from the finite number of discrete single-particle Floquet levels give a vanishing contribution. This happens, for instance, for all the $\hat{m}_j$ centred on sites j outside the inhomogeneity in $L/2$ ($|j - L/2| \gg l$, here the discrete single-particle modes localized in the inhomogeneity have a vanishingly small amplitude). We can see one instance of that in Fig. 3.6, where we plot the stroboscopic magnetization $m_j(n\tau)$ on the site $j = 3L/4$. We can see that the fluctuations around the Floquet-diagonal value tend to vanish when L increases, the observable converges to the asymptotic value before a finite-size revival sets up at a time $\sim L$; for $L \to \infty$ we would see a perfect convergence lasting for an infinite time. We could see the same behaviour for all the single-particle operators and Green functions involving only $\hat{c}_j$ and $\hat{c}_i$ outside the inhomogeneity (still $|j - L/2| \gg l$, $|i - L/2| \gg l$).

Operators localized inside the inhomogeneity, instead, couple mainly to Floquet states in the discrete part of the spectrum (as we have noticed, these states are not extended but localized in the inhomogeneity). The Riemann-Lebesgue lemma does not apply and we can see fluctuations persisting in the thermodynamic limit. We show an instance of that in the lower right panel of Fig. 3.5, where we consider the stroboscopic value of the magnetization in the central site of the system $m_{L/2}(n\tau)$. It never relaxes to a stationary value, however large we take L. This result of course is valid for all single particle operators and Green functions involving only $\hat{c}_i$ and $\hat{c}_j$ inside the inhomogeneity.

This discussion and Eq. (3.35) imply that generic many-particle observables $\hat{O}$ relax to the Floquet-diagonal ensemble if we are in the thermodynamic limit and we consider operators involving mainly $\hat{c}_j$ centred on sites outside the inhomogeneity. All the extensive observables fall in this class and only a minority of operators, involving mainly $\hat{c}_j$ centred on the central site, do not become periodic after a transient. An instance of convergence of an extensive (single-particle) operator is given in the upper-right panel of Fig. 3.5, where we plot the stroboscopic value of the average transverse magnetization $\hat{m} = \frac{1}{L} \sum_{j=1}^{L} \hat{\sigma}_j^x$ for different lengths. Indeed, one can see by
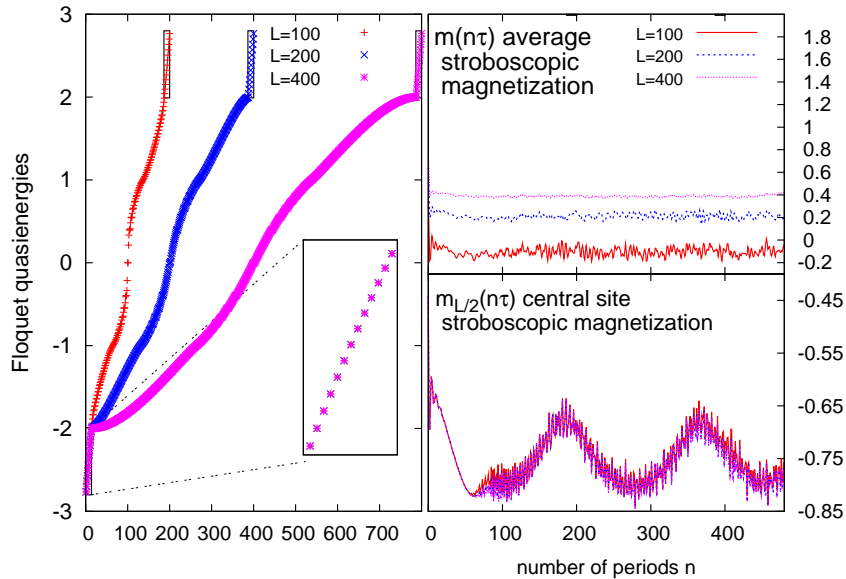
Figure 3.5: (Left panel) The single-particle Floquet spectrum for an Ising chain with a Gaussian inhomogeneity with $l = 20$, $h_G = 2.8$, $\omega_0 = 10$, $A = 1$ and different values of L. Notice a finite, L-independent number of discrete quasi-energies. (Upper right panel) The average transverse magnetization $m(t)$ probed at $t = n\tau$, showing fluctuations that decrease for increasing L. (Lower right panel) The transverse magnetization at the centre of the inhomogeneity, $m_{j_c}(t = n\tau)$, whose fluctuations persist for all L.

inspection that fluctuations around the asymptotic limit get smaller when the chain is made longer.

3.4 Work distribution and dynamical fidelity

Many recent works have considered the work probability distribution in classical and quantum systems [81, 84, 86, 87, 88, 89, 83]. Applying many times the same non-equilibrium perturbation to a system, we can see that the performed work changes in any realization of the protocol because of quantum or thermal fluctuations. Very well known are the works (see Ref. [83] for a review) stemming from the seminal paper by Jarzynski [82] which show how the properties of the work statistics in a generic non-equilibrium protocol are related to the change of free-energy in the corresponding quasi-equilibrium thermodynamical process. The most important result in this class are the Jarzynski-Crooks relations [83]. They have been demonstrated originally for classical systems where only thermal fluctuations matter [82, 124]; then they have been extended to unitarily evolving quantum systems [125, 81, 126]
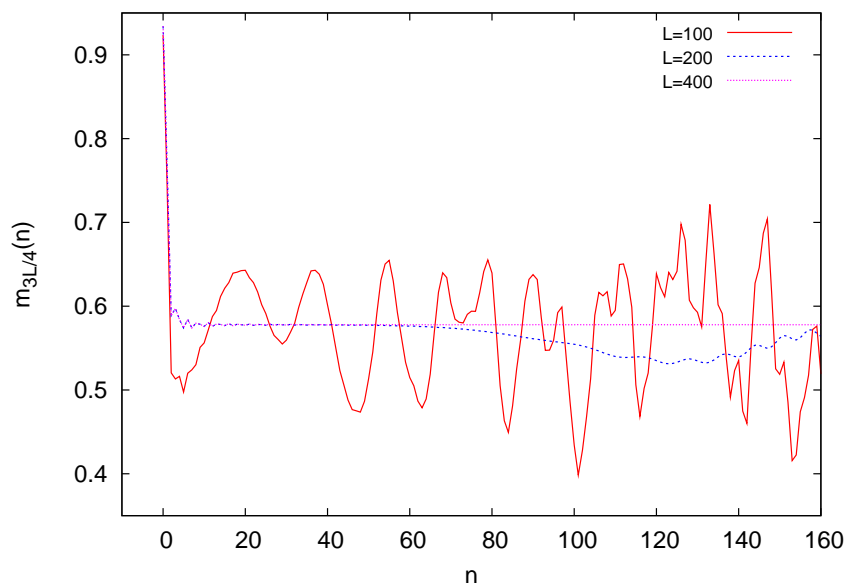
Figure 3.6: The stroboscopic value of the magnetization centred in a site far from the inhomogeneity $m_{3L/4}(t = n\tau)$. We can see that the fluctuations around the Floquet diagonal value decrease for larger L; indeed the observable always tends to converge to this value, before a finite size revival sets up at a time which is longer as L is larger.

where work fluctuations arise from quantum fluctuations in the energy provided to the system. Recently, many works have appeared concerning the work statistics in many body quantum systems where the properties of the work probability distribution are related to the presence of quantum phase transitions [86, 87, 88, 89]. Moreover, for small W, the work distribution $P(W)$ seems to assume a power-law behaviour independent of the precise details of the system and the protocol [84, 86, 87, 88, 89]. This probability distribution is an object of experimental interest, thanks to the techniques which allow to detect the statistics of quantum fluctuations of observables [10, 80]. Here we consider the properties of the work distribution for a periodically-driven quantum Ising chain in transverse field. We assume to start in the ground state of the initial Hamiltonian. We measure the work performed on the system after it has evolved for a time t; the probability distribution of the work fluctuations is [81, 126, 83]

$$P_t(W) = \sum_m \delta(W - (E_m^t - E_{\mathrm{GS}}(0))) \left| \langle \Psi_m^t | \Psi(t) \rangle \right|^2. \tag{3.37}$$

Here, $E_{\mathrm{GS}}(0)$ is the energy of the initial ground state, E_m^t are the eigenenergies of the final Hamiltonian and $\left| \Psi_m^t \right\rangle$ the corresponding eigenstates. We apply a periodic driving and probe the system stroboscopically at intervals of an integer number of periods; in this way eigenstates and eigenvalues of the initial and final Hamiltonian coincide and the minimum work that can be performed is $W = 0$. We start our discussion just considering the weight of the δ function in $W = 0$ for the cyclic protocol; this object is called dynamical fidelity[6]. It is the squared overlap of the state of the system at the stroboscopic time $t = n\tau$ with the initial state (coinciding in our case with the initial ground state)

$$\mathcal{F}(t) = |\langle \Psi_0 | \Psi(t) \rangle|^2 = \left| \langle \Psi_{\mathrm{GS}}^0 | \hat{U}(t,0) | \Psi_{\mathrm{GS}}^0 \rangle \right|^2. \tag{3.38}$$

This object is also important in itself. Its asymptotic behaviour in time gives us information about the localization properties of a generic initial state $|\Psi_0\rangle$ in the Hilbert space [127]: if it is localized the squared overlap with its value $|\Psi(t)\rangle$ at time t will remain finite, instead it will vanish. In case of sudden quench (periodic driving) the two distinct behaviours are strictly related to the properties of the energy (Floquet) spectrum: pure point in the first case, continuous in the second [128]. Moreover, quantities strictly related to the fidelity are used to detect quantum phase transitions [129, 130] and quantum entanglement [131] and are useful measures in quantum information science [132].

We specialize our discussion to the case of the uniformly driven quantum Ising chain discussed in detail in Secs. 3.1 and 3.2. The Hamiltonian is the

---

[6]We have published the results we are going to present on the dynamical fidelity in the periodically driven quantum Ising chain in Ref. [90].

translationally-invariant version of Eq. (3.1) and we choose to drive the system around the quantum critical point with a field given by Eq. (3.11) (fixing $A = 1$, $\varphi_0 = 0$). We expect the fidelity Eq. (3.38) to vanish in the thermodynamic limit. Indeed, we can see that the modulus square product of the states Eqs. (3.5) and (3.7) is given by

$$
\mathcal{F}(n\tau) = \prod_{k>0}^{\text{ABC}} \mathcal{F}_k(n\tau) \quad \text{where} \quad \mathcal{F}_k(n\tau) = \left| u_{k\,0}^{0}{}^{*} u_k(n\tau) + v_{k\,0}^{0}{}^{*} v_k(n\tau) \right|^2 .
\tag{3.39}
$$

Unless the unlikely occurrence that the initial ground state coincides with a many-body Floquet state (and all the $u_{k\,0}^{0}$, $v_{k\,0}^{0}$ are components in the standard basis of single-particle Floquet states $\left|\phi_k^+(0)\right\rangle$, $\left|\phi_k^-(0)\right\rangle$), we find $\mathcal{F}_k(n\tau) < 1$. So the fidelity is the product of $L/2$ less-than-one factors and in the thermodynamic limit ($L \to \infty$), it vanishes exponentially with L. Nevertheless, for finite L, although exponentially small in L, this object is a finite quantity of experimental interest. We are going to show that, before finite-size revivals set up, it tends towards a steady regime where its value does not change from a cycle of the driving to the next. By means of Eqs. (3.7) and (3.5) and using the Floquet expansion Eq. (3.10), we can find the fidelity after n complete cycles of the driving field

$$
\mathcal{F}(n\tau) = e^{\sum_{k>0} \log |b_k(n\tau)|^2} ,
\tag{3.40}
$$

where $b_k(n\tau) = |r_k^+|^2 e^{-i\mu_k n\tau} + |r_k^-|^2 e^{i\mu_k n\tau}$. If L is large, we can approximate the sum over k into an integral, easily establishing that $\mathcal{F}(n\tau) \sim e^{-Lg_n}$; the quantity

$$
g_n(\omega_0) = - \int_0^\pi \frac{dk}{2\pi} \log |b_k(n\tau)|^2 .
\tag{3.41}
$$

is non-negative and well defined for $L \to \infty$. Defining $q_k \equiv 2|r_k^+|^2|r_k^-|^2/(|r_k^+|^4 + |r_k^-|^4) \in [0,1]$ we can recast this formula as

$$
g_n(\omega_0) = - \int_0^\pi \frac{dk}{2\pi} \log \frac{1 + q_k \cos(2\mu_k n\tau)}{1 + q_k} .
\tag{3.42}
$$

Whenever the frequency does not match any unperturbed resonance of the system ($\omega_0 > 4$ in the present case), then $q_k < 1$ for all k. Therefore, we can expand the argument of the logarithm and then apply the Riemann-Lebesgue lemma to all the oscillating terms. Defining $g_{\mathrm{d}}(\omega_0) \equiv \int_0^\pi \frac{dk}{2\pi} \log(1 +$

q_k) we find

$$
\begin{aligned}
g_\infty(\omega_0) \equiv \lim_{n\to\infty} g_n(\omega_0) &= g_{\mathrm{d}}(\omega_0) + \sum_{p=1}^{\infty} \frac{(2p-1)!!}{2p(2p)!!} \int_0^\pi \frac{dk}{2\pi} q_k^{2p} \\
&= g_{\mathrm{d}}(\omega_0) + \int_0^\pi \frac{dk}{2\pi} \log \frac{2}{1+\sqrt{1-q_k^2}} \\
&= \int_0^\pi \frac{dk}{2\pi} \log \frac{2(1+q_k)}{1+\sqrt{1-q_k^2}} \ .
\end{aligned}
\tag{3.43}
$$

We can see in Fig. 3.7 that our formula works well also when $\omega_0 < 4$ (for a precise mathematical justification of this fact, see Appendix C): here we plot the asymptotic g_∞ vs ω_0 comparing it with its finite n counterparts for many values of n. (As done in Sec. 3.2, we obtain Floquet states and time evolution by means of the numerical solution of Bogoliubov-de Gennes equations Eq. (3.8) and the methods explained in Chapt. 2.) In Fig. 3.7 we can clearly see that the stroboscopic fidelity tends to a steady value after a transient; this fact is rigorously true only in the limit $L \to \infty$.

We can see in $g_\infty(\omega_0)$ features similar to those we have noticed in the periodic-steady-regime asymptotic stroboscopic work w_∞ (lower panel of Fig. 3.3) [7]: dips at the zeros of $J_0(2/\omega_0)$, peaks at $\omega_0 = 4/p$ and an high frequency plateau. At the zeros of $J_0(2/\omega_0)$ the rate $g_\infty(\omega_0)$ shows minima as a consequence of Coherent Destruction of Tunneling [120] but is nevertheless non-vanishing. We can see that the rate of exponential decay with L, $g_\infty(\omega_0)$, is never vanishing. Therefore, whatever we take the frequency ω_0, the fidelity converges to a value $\mathcal{F}_\infty = 0$ in the thermodynamic limit; matter of fact in this limit it is always $\mathcal{F}(n\tau) = 0$ but at $n = 0$. By means of Eq. (3.39), we can notice that the only other possibility in the thermodynamic limit could be $\mathcal{F}_\infty = 1$ (corresponding to a vanishing $g_\infty(\omega_0)$) which would mean that the state comes back to its initial value. We can see indeed that this never happens: this fact implies that the ground state never coincides with a many-body Floquet state. We can see, therefore, a convergence to a periodic steady regime for the observables but not for the state. The Floquet diagonal ensemble density matrix Eq. (2.14) is indeed only a convenient way to express the expectations of the observables in the asymptotic regime.

In this context, convergence to a steady regime of the stroboscopic fidelity may seem not interesting: From one side the fidelity is exponentially small in L ($\mathcal{F}(n\tau) \sim \mathrm{e}^{-Lg_n}$) and always vanishing (but at the initial time) in the thermodynamic limit, from the other, only in this limit convergence

---

[7]This quantity is $1/L \times$ the first moment of the asymptotic work probability distribution (see Eq. (3.51)), while g_∞ is related to the value in $W = 0$ of the same distribution, so (with hindsight bias) we are not surprised to see this similarity.
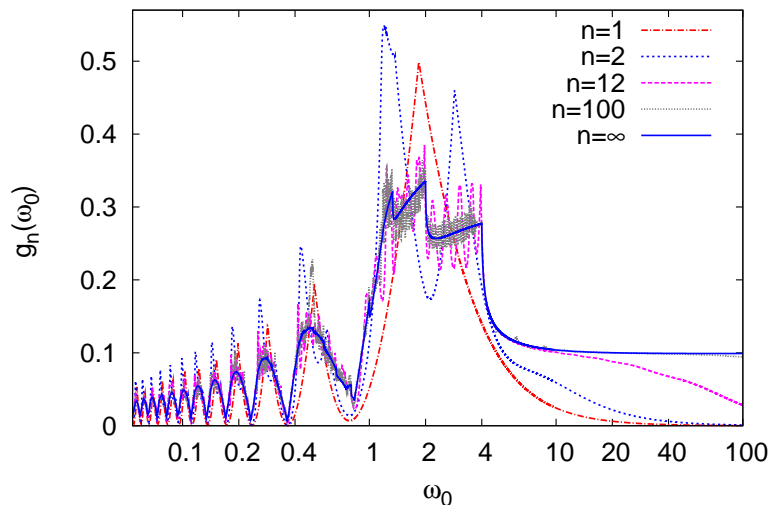
Figure 3.7: $g_n = -[\log \mathcal{F}(n\tau)]/L$, minus the logarithm of the fidelity per-site, as a function of the frequency ω_0 of the driving field $h(t) = 1 + \cos(\omega_0 t)$ for $n = 1, 2, 12, 100$. The value of g_∞, Eq. (3.43), is also shown. Notice how, for any n finite, $g_n(\omega_0) \to 0$ for $\omega_0 \to \infty$ (for $n = 100$ such a rise towards 0 is visible right before $\omega_0 \sim 100$).

happens rigorously. Nevertheless, the steady-regime fidelity is an object of experimental interest in chains with a finite L. Indeed, as we can see in Fig. 3.7, the fluctuations at large but finite n around the steady value are very small, even for low frequencies where the finite-size revival has already set up (data refer to $L = 1000$ and the finite size revival sets up at $n \sim L\omega_0/(2\pi)$. The only point is to keep coherence for many periods, but this is not an issue in cold atom experiments [1].

Moreover, we have to notice an important point: the GGE ensemble Eq. (3.19) miserably fails in predicting the asymptotic stroboscopic value of the fidelity. As we show in Ref. [90] (where we define the GGE ensemble as "decohered density matrix") it predicts for the asymptotic value of $g_n(\omega_0)$

$$g_{\text{GGE}}(\omega_0) = g_{\text{d}}(\omega_0) = \int_0^\pi \frac{dk}{2\pi} \log(1 + q_k),$$

which (as we can see in Eq. (3.43)) is systematically larger than the exact asymptotic value Eq. (3.43). Therefore we see that the GGE misses important quantum correlations which are still existing in the system but cannot be seen in the local observables because of dephasing: the dynamical fidelity makes transparent this hidden phase information.

44

3.4.1   The work distribution and its characteristic function

Actually, we are able to discuss not only the properties of the peak at $W = 0$, but the whole work-distribution function of our system. To do that, we introduce the characteristic function [126, 81] of the distribution as its Fourier transform

$$G_t(u) = \int_{-\infty}^{+\infty} dW\, \mathrm{e}^{iuW} P_t(W)\,. \qquad (3.44)$$

This gives us all the information on the distribution, because all its moments $\mu_n(t) = \int_{-\infty}^{+\infty} dW\, W^n P_t(W)$ can be obtained as

$$\mu_n(t) = (-i)^n\, \partial_u^n G_t(u)\big|_{u=0}\,.$$

If we substitute in Eq. (3.44) the expression for the work probability distribution [8] given by Eq. (3.37), we find [86] after few manipulations

$$G_t(u) = \langle \Psi(t)|\, \mathrm{e}^{-iu\widetilde{H}(t)}\, |\Psi(t)\rangle\,; \qquad (3.45)$$

here we shift the zero of the energy by defining the operator $\widetilde{H}(t) \equiv \hat{H}(t) - E_{\mathrm{GS}}(0)$. In what follows we will use, instead of the Fourier transform, the Laplace transform defined as $G_t(-is)$ with $s \geq 0$. Substituting in the integral Eq. (3.44) we see that this object is real and converges because $P(W)$ is vanishing below the threshold $E_0(t) - E_{\mathrm{GS}}(0)$. We move to consider the cumulant generating function defined as

$$\mathcal{G}_t(s) = \log G_t(-is)\,.$$

From it we can find all the cumulants of the distribution $P_t(W)$ [86] as $K_n(t) = (-1)^n\, \partial_s^n \mathcal{G}_t(s)\big|_{s=0}$. If we consider explicitly the case of the quantum Ising model and substitute in Eq. (3.45) the expressions Eq. (3.7) for the state and Eq. (3.2) for the Hamiltonian we find, for large L

$$\frac{\mathcal{G}_t(s)}{L} = \int_{-\infty}^{\infty} \frac{dk}{2\pi} \log\left[\langle \psi_k(t)|\, \mathrm{e}^{-s(\hat{H}_k(t)+\epsilon_k(0))}\, |\psi_k(t)\rangle \right] \qquad (3.46)$$

where $-\epsilon_k(0)$ is the ground state energy for the mode k at time 0 (Eq. (3.4)). As we have seen, for each mode k the Hilbert space is bidimensional, so we can expand the k-component of the Hamiltonian $\hat{H}_k(0)$ in the basis of its instantaneous eigenstates

$$\hat{H}_k(t) = \epsilon_k(t)\, \big|\psi_{k\,\mathrm{ex}}^t\big\rangle \big\langle \psi_{k\,\mathrm{ex}}^t\big| - \epsilon_k(t)\, \big|\psi_{k\,\mathrm{GS}}^t\big\rangle \big\langle \psi_{k\,\mathrm{GS}}^t\big|$$

where the eigenvalues $\pm\epsilon_k(t)$ are given by Eq. (3.4), $\big|\psi_{k\,\mathrm{GS}}^t\big\rangle$ is the k-component of the ground state Eq. (3.5) and the excited state is obtained by creating two

---

[8]we are taking as initial state of the evolution the initial ground state, but also more general cases can be considered [126, 81].

elementary excitations on top of this: $\left|\psi_{k\,\text{ex}}^t\right\rangle = \hat{\gamma}_k^\dagger(t)\hat{\gamma}_{-k}^\dagger(t)\left|\psi_{k\,\text{GS}}^t\right\rangle$ where the operators $\hat{\gamma}_k(t)$ are defined in Eq. (3.6). In this way it is easy to see that [86]

$$\frac{\mathcal{G}_t(s)}{L} = \int_{-\infty}^{\infty}\frac{\mathrm{d}k}{2\pi}\log\left[|a_k(t)|^2\mathrm{e}^{-s(\epsilon_k(t)+\epsilon_k(0))} + |b_k(t)|^2\mathrm{e}^{-s(-\epsilon_k(t)+\epsilon_k(0))}\right]$$

(3.47)

where we have defined the overlaps $a_k(t) = \left\langle\psi_{k\,\text{ex}}^t\,|\psi_k(t)\right\rangle$ and $b_k(t) = \left\langle\psi_{k\,\text{GS}}^t\,|\psi_k(t)\right\rangle$. As in the foregoing section, we specialize to the stroboscopic case where these amplitudes can be expressed quite easily in terms of Floquet states and quasi-energies. Indeed, if the system starts in the ground state, we have $b_k(n\tau) = |r_k^+|^2\mathrm{e}^{-i\mu_k n\tau} + |r_k^-|^2\mathrm{e}^{i\mu_k n\tau}$. Exploiting the normalization condition of the state $|\psi_k(t)\rangle$ expressed in the basis of the eigenstates $(|a_k(t)|^2 + |b_k(t)|^2 = 1)$, we easily find

$$\begin{aligned}|b_k(n\tau)|^2 &= |r_k^+|^4 + |r_k^-|^4 + 2|r_k^+|^2|r_k^-|^2\cos\left(2\mu_k n\tau\right)\\ |a_k(n\tau)|^2 &= 2|r_k^+|^2|r_k^-|^2\sin\left(2\mu_k n\tau\right).\end{aligned}$$

(3.48)

Substituting in Eq. (3.47) and using the definition $q_k \equiv 2|r_k^+|^2|r_k^-|^2/(|r_k^+|^4 + |r_k^-|^4)$ we find

$$\frac{\mathcal{G}_{n\tau}(s)}{L} = \int_0^\pi\frac{\mathrm{d}k}{2\pi}\log\left[1 - 2\frac{q_k}{1+q_k}\left(1-\mathrm{e}^{-2s\epsilon_k(0)}\right)\sin^2\left(\mu_k n\tau\right)\right].$$

(3.49)

Quite interestingly, we can check that $\lim_{s\to\infty}\frac{\mathcal{G}_{n\tau}(s)}{L} = -g_{n\tau}$ where $g_{n\tau}$ is minus the logarithm of the fidelity per site given in Eq. (3.41). This is a general result related to the fact that, in the stroboscopic case, $\lim_{s\to\infty}G_t(-is)$ is just the dynamical fidelity. Whenever $s < \infty$, we can apply an argument [9] (reported in Appendix C) strictly analogous to the one leading to Eq. (3.43) and find that this object converges for large n to a steady state value

$$\frac{\mathcal{G}_\infty(s)}{L} \equiv \lim_{n\to\infty}\frac{\mathcal{G}_{n\tau}(s)}{L} = 2\int_0^\pi\frac{\mathrm{d}k}{2\pi}\log\left[\frac{1+\sqrt{1-\xi_k(s)}}{2}\right]$$

(3.50)

where $\xi_k(s) \equiv 4\left|r_k^+\right|^2\left|r_k^-\right|^2\left(1-\mathrm{e}^{-2s\epsilon_k(0)}\right)$. In Fig. 3.8, we can see two examples of convergence under the driving, here we plot $\frac{\mathcal{G}_{n\tau}(s)}{L}$ versus s for different values of n, seeing that it approaches $\frac{\mathcal{G}_\infty(s)}{L}$ when n is increased. The form of the driving is that reported in Eq. (3.11) (fixing $A = 1$, $\varphi_0 = 0$) and we consider two different frequencies: $\omega_0 = 2$ in the

---

[9]For $s \to \infty$, $\frac{\mathcal{G}_{n\tau}(s)}{L}$ reduces to the $-g_{n\tau}$ which we have discussed in the former Subsection. As stated there, in this case we can apply the expansion Eq. (3.43) only if $q_k < 1 \,\forall\, k$, condition true whenever $\omega_0 > 4$. If $\omega_0 < 4$, we have to perform the expansion reported in Appendix C for s finite and then take the limit $s \to \infty$, in this way we give a rigorous justification of Eq. (3.43) also in this range of frequencies.
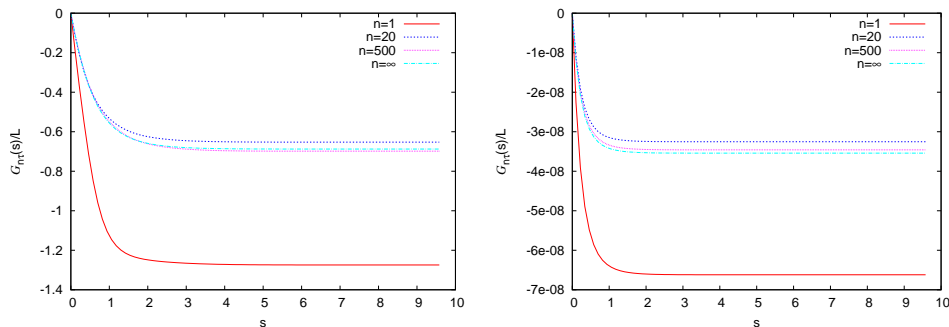
Figure 3.8: Plot versus s of $\frac{\mathcal{G}_{n\tau}(s)}{L}$ for different n and $\frac{\mathcal{G}_\infty(s)}{L}$; the driving is that in Eq. (3.11) and we consider two different values of the frequency, $\omega_0 = 2$ (left panel) and $\omega_0 = 0.3623$ (right panel). Numerical data are for $L = 1000$.

left panel and $\omega_0 = 0.3623$ in the right one. The latter value is approximately such that $J_0(2/\omega_0) = 0$: here we can see that $\frac{\mathcal{G}_{n\tau}(s)}{L}$ takes, for large s, a very small value, consistently with the results shown in Fig. 3.7 for $g_{n\tau} = -\lim_{s\to\infty} \frac{\mathcal{G}_{n\tau}(s)}{L}$. We can evaluate the cumulants of the asymptotic work distribution. They can be obtained as

$$K_n = (-1)^n \frac{\partial^n}{\partial s^n} \log G_\infty(s)\big|_{s=0} \ .$$

The first cumulant (which has the physical meaning of asymptotic stroboscopic quantum average of the performed work) is given by

$$K_1 = \langle W \rangle_\infty = L \int_0^\pi \frac{\mathrm{d}k}{2\pi} \left(4 \left| r_k^+ \right|^2 \left| r_k^- \right|^2 E_k(0) \right) \ . \tag{3.51}$$

We are happy, because this is just the result we would obtain by evaluating $\int_0^\pi \frac{\mathrm{d}k}{2\pi} \left[\langle \psi_k(n\tau)| \hat{H}_k(0) | \psi_k(n\tau) \rangle - E_{\mathrm{GS}\,k}(0) \right]$ which we have done in Sec. 3.2 and represented in Fig. 3.3.

The second cumulant has the physical meaning of variance of the work distribution and is given by

$$K_2 = \sigma_\infty^2 = L \int_0^\pi \frac{\mathrm{d}k}{2\pi} \left[4 \left| r_k^+ \right|^2 \left| r_k^- \right| \left(1 + 3 \left| r_k^+ \right|^2 \left| r_k^- \right| \right) E_k^2(0) \right] \ . \tag{3.52}$$

We can notice that the distribution of the work in the thermodynamic limit tends to become a δ [86] because

$$\frac{\sigma_\infty}{\langle W \rangle_\infty} \sim \frac{1}{\sqrt{L}} \ .$$

Nevertheless, fluctuations around it are visible for L finite and, as we are going to see, they remarkably show for small W a behaviour independent of the periodic driving protocol.

47

3.4.2 Universal edge singularity at small W in the synchronized probability distribution

Inspiring ourselves to the beautiful paper Ref. [86], we seek for understanding the behaviour of the asymptotic work probability distribution at small values of the work, especially in connection with aspects independent of the specific protocol (this independence is improperly referred to as "universal"). The behaviour of $P_\infty(W)$ at small W is written in the behaviour of $G_\infty(-is)$ at large s. We can obtain an approximate analytical formula valid for $s \gg 1/|h_i - 1|$ (see Appendix C for the derivation)

$$\frac{\mathcal{G}_\infty(s)}{L} \simeq -g_\infty + \frac{a}{\sqrt{s}} e^{-2s|h_i - 1|} . \tag{3.53}$$

Here g_∞ is minus the asymptotic logarithmic fidelity (see Eq. (3.43)), h_i is the initial value of the field and

$$a \equiv \frac{1}{2} \left(\frac{1}{\sqrt{1 - 4 |r_0^+|^2 |r_0^-|^2}} - 1 \right) \sqrt{\frac{|h_i - 1|}{4\pi h_i}} .$$

Using the relation $G_\infty(s) = e^{L\mathcal{G}_\infty(s)}$, this formula implies

$$G_\infty(-is) \simeq e^{-Lg_\infty} \left(1 + \frac{La}{\sqrt{s}} e^{-2s|h_i - 1|} \right)$$

In appendix C, applying the Laplace transform, we obtain from this equation an interesting approximation for the probability distribution at small W

$$P_\infty(W) \simeq e^{-Lg_\infty} \left(\delta(W) + \frac{aL\theta\left(W - 2|h_i - 1|\right)}{\sqrt{\pi}\left(W - 2|h_i - 1|\right)^{1/2}} \right) ; \tag{3.54}$$

Eq. (3.54) embodies a very strong statement, predicting an edge singularity in the asymptotic work distribution function at a precise value of W which is totally independent of the details of the periodic protocol (and even of the frequency) but depends only on the initial value h_i of the field [10]. The details of the protocol enter into the strength of the singularity (the coefficient a) by means of the factors $|r_0^+|^2$ and $|r_0^-|^2$. We can notice that those pertain to the mode at $k = 0$ and also the threshold $2|h_i - 1|$ is the energy which has to be provided to the system to generate an excitation in the mode at $k = 0$. So, the low energy behaviour of the work distribution function is dominated by the mode of lowest energy [86]; with hindsight bias we recognize we could have guessed that until the first moment.

---

[10]In Ref. [86] the authors find – for the Ising chain under a generic, non-necessarily periodic protocol – that $P_t(W)$ at small W (for a finite time t) depends only on the initial and the final value of the driving field. In our case, the initial and the final value coincide.

The only condition for the validity of these approximate formulae is a driving field not starting with the critical point value ($h_i \neq 1$): if not so, the approximations leading to it fail as we show in Appendix C.

We can check numerically the validity of the foregoing approximations. We fix $A = 1$ in Eq. (3.11), considering a driving field of the form

$$h(t) = 1 + \cos(\omega_0 t + \varphi_0). \qquad (3.55)$$

In the left panel of Fig. 3.9 we show $\frac{\mathcal{G}_\infty(s)}{L} + g_\infty$ for different values of φ_0 and $\omega_0 = 2.0$; for each φ_0 there is a different value of $h_i = 1 + \cos(\varphi_0)$ and here we choose the parameters so that $h_i \neq 1$ for all the curves. We can see that, for s large enough, the agreement with the approximate formula Eq. (3.53) is perfect. If we take $\varphi_0 = -\pi/2$, we have $h_i = 1$ and Eq. (3.53) is no more valid. We can see in some examples in the right panel of Fig. 3.9 that $\frac{\mathcal{G}_\infty(s)}{L} + g_\infty$ has not an exponential, but a polynomial decay of the form $1/s$. We notice that if we take $|h_i - 1|$ small but non-vanishing ($\varphi_0 = -0.498\,\pi$), the polynomial decay lasts for a long range of s before we can see some deviation. It seems indeed that this $1/s$ decay when $h_i = 1$ is quite general: we have observed it when the system undergoes the driving in Eq. (3.55) with $\varphi_0 = -\pi/2$ for many different frequency choices (some are shown in the figure) and we have checked it also for other forms of driving, like $h(t) = \cos(\omega_0 t)$. If $\frac{\mathcal{G}_\infty(s)}{L} \simeq -g_\infty + A/s$ for large s, then $G_\infty(-is) \simeq \mathrm{e}^{-g_\infty}(1 + A/s)$ and, at small W, we have the approximation for the probability distribution

$$P(W) \simeq \mathrm{e}^{-Lg_\infty}(\delta(W) + A\,\theta(W))$$

where θ is the Heaviside function. We notice that in Ref. [86] the authors find a very similar formula for $P_t(W)$ (when the time t is finite) in an Ising chain undergoing a generic, non-necessarily periodic, driving which ends at the critical point. In our case we consider the asymptotic behaviour and, thanks to time periodicity, whenever $h_i = 1$ the driving not only ends but also starts at the critical point.

3.5 Conclusion

In conclusion, in this Chapter we have shown an example of the relaxation to the Floquet diagonal ensemble by means of the quantum Ising chain in transverse field, with or without translational symmetry. Because of integrability, only the continuity of single-particle Floquet spectrum matters to attain relaxation of the local observables and their asymptotic value depends only on the properties of single-particle Floquet modes, Because of integrability, this asymptotic value depends strongly on the parameters of the driving and can be described by means of a GGE ensemble. This fact
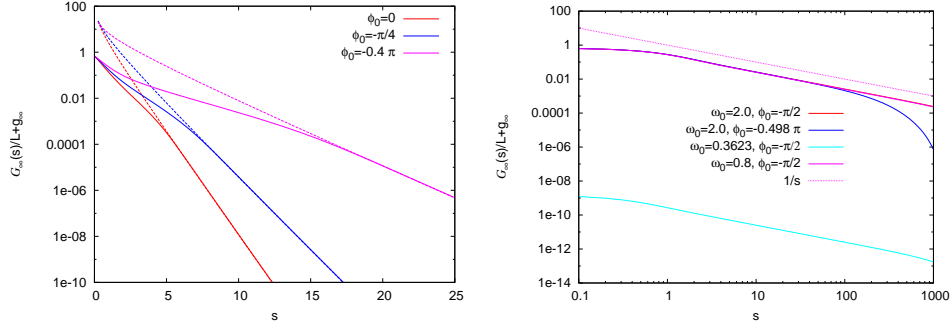
49

Figure 3.9: (Left panel) $\frac{\mathcal{G}_\infty(s)}{L} + g_\infty$ versus s when the driving is (3.55) ($\omega_0 = 2$) and φ_0 such that $h_{\mathrm{i}} \neq 1$ (continuous lines) compared with Eq. (3.53) (broken lines), there is a perfect agreement when s is large. Data are for $L = 1000$. (Right panel) The same for $h_{\mathrm{i}} = 1$ ($\varphi_0 = -\pi/2$) and different frequencies, we can see a polynomial decay like $1/s$; when h_{i} is slightly different from 1 ($\varphi_0 = -0.498\pi$) this decay is still valid for a large range of s. Data are for $L = 4000$.

is true only for local observables, we have shown how the state of the system does not become periodic after a transient and how the work statistics attains an asymptotically periodic condition not described by the GGE.

In the next chapter we move to consider the picture of relaxation to the Floquet diagonal ensemble in the Linear Response Limit, and the quantum Ising chain in transverse field will be still the system on which we will do our numerical analyses.

Chapter 4

Periodic steady regime and linear response theory

Linear Response Theory (LRT) is a tool of the utmost importance in condensed matter physics [133, 134]. It allows to express the response of a system to a small perturbation in terms of its static unperturbed properties. It is therefore invaluable when a system is experimentally investigated by means of small-amplitude probes.

Our focus in this Chapter will be on the linear response of many-body quantum systems. Adding a small perturbation to the static Hamiltonian of a system, and solving the evolution equations up to first-order in the perturbation, we can give a first-order approximation to the response of any observable. Everything can be expressed in terms of response functions, i.e., time-retarded correlators of the operator whose response we want to study, and the operator which couples to the perturbation [134].

An essential aspect of the theory is the assumption of a quantum coherent evolution. Van Kampen has argued that this is a very strong hypothesis, valid on time-scales many orders of magnitude smaller than those on which the theory is successfully applied [135]. Notwithstanding this crucial issue, the theory is valid; in Van Kampen's opinion this is due to the assumption of a thermal initial state which mimics the random correlations induced by the interaction with the environment.

Experimental progress has made the issue of phase coherence in the evolution very important: experiments on cold atoms in optical lattices allow us to observe the coherent dynamics of an artificial many-body quantum system up to times of ~ 1 ms. It is not difficult to engineer small-amplitude perturbations to compare the exact evolution with the linearized one. Moreover, the question is very interesting because, under the hypothesis of coherent evolution, LRT predicts in some regimes a relaxation of the observables to a periodic steady condition which is different from the one corresponding to the Floquet diagonal ensemble (Eq. (2.14)).

Indeed let us consider, in general, an ordered quantum many-body system in the thermodynamic limit $L \to \infty$, and a small periodic perturbation $v(t)\hat{A}$ applied to the Hamiltonian. Let us assume that the perturbation is resonant with one of the internal frequencies of the system; we assume that the system is such that the unperturbed spectrum and the Floquet spectrum are both continuous. LRT predicts that the system absorbs a constant amount of energy in each cycle of the driving; this contrasts with the expected relaxation of the energy to the periodic value given by the Floquet diagonal ensemble, which must be finite if the energy-per-site spectrum is bounded (as indeed happens in lattice-spin or Fermionic systems, see Fig. (3.2)). This leads to different predictions of $\langle \hat{A} \rangle_t$, the response of the observable coupling to the external field. Both theories predict a periodic steady regime, after a transient, but LRT predicts an additional term, out-of-phase with the driving and responsible for a steady energy absorption.

We will use the general Floquet and LRT theories to discuss this question, and we will substantiate our results by means of a "numerical experiment". We will consider the uniform quantum Ising chain in transverse field discussed in Chapt. 3, and we will apply to it a time-periodic perturbation with small amplitude. We will compare the exact dynamics, obtained numerically (see Chapt. 3), with the results of LRT. We will show that the solution to the previous contradiction is rather different when, in the thermodynamic limit, we consider an extensive or a localized driving. For a driving coupled to an extensive operator, we show that the steady energy absorption and out-of-phase response predicted by LRT hold for a finite time, after which the energy saturates; this time goes to infinity in the LRT limit of vanishing amplitude v_0 of the perturbation. In such a limit, the Floquet spectrum develops a degeneracy which gives rise to periodic terms in the Floquet off-diagonal response (see Eq. (2.13)), leading in turn to the appearance of the out-of-phase term in the response. Because of this degeneracy, the off-diagonal density of states $F_{A,t}(\omega)$ (see Eq. (2.16)) develops a singularity which makes the application of the Riemann-Lebesgue lemma tricky. Quite interestingly, for reasonably small amplitudes, the in-phase term of the response is well predicted by LRT up to infinite time.

For a driving coupled to a local operator, i.e., such that the limit of large L is performed while keeping the perturbation localized to few sites, LRT correctly predicts the response for a time scaling with the length of the chain L. In the thermodynamic limit, therefore, LRT is valid for an infinite time. From the point of view of the mathematics, small gaps in the Floquet spectrum close up in the thermodynamic limit, giving rise to periodic terms in the Floquet off-diagonal component of the response. From the physical point of view, the excitations generated in each period by the localized driving are a finite number and they have an infinite space where they can propagate: the quantum many body system acts as a thermal bath for itself [134] and the energy-per-site absorbed is always infinitesimal.

Therefore, the energy of the system changes only by an infinitesimal amount, and this is consistent with the prediction of energy relaxation.

We can see how the validity of LRT is strictly connected with the energy-per-site absorbed being infinitesimal: in a coherent dynamics framework this is only possible for a system in the thermodynamic limit with localized driving. If the driving is extensive, the energy-per-site absorbed is not infinitesimal, and LRT agrees with the exact dynamics only for a finite time. The steady energy absorption predicted by LRT can last forever only if there are dissipation channels towards an environment [134].

In the following sections we will summarize LRT for the case of a suddenly switched-on periodic driving, we will do some observations on the energy absorption and then we will present our results. We will conclude the Chapter by discussing possible experimental verifications and arguing about the generality of our conclusions.

4.1   Linear response theory

Here, we summarize the relevant LRT results, specializing soon to the case of a suddenly switched-on periodic driving. Indeed, our aim is to compare the LRT results with those provided by the Floquet theory, which does not apply if the usual adiabatic switching-on of the perturbation is used. We start by considering a quantum system subject to a small generic time-dependent perturbation, with Hamiltonian:

$$\hat{H}(t) = \hat{H}_0 + v(t)\hat{A} \, , \tag{4.1}$$

where $\hat{A}$ is some Hermitian operator and $v(t)$ a (weak) perturbing field. We assume to perturb the system around the thermal equilibrium condition, with (possibly vanishing) temperature $T = 1/(k_B \beta)$:

$$\hat{\rho}_{\text{eq}} = \sum_n \frac{\mathrm{e}^{-\beta E_n^{(0)}}}{Z} \left| \Phi_n^{(0)} \right\rangle \left\langle \Phi_n^{(0)} \right| \, . \tag{4.2}$$

Here $\left| \Phi_n^{(0)} \right\rangle$ are the eigenstates of $\hat{H}_0$, $E_n^{(0)}$ the corresponding eigen-energies, and $Z = \sum_n \mathrm{e}^{-\beta E_n^{(0)}}$ the partition sum. If we assume a quantum unitary evolution induced by the Hamiltonian $\hat{H}(t)$, we can use LRT to approximate, at first-order in $v(t)$, the expectation value of any observable $\langle \hat{B} \rangle_t$. Restricting to the case $\hat{B} = \hat{A}$ we find [134]

$$\langle \hat{A} \rangle_t = \langle \hat{A} \rangle_{\text{eq}} + \int_{-\infty}^{+\infty} \mathrm{d}t' \, \chi(t - t') \, v(t') \, , \tag{4.3}$$

where $\langle \hat{A} \rangle_{\text{eq}} = \text{Tr}[\hat{\rho}_{\text{eq}} \hat{A}]$ is the equilibrium value, and the retarded susceptibility is defined as

$$\chi(t) \equiv -\frac{i}{\hbar}\theta(t)\langle \left[\hat{A}(t), \hat{A} \right] \rangle_{\text{eq}} = -\frac{i}{\hbar}\theta(t) \sum_{n,m} (\rho_m - \rho_n) |A_{mn}|^2 \, e^{-i\omega_{nm}t} \; , \quad (4.4)$$

with $\rho_n = e^{-\beta E_n^{(0)}}/Z$, $A_{mn} = \left\langle \Phi_m^{(0)} \middle| \hat{A} \middle| \Phi_n^{(0)} \right\rangle$, and $\hbar\omega_{nm} = E_n^{(0)} - E_m^{(0)}$. All the relevant information on the susceptibility is contained in its spectral function

$$\chi''(\omega) = -\frac{\pi}{\hbar} \sum_{n,m} (\rho_m - \rho_n) |A_{mn}|^2 \, \delta(\omega - \omega_{nm}) \; . \quad (4.5)$$

This manifestly odd function ($\chi''(-\omega) = -\chi''(\omega)$) is the imaginary part of the Fourier transform of the susceptibility; thanks to causality [134], the whole Fourier transform $\chi(\omega)$ can be reconstructed, and then $\chi(t)$ obtained. Indeed, considering the Fourier transform $\chi(z)$ for $z = \omega + i\eta$ in the limit $\eta \to 0^+$, we find

$$\chi(z) = \int_{-\infty}^{+\infty} dt \, \chi(t) \, e^{izt} = \int_{-\infty}^{+\infty} \frac{d\omega}{\pi} \frac{\chi''(\omega)}{\omega - z} \; . \quad (4.6)$$

We will always consider (unless otherwise stated) an extended ordered system in the thermodynamic limit, in this way the spectrum is a continuum and (as in Eq. (2.16)) the discrete Dirac's deltas in Eq. (4.5) merge together, making $\chi''(\omega)$ a regular function of ω.

We restrict here to the case of a perfectly periodic perturbation of frequency ω_0, for definiteness $v_0 \sin(\omega_0 t)$. As already mentioned, textbook approaches usually consider an adiabatic switching-on of the perturbation from $t = -\infty$ to $t = 0$, writing $v(t) = v_0 \sin(\omega_0 t) \left[e^{\eta t}\theta(-t) + \theta(t) \right]$ with η small and positive, which is sent to $\eta \to 0^+$ at the end of the calculation. Since we are interested in comparing LRT results with a Floquet analysis and associated numerical results, we are forced, on the contrary, to assume a sudden switching-on of the periodic perturbation at $t = 0$, taking $v(t) = v_{\text{per}}(t) = v_0 \theta(t) \sin(\omega_0 t)$. We define $\delta\langle \hat{A} \rangle_t^{\text{per}} = \langle \hat{A} \rangle_t^{\text{per}} - \langle \hat{A} \rangle_{\text{eq}}$ the (possibly non periodic) response to the periodic perturbation; using Eqs. (4.3)-(4.6) it is not difficult to find

$$\delta\langle \hat{A} \rangle_t^{\text{per}} = v_0 \int_{-\infty}^{+\infty} \frac{d\omega}{2\pi i} \, \chi''(\omega) \left(\frac{e^{i\omega_0 t} - e^{-i\omega t}}{\omega + \omega_0} - \frac{e^{-i\omega_0 t} - e^{-i\omega t}}{\omega - \omega_0} \right) \; . \quad (4.7)$$

We notice that, notwithstanding the singular denominators at $\omega = \pm\omega_0$ and the absence of $\pm i\eta$ regularizing terms, the integrand is regular, since it is finite in the limit $\omega \to \pm\omega_0$. We need to pay attention only if we split the terms with $e^{\pm i\omega_0}$ from those with $e^{-i\omega t}$ in the sum of two integrals: because of the singularities of the denominators in $\pm\omega_0$ we would need to use the

Cauchy principal value prescription in both integrals. Exploiting the fact that $\chi''(\omega)$ is odd, we can readily find

$$\delta \langle \hat{A} \rangle_t^{\mathrm{per}} = v_0 \chi'(\omega_0) \sin(\omega_0 t) - 2 v_0 \omega_0 \!\!\!\fint_0^{+\infty} \!\!\frac{\mathrm{d}\omega}{\pi} \, \frac{\chi''(\omega)}{\omega^2 - \omega_0^2} \sin(\omega t) \ . \qquad (4.8)$$

Here $\chi'(\omega_0)$ is obtained as the real part of the Fourier-transformed susceptibility Eq. (4.6) for $z = \omega_0 + i\eta$, the so-called Kramers-Krönig transform [134]

$$\chi'(\omega_0) \equiv \fint_{-\infty}^{+\infty} \frac{\mathrm{d}\omega}{\pi} \frac{\chi''(\omega)}{\omega - \omega_0} \ . \qquad (4.9)$$

If the term multiplying $\sin(\omega t)$ in Eq. (4.8) were a regular function of ω, we could proceed as we have done in general for the out-of-diagonal Floquet term (Eq. (2.17)). We could apply the Riemann-Lebesgue lemma and show that the integral in ω vanishes after a transient; only the periodic term proportional to $\chi'(\omega_0)$, and in-phase with the driving, would be left. In the case of resonant perturbation ($\chi''(\omega_0) \neq 0$) this is impossible, because the integrand is singular in $\pm\omega_0$ (we will see how this singularity emerges from a degeneracy in the Floquet spectrum). Nevertheless, we can isolate this singularity in a term proportional to $\chi''(\omega_0)$. Simple calculations (see appendix D.1) show that this term equals $-v_0 \chi''(\omega_0) \cos(\omega_0 t)$, and is out-of-phase with the driving. Having taken out this singular term, the integral in ω involves a regular function

$$F^{\mathrm{trans}}(\omega_0, t) = -v_0 \int_{-\infty}^{\infty} \frac{\mathrm{d}\omega}{\pi} \, \frac{[\chi''(\omega) - \chi''(\omega_0)]}{\omega - \omega_0} \sin(\omega t) \ . \qquad (4.10)$$

This is a transient term vanishing for long times, due to the Riemann-Lebesgue lemma. In conclusion, the response of the system in LRT has the form

$$\delta \langle \hat{A} \rangle_t^{\mathrm{per}} = v_0 [\chi'(\omega_0) \sin(\omega_0 t) - \chi''(\omega_0) \cos(\omega_0 t)] + F^{\mathrm{trans}}(\omega_0, t) \ . \qquad (4.11)$$

As already anticipated, we see in this expression that LRT predicts a result qualitatively similar to relaxation in the periodic Floquet diagonal ensemble: the response becomes periodic for long times. There is a term in-phase with the driving, proportional to $\chi'(\omega_0)$, and a term out-of-phase with it, proportional to $\chi''(\omega_0)$. The last out-of-phase term is associated with energy absorption, as we will discuss in the next section. We will also see that, because of general energy considerations, it has to be vanishing in the Floquet diagonal ensemble prediction. We will verify this explicitly for the quantum Ising chain in Sec. 4.3, connecting this fact with the properties of the Floquet spectrum when the external frequency is resonant with the unperturbed Hamiltonian.

4.2 Energy absorption and periodic steady state

In this section we describe the energy absorption of a system which is periodically driven by an external field, $\hat{H}(t) = \hat{H}_0 + v(t)\hat{A}$. We distinguish among two energy functions, the exclusive energy $E_0(t) = \text{Tr}[\hat{\rho}(t)\hat{H}_0]$, which is the energy expectation of the unperturbed system on the state $\hat{\rho}(t)$ evolving with the perturbation, and the inclusive energy, which is the expectation value on $\hat{\rho}(t)$ of the total Hamiltonian $\hat{H}(t)$ including the perturbing term. The von Neumann's equation for the unitary dynamics $i\hbar\dot{\hat{\rho}}(t) = [\hat{H}(t), \hat{\rho}(t)]$ and the cyclicity of the trace give us an expression for the power instantaneously absorbed by the system

$$\frac{d}{dt}E(t) = \text{Tr}\left[\hat{\rho}(t)\frac{d}{dt}\hat{H}(t)\right] = \dot{v}(t)\langle\hat{A}\rangle_t \qquad (4.12)$$

which is very similar to the Hellmann-Feynman formula. Exploiting that $E_0(t) = E(t) - v(t)\langle\hat{A}\rangle_t$ we readily find

$$\frac{d}{dt}E_0(t) = -v(t)\frac{d}{dt}\langle\hat{A}\rangle_t \ . \qquad (4.13)$$

From now on we specialize to a simple time-periodic case taking, as before, $v(t) = v_0 \sin(\omega t)$. We are interested in the energy absorption over each cycle of the driving. Accordingly, we consider the time interval corresponding to the n-th cycle $[(n-1)\tau, n\tau]$. Defining the energy changes over this interval as $\Delta E(n) = E(n\tau) - E((n-1)\tau)$ and $\Delta E_0(n) = E_0(n\tau) - E_0((n-1)\tau)$, we can use the previous relationships to find

$$\Delta E(n) = \Delta E_0(n) = v_0\omega_0 \int_{(n-1)\tau}^{n\tau} dt \ \cos{(\omega_0 t)}\langle\hat{A}\rangle_t \ . \qquad (4.14)$$

From this formula, we see that a net absorption of energy over a cycle depends on the presence of a term in the response $\langle\hat{A}\rangle_t$ which is out-of-phase with the driving. To show this, we define $\left[\langle\hat{A}\rangle_t\right]_n$ as the restriction of $\langle\hat{A}\rangle_t$ to the time interval $[(n-1)\tau, n\tau]$; hence, we can expand it in a Fourier series

$$\left[\langle\hat{A}\rangle_t\right]_n = \widetilde{A}_0(n) + \sum_{m=1}^{+\infty}\left[\widetilde{A}_m^{(c)}(n)\cos(m\omega_0 t) + \widetilde{A}_m^{(s)}(n)\sin(m\omega_0 t)\right] \ . \quad (4.15)$$

The Fourier coefficients $\widetilde{A}_m^{(c,s)}$ depend on the period index n because $\langle\hat{A}\rangle_t$ is not strictly periodic. From the point of view of the Floquet theory, there are off-diagonal terms in the Floquet expansion (the term $\langle\hat{A}\rangle_t^{\text{off}-\text{diag}}$ in Eq. (2.13)) which give rise to fluctuations around the asymptotic periodic regime for the first periods; the same happens within LRT, because of the transient term in Eq. (4.10). For long times, these fluctuations vanish,

thanks to the continuity of the Floquet spectrum, and the Fourier coefficients tend to become constant for $n \to \infty$. Substituting this formula in Eq. (4.14) we see that the only term in this Fourier series responsible for energy absorption is $\widetilde{A}_1^{(c)}(n) \cos(\omega_0 t)$. This is the well known term out-of-phase with the driving, and the rate of energy absorption depends only on its Fourier coefficient $\widetilde{A}_1^{(c)}(n)$

$$\mathcal{W}_n = \frac{\Delta E(n)}{\tau} = \frac{1}{2} v_0 \omega_0 \widetilde{A}_1^{(c)}(n) \ . \tag{4.16}$$

Looking at Eq. (4.11), we see that LRT predicts $\widetilde{A}_1^{(c)}(n) \xrightarrow{n \to \infty} -v_0 \chi''(\omega_0)$; this implies that, after a few cycles of the driving, we should see a steady rate of energy absorption given by [134]

$$\mathcal{W}_{n \to \infty}^{\mathrm{LRT}} = -\frac{1}{2} \omega_0 v_0^2 \chi''(\omega_0) > 0 \ . \tag{4.17}$$

As appropriate, this object is positive, since $\chi''(\omega_0 > 0) < 0$.

A steady energy absorption in the unitary dynamics of an isolated system is not always possible. We can see a saturation of energy absorption even in periodically driven few particle systems without an upper bound in the energy spectrum, whenever there is dynamical localization, like in mesoscopic disordered conducting rings in a time-dependent magnetic field [136] and quantum kicked rotors [137, 138]. In the many-body case, we do not have the discrete spectrum necessary for dynamical localization; nevertheless we can see saturation of the energy absorption whenever the driving is extensive and the energy-per-site spectrum is bounded. Indeed, in many closed systems on a lattice, say a Fermionic Hubbard-like model, the transverse field quantum Ising model, or any spin model in any dimension, one can show by simple arguments that the spectrum of the Hamiltonian should be bounded in a region $[e_L N, e_U N]$. (Here e_L and e_U are appropriate finite lower and upper bounds on the energy-per-site spectrum, and N is the number of sites.) Perturbing such a system with an extensive operator $\hat{A}$ must necessarily lead to a saturation of energy. In this case, the rate of energy absorption scales with N (like the operator $\hat{A}$ and the coefficient $\widetilde{A}_1^{(c)}(n)$ – see Eq. (4.16)); if the rate is constant, it would lead, in a finite number of periods, to a violation of the bounds of the spectrum. In other words, we must always have $|E(t) - E(0)|/N < |e_U - e_L|$. We therefore expect that, when the driving is extensive, LRT is valid only for a finite number of periods. The previous argument does not apply when the driving couples to a localized perturbation: the rate of energy absorption is, in that case, of order $1/N$ with respect to the energy bound, hence infinitesimal in the thermodynamic limit $N \to \infty$.

The saturation of energy absorption under an extensive driving is reflected in the behaviour of the expectation value $\langle \hat{A} \rangle_t$ of the operator coupled to the field. If the observables relax to the Floquet diagonal ensemble,

$\langle \hat{A} \rangle_t \to \langle \hat{A} \rangle_t^{\text{diag}}$ (see Sec. 2.3), the asymptotic periodic condition implies that all the Fourier coefficients of Eq. (4.15) need to converge to a constant for $n \to \infty$. The only way in which this is consistent with an asymptotic saturation of energy absorption is (see Eq. (4.16)) that $\widetilde{A}_1^{(c)}(n) \to 0$. This gives rise to a response asymptotically in-phase with the driving

$$\langle \hat{A} \rangle_t \longrightarrow \langle \hat{A} \rangle_t^{\text{diag}} = \widetilde{A}_0 + \widetilde{A}_1^{(s)} \sin(\omega_0 t) + (\text{higher harmonics}) , \qquad (4.18)$$

consistent with an energy $E(t)$ relaxing to the Floquet diagonal ensemble. We see, therefore, that energy considerations suggest that the out-of-phase term predicted by LRT (see Eq. (4.11)) should be vanishing. In the next section, we will see all these results explicitly verified for the quantum Ising chain in transverse field.

Before going into details, we illustrate an instance of what we have just discussed in Fig. 4.1. Here we show the exclusive energy-per-site $((E_0(t) - E(0))/L)$ obtained numerically for a uniform periodically driven quantum Ising chain (see Eq. (4.1)), compared with the LRT result of steady energy absorption. The field is modulated around the critical point $h_c = 1$, as $h(t) = h_c + \Delta h \sin(\omega_0 t)$ with a small Δh, and the driving frequency $\omega_0 = 0.5$ is inside the resonance spectrum $[-4, 4]$ of the Ising chain, discussed in Sec. 3.1. Everything is rescaled by $1/(\Delta h)^2$ to make the comparison possible; we see that, consistently with our discussion, after a few periods the exact results deviate from the LRT prediction, and the energy saturates to a condition where it shows oscillations at different time scales. As a second example of the saturation of energy absorption, and deviation from LRT, we mention the results shown in Fig. 1 of Ref. [20], where this effect is apparently observed for a periodically modulated uniform Hubbard model, studied by means of t-DMRG [139, 140]. We will discuss later the possible experimental verification of these effects.

To conclude this section, we mention that when there is no convergence to a steady periodic regime but the spectrum is limited (like in disordered systems), saturation of energy absorption can manifest itself with a fluctuating absorbed energy and a $\widetilde{A}_1^{(c)}(n)$ which fluctuates around a vanishing average.

4.3 Results for the quantum Ising chain in transverse field

The Ising Hamiltonian in Eq. (3.1), and the way to solve its dynamics, have been discussed in detail in Chap. 3; here we analyze what happens in the case of a small-amplitude periodic driving, comparing our numerical findings with the analytical results of LRT. The unperturbed Hamiltonian $\hat{H}_0$ in Eq. (4.1) will be a uniform Ising chain of length L at the critical point
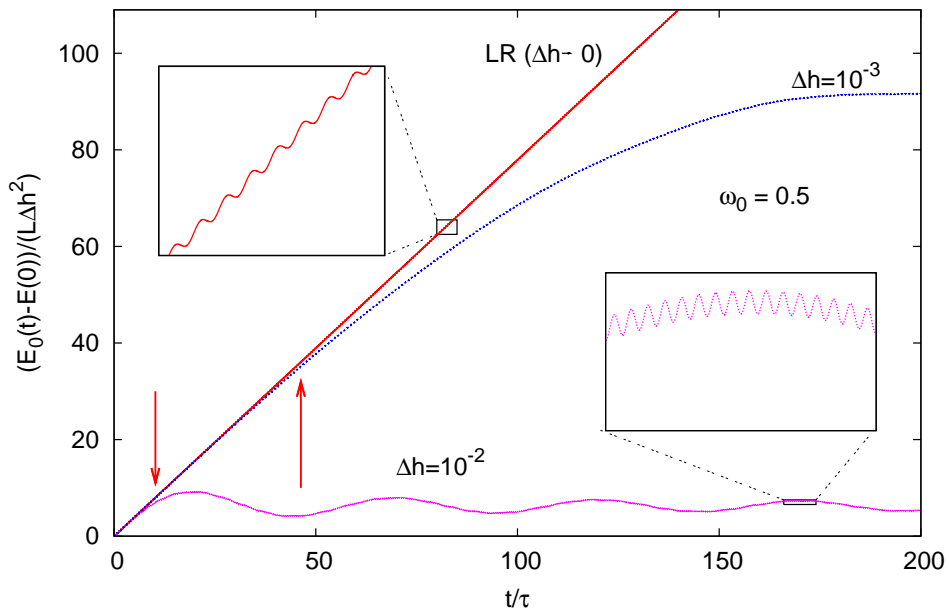
Figure 4.1: Plot of the absorbed energy-per-site, vs t/τ, for $\omega_0 = 0.5$, for a transverse field Ising chain which is perturbed, around the critical point, with a uniform transverse field modulation $(\Delta h)\sin(\omega_0 t)$. Details are explained in Sec. 4.3. The red solid line is the LRT result, compared to the exact results for $\Delta h = 10^{-2}$ (purple dotted line) and $\Delta h = 10^{-3}$ (blue dashed line). All the results are rescaled by $1/(\Delta h)^2$ so as to make the comparison meaningful. The limit $\Delta h \to 0$ is evidently singular.

($h_c = 1$). We will take as perturbation

$$v(t)\hat{A} = -\frac{\Delta h}{2}\theta(t)\sin(\omega_0 t)\sum_{j=1}^{l}\hat{\sigma}_j^x \ .$$

By choosing different values of l we can make the driving localized to few sites, when l is finite for $L \to \infty$, or extensive, i.e., coupled to a sub-chain of length l with $\lim_{L\to\infty} l/L =$ constant, or even uniform, when $l = L$. We will start considering the uniform $l = L$ case.

4.3.1 Uniform driving

In the uniform extensive case, the operator coupled to the driving is the transverse magnetization $\hat{A} = \hat{M}_L = \sum_{j=1}^{L}\hat{\sigma}_j^x$; we are going to measure the corresponding intensive observable, the transverse magnetization per site: $\hat{m} = \frac{1}{L}\sum_{j=1}^{L}\hat{\sigma}_j^x$. Due to the translational invariance, the expectation value of this observable can be decomposed in Floquet diagonal and off-diagonal parts, see Eqs. (3.12)-(3.14) where we have to take

$$\hat{B}_k = \hat{M}_k = 2(\hat{c}_{-k}\hat{c}_{-k}^{\dagger} - \hat{c}_k^{\dagger}\hat{c}_k) \ . \tag{4.19}$$

Eq. (3.14) gives the transient off-diagonal term; it lasts longer the smaller we take Δh: in the limit $\Delta h \to 0$, it lasts forever and gives rise to a term out-of-phase with the driving, as we are going to see.

We consider a perturbation around the critical field $h_c = 1$ assuming that the system is initially in its ground state. LRT provides us an approximation, linear in Δh, for the deviation of $m(t)$ from the ground state equilibrium value m_{eq} which, in the thermodynamic limit, is $m_{eq} = 2/\pi$. Using the notations of Sec. 4.1, here we have $v_0 = -\Delta h/2$ and $\hat{A} = \hat{M}_L = L\hat{m}$. We consider the response of the intensive operator $\hat{m}$ to the extensive one $\hat{M}_L$, in such a way that we have meaningful results in the thermodynamic limit. The response function is given by

$$\chi(t) \equiv -\frac{i}{\hbar}\,\theta(t)\,\langle\Psi_{\text{GS}}^0|\,\left[\hat{m}(t),\hat{M}_L\right]\,|\Psi_{\text{GS}}^0\rangle \ . \tag{4.20}$$

The ground state at time $t = 0$ is the one in Eq. (3.5) with $h(0) = 1$. As shown in appendix D.2, the spectral function $\chi''(\omega_0)$ is given, in the thermodynamic limit $L \to \infty$, by

$$\chi''(\omega_0) = -\text{sign}(\omega_0)\,\theta(4 - |\omega_0|)\,\sqrt{1 - \left(\frac{\omega_0}{4}\right)^2} \ . \tag{4.21}$$

We notice that the manifestly odd $\chi''(\omega_0)$ is non-vanishing only for $|\omega_0| < 4$, which means that the driving frequency needs to fall inside the spectrum of the natural resonance frequencies of the system (see Sec. 3.1) in order

to have dissipation. The corresponding $\chi'(\omega_0)$ is calculated using Eq. (4.9). The functions $\chi'(\omega_0)$ and $\chi''(\omega_0)$ will be shown in Fig. 4.3. Summarizing, the LRT prediction for the transverse magnetization density is:

$$m_{\text{LRT}}^{\text{per}}(t) = m_{\text{eq}} - \frac{\Delta h}{2} \left[\chi'(\omega_0) \sin(\omega_0 t) - \chi''(\omega_0) \cos(\omega_0 t) \right] + F^{\text{trans}}(\omega_0, t) \,, \tag{4.22}$$

where the transient part $F^{\text{trans}}(\omega_0, t)$ is given by Eq. (4.10) with $v_0 = -(\Delta h)/2$.

We can see in Fig. 4.2 a comparison of the exact response, obtained by numerical integration of the Bogoliubov-de Gennes equations Eq. (3.8), with the LRT results. We plot there $m(t) - m_{eq}$ versus time in both cases, considering a resonant frequency $\omega_0 = 0.5$ (upper panel) and an off-resonant one $\omega_0 = 5$ (lower panel), both for $\Delta h = 10^{-2}$. While in the off-resonant case the agreement is perfect at all times, in the resonant one there is a good agreement (even in the transient) only for the first periods; later on, the exact evolution and the LRT approximation settle to two different periodic steady regimes. The most striking feature is that they are out-of-phase with respect to each other: the LRT result in Eq. (4.22) contains the out-of-phase cosine term which is absent in the exact response. In the central panel we see how, in the latter case, the Fourier cosine component on the n-th period (see Eq. (4.15)) $\widetilde{m}_1^{(c)}(n)$ tends to vanish, with oscillations, as $n \to \infty$. Consistently, the extensive energy absorption rate $-(\Delta h/4)\omega_0 L \widetilde{m}_1^{(c)}(n)$ vanishes, in agreement with the results of Sec. 4.2. In the same panel, we see how the sine component $\widetilde{m}_1^{(s)}(n)$ is well predicted by LRT at all periods and, for $n \to \infty$, tends to $-\frac{\Delta h}{2}\chi'(\omega_0)$. Remarkably, LRT describes accurately the in-phase component of the response up to infinite time; this can be seen also in the upper panel of the figure. LRT does not give an exact prediction of the average $\widetilde{m}_0$ around which the response oscillates: it differs from m_{eq} by terms linear in Δh. To summarize, the Floquet theory predicts an asymptotic response of the form

$$m(t) \xrightarrow{t \to \infty} m^{\text{diag}}(t) = \widetilde{m}_0 + \widetilde{m}_1^{(s)} \sin(\omega_0 t) + (\cdots) \,, \tag{4.23}$$

where $\widetilde{m}_1^{(s)} = -\frac{\Delta h}{2}\chi'(\omega_0) + o(\Delta h)$, $\widetilde{m}_0 = m_{eq} + O(\Delta h)$ and the terms marked by $\cdots$ are of higher order in Δh. The remarkable absence of the cosine term is consistent with the saturation of energy absorption. We have verified this picture for all frequencies, and the results are summarized in Fig. 4.3. The quick deviation of the absorbed energy from the steadily increasing LRT prediction is shown in Fig. 4.1, which we have described before. Here we only comment on the red arrows shown, which mark the time t^* at which the exact absorbed energy per site $(E_0(t) - E(0))/\Delta h$ deviates from the LRT prediction by an amount Δh^2. This time grows larger as Δh becomes smaller, and can be quite interesting from the experimental point of view.
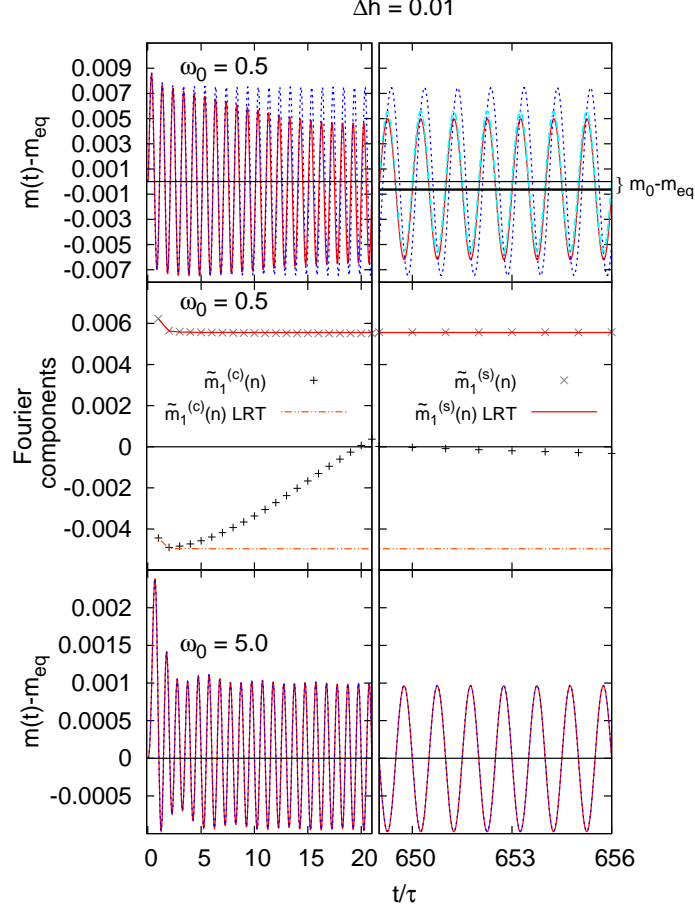
Figure 4.2: Plot of the exact transverse magnetization per spin $m(t) - m_{\text{eq}}$ (red solid line) versus t for a small driving field amplitude $\Delta h = 10^{-2}$, compared to the LRT prediction (blue dotted line). The upper panels refer to $\omega_0 = 0.5$, where $\chi''(\omega_0) \neq 0$; the lower ones to $\omega_0 = 5$, where $\chi''(\omega_0) = 0$. The upper right panel illustrates the disagreement between the exact $m(t)$ and LRT: the exact $m(t)$ lacks any asymptotically out-of-phase term proportional to $\chi''(\omega_0)$ and is slightly shifted downwards. The exact value is, on the contrary, well reproduced, apart a small downwards shift, by the in-phase LRT term (proportional to $\chi'(\omega_0)$) (light blue dashed line). The two central panels represent the Fourier coefficients $\widetilde{m}_1^{(c,s)}(n)$ of the $\cos(\omega_0 t)$ and $\sin(\omega_0 t)$ components of $m(t)$ in the time-window $[(n-1)\tau, n\tau]$ for $\omega_0 = 0.5$. While the latter tends, as expected, to its LRT counterpart for $n \to \infty$, the former tends to 0.
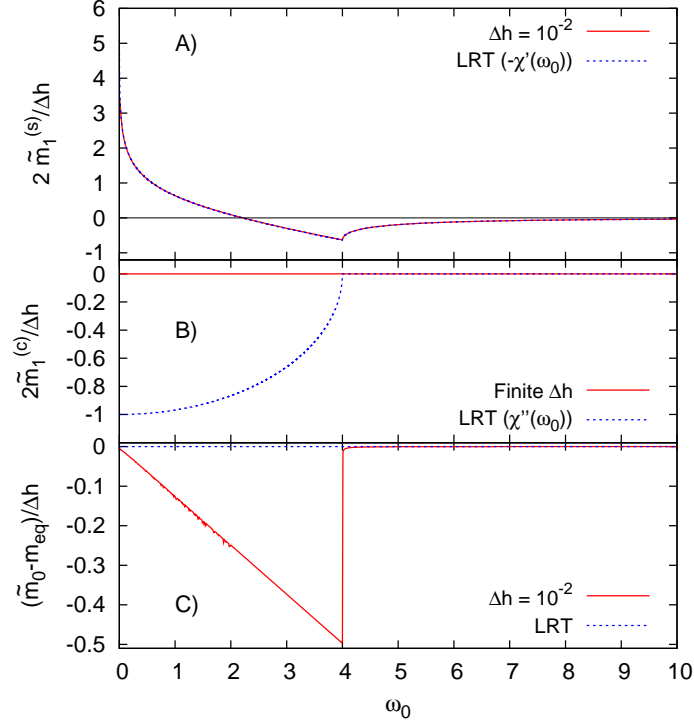
Figure 4.3: (A) Plot of $2\widetilde{m}_1^{(s)}/(\Delta h)$, where $\widetilde{m}_1^{(s)}$ is the Fourier coefficient of the $\sin(\omega_0 t)$ in Eq. (4.23), versus ω_0, compared with the LRT prediction $-\chi'(\omega_0)$. (B) A similar plot for $2\widetilde{m}_1^{(c)}/(\Delta h)$, where $\widetilde{m}_1^{(c)}$ is the Fourier coefficient of the $\cos(\omega_0 t)$ term, which vanishes exactly, while it is predicted to be $\chi''(\omega_0)$ within LRT. (C) Plot of $(\widetilde{m}_0 - m_{\mathrm{eq}})/(\Delta h)$, where $\widetilde{m}_0$ is the zero-frequency (i.e., constant) Fourier coefficient in Eq. (4.23). In all the panels, the exact Fourier coefficients are shown with red solid lines, the corresponding LRT results by blue dotted lines.
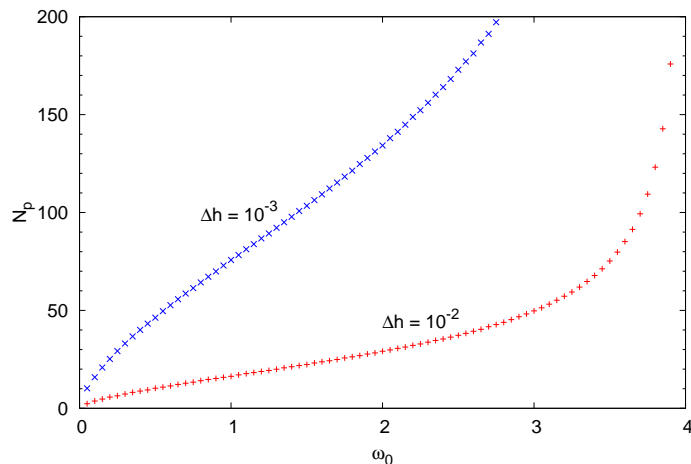
Figure 4.4: Plot of the approximate number of periods t^*/τ over which LRT is accurate for a uniformly driven quantum Ising chain, as a function of the frequency ω_0, for two values of Δh.

In Fig. 4.4 we plot the dependence on ω_0 of the number of periods $\omega_0 t^*/(2\pi)$ at which LRT fails.

To conclude this section we describe how Eq. (4.22) emerges from the Floquet picture, Eqs. (3.12)-(3.14), in the limit of vanishing Δh. The diagonal Floquet component gives rise to the term in-phase with the driving, while the out-of-phase term stems from the off-diagonal component. Whenever Δh is finite, the Floquet off-diagonal term (Eq. (3.14)) decays asymptotically, because the integrand is perfectly regular; for $\Delta h \to 0$, however, it develops a singularity giving rise to the cosine term in Eq. (4.8). Therefore a finite Δh has a kind of regularizing effect. For a better comparison with Eq. (3.14), we specialize the integral in Eq. (4.8) to the case of the Ising model; we change the integration variable to k and obtain

$$m_{\text{LRT}}^{\text{o.o.p.}}(t) = 2\omega_0 \Delta h \int_0^\pi \frac{\mathrm{d}k}{\pi} \frac{\cos^2(k/2)}{\omega_0^2 - (2\epsilon_k^0)^2} \sin(2\epsilon_k^0 t) , \qquad (4.24)$$

where o.o.p. stands for out-of-phase. This formula is the $\Delta h \to 0$ limit of Eq. (3.14); indeed, in this limit the Floquet modes and quasi-energies tend, respectively, to the unperturbed eigenvectors and eigen-energies folded in the appropriate Brillouin zone (see Chapt. 2). This limit is not always regular, indeed we can see in the upper panel of Fig. 4.5 that the quasi-energies are very close to the unperturbed energies everywhere but at those values of k corresponding to a resonance in the unperturbed spectrum ($\epsilon_k^0 = -\epsilon_k^0 + \omega_0$): while the unperturbed energies coincide up to a translation of ω_0, the quasi-energies at any finite value of Δh show an avoided crossing. When $\Delta h \to 0$, this gap closes and a degeneracy in the Floquet spectrum appears:

64

$\mu_k^+ = \epsilon_k^0$ and $\mu_k^- = -\epsilon_k^0$ coincide up to a translation of ω_0. The limit is singular because, when it is attained, there is a change in the topology of the bands. Because of this degeneracy, periodic terms in the off-diagonal Floquet component Eq. (3.14) appear and they give rise to the cosine out-of-phase component. From the point of view of the Floquet joint density of states (see Eq. (2.16)), we can see that this function develops a singularity in the limit of $\Delta h \to 0$; in this way the persisting cosine term emerges. To explicitly show how all this works in our case, by taking due care of the folding in the first Brillouin zone, we can write the fluctuating part of $m(t)$ (Eq. (3.14)) as

$$m^{\mathrm{off-diag}}(t) \approx \int_0^\pi \frac{\mathrm{d}k}{\pi} \left[g_k(t) \cos(2\epsilon_k^0 t) + f_k(t) \sin(2\epsilon_k^0 t) \right] , \qquad (4.25)$$

where the two τ-periodic quantities $g_k(t)$ and $f_k(t)$ originate from appropriate combinations of the real and imaginary parts of the matrix element $F_k(t) = r_k^{+*} r_k^- \left\langle \phi_k^+(t) \right| \hat{m}_k \left| \phi_k^-(t) \right\rangle$ appearing in Eq. (3.14). Both $g_k(t)$ and $f_k(t)$ are regular functions with, at most, a discontinuity across the resonance, while the corresponding LRT integrand $f_k^{\mathrm{LRT}} = 2\omega_0 \Delta h \cos^2(k/2)/[\omega_0^2 - (2\epsilon_k^0)^2]$ is highly singular and requires a principal value prescription. The lower part of Fig. 4.5 shows the behaviour of $f_k(t = \tau)$ compared to its LRT counterpart: quite evidently, there is a finite discontinuity in $f_k(\tau)$ which develops, for $\Delta h \to 0$, into the singular denominator $(\omega_0 - 2\epsilon_k^0)^{-1}$ appearing in LRT.

4.3.2 Perturbation acting on a sub-chain of length $l < L$

We consider now the case of a non-uniform perturbation acting on a sub-chain of length l, $\hat{A} = \hat{M}_l = \sum_{j=1}^l \hat{\sigma}_j^x$. From now on we will define $\hat{m}_j \equiv \hat{\sigma}_j^x$. Thanks to the linearity, the response function

$$\chi_l(t) = -i\hbar^{-1}\theta(t) \left\langle \Psi_{\mathrm{GS}}^0 \right| \left[\hat{M}_l(t),\, \hat{M}_l \right] \left| \Psi_{\mathrm{GS}}^0 \right\rangle$$

is completely determined by the response of the j'-th site to a perturbation localized on the j-th one $\chi_{j'j}(t) \equiv -i\hbar^{-1}\theta(t)\langle[\hat{m}_{j'}(t), \hat{m}_j]\rangle_{\mathrm{GS}^0}$; the calculation of this object is given in appendix D.3. From the other side, the exact dynamics can be found using the Bogoliubov-de Gennes equations Eq. (3.24), and the corresponding Floquet analysis detailed in Subsec. 3.3.2. Let us consider the cosine and sine ω_0-Fourier components of $\langle \hat{A} \rangle_t = \langle \hat{M}_L \rangle_t$ (see Eq. (4.15)), $\widetilde{A}_1^{(c,s)}(n)$. We plot them in Fig. 4.6: on the left panel we show the results for an extensive driving $l = L/2$, on the right panel the results for localized driving ($l = 1$); in both cases we compare the exact results with LRT.

We see that there are always finite-size revivals at a time $\sim (L-l)$. Physically, at this time, the excitations generated by the driving and propagating
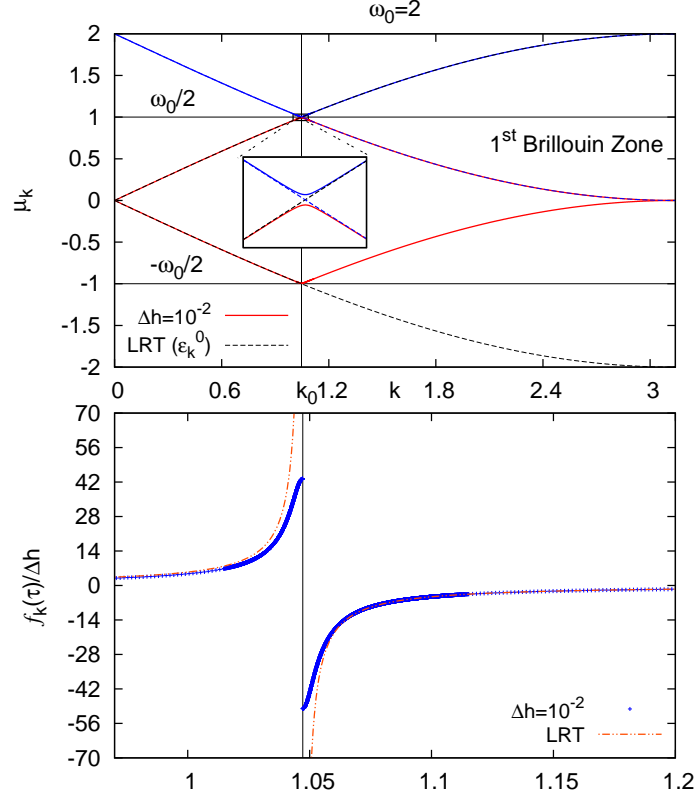
Figure 4.5: (Top) The Floquet quasi-energies $\pm\mu_k$ (continuous lines) versus k for a weak driving of $\Delta h = 10^{-2}$ at $\omega_0 = 2$, compared to the unperturbed excitation energies $\pm\epsilon_k^0$ (dashed lines). μ_k coincides with ϵ_k^0 up to terms of order $(\Delta h)^2$ everywhere but around the (one-photon) resonance occurring at $2\epsilon_{k_0}^0 = \omega_0$ (here $k_0 = \pi/3$). The inset shows that the resonance is an avoided crossing of the Floquet exponents. (Bottom) Plot of $f_k(\tau)$ (see Eq. (4.25)) compared to the corresponding LRT diverging integrand f_k^{LRT} (see Eq. (4.24)) close to the resonance point k_0, both rescaled by Δh.

at the maximum velocity $v = 1$ reach the boundaries of the chain and the system discovers to be finite [1]. Before this revival (which moves to infinite time in the thermodynamic limit), we see a different behaviour for the two cases. While, in both cases, the sine component $\widetilde{A}_1^{(s)}(n)$ is well described by LRT up to the revival time, this does not happen for the cosine component. The latter agrees with the LRT prediction until the revival sets up only in the case of localized perturbation; when the perturbation is extensive, we can see marked deviations after a few periods. If we extrapolate to the thermodynamic limit, we find fluctuations around 0 which likely vanish for long times. When the perturbation is extensive, this implies the asymptotic vanishing of the absorption rate $-(\Delta h/4)\omega_0\widetilde{A}_1^{(c)}(n)$, in agreement with the discussion in Sec. 4.2. When the perturbation is localized, on the contrary, the energy absorption lasts forever (up to usual finite-size revival time, in the finite L case). There is no contradiction with the boundedness of the spectrum, since the energy-per-site absorbed per cycle is order $1/L$, hence becomes infinitesimal in the thermodynamic limit.

We can understand the difference among the two cases by means of an interesting physical picture. When the perturbation is localized, and we are in the thermodynamic limit, the driving generates a finite amount of excitations per cycle which have an infinite space where to propagate: so, the excitation energy-per-site is always infinitesimal and LRT is valid. When the perturbation is instead extensive, the space where to accommodate the excitations scales still with L, but an equally extensive number of them is generated in each cycle. In this way, we see that the energy bound is soon saturated and the phenomenology does not change if we take the thermodynamic limit $L \to \infty$.

To conclude, we can give an interpretation in terms of the Floquet analysis of Sec. 2.3 of the persisting off-diagonal cosine term appearing when the perturbation is localized. This term comes from the Floquet off-diagonal component of the response (see Eq. (2.13)); it persists for a long time because there are quasi-degenerate pairs of single-particle [2] Floquet quasi-energies μ_α associated to the Bogoliubov-de Gennes equations (see Subsec. 3.3.2). The intra-pair gap is two orders of magnitude smaller than the inter-pair gap and both the gaps close in the thermodynamic limit as $1/L$; the small intra-pair gaps make the Floquet off-diagonal terms (see Eq. (2.13)) between quasi-degenerate states essentially periodic (deviations from periodicity cannot be

---

[1] Indeed, we assume periodic boundary conditions in the spins, so it would be more correct to say that at time $L - l$ the excitations propagating towards the two sides reach each other.

[2] Here we only consider the dynamics of a single-particle quadratic operator, but – as we have seen in Sec. 3.3.3 – also for many-body operators only the properties of single-particle Floquet objects matter, thanks to Wick's theorem. There is relaxation if the single-particle Floquet spectrum is a continuum and the asymptotic periodic regime is fully determined by the single-particle Floquet modes.
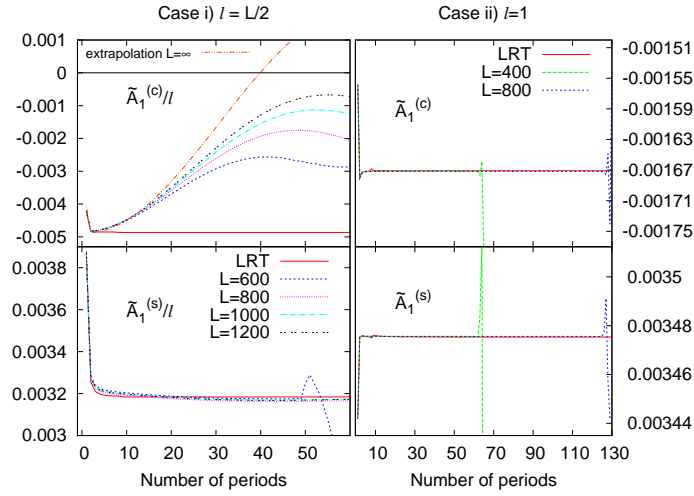
Figure 4.6: (Upper panels) $\widetilde{A}_1^{(c)}(n)$, the $\cos(\omega_0 t)$-component of $\langle M_l \rangle_t$ in the nth-period, rescaled by l, for an extensive perturbation $l = L/2$ (left, case (i)) and a local one $l = 1$ (right, case (ii)). (Lower panels) Same as above, but for $\widetilde{A}_1^{(s)}(n)$, the $\sin(\omega_0 t)$-component of $\langle \hat{M}_l \rangle_t$ in the nth-period. LRT predicts $\widetilde{A}_1^{(s)}(n) = -(\Delta h/2)\chi_l'(\omega_0)$, in excellent agreement with the exact results before the revivals at t^* for both $l = L/2$ and $l = 1$. $\widetilde{A}_1^{(c)}(n)$ quickly deviates from the LRT value $(\Delta h/2)\chi_l''(\omega_0)$ and approaches 0 (with oscillations) for $l = L/2$, while it agrees with the LRT value for $l = 1$. Here $\omega_0 = 1$ and $\Delta h = 10^{-2}$.

68

seen before the finite-size revival sets up), they give an additional contribution to the Floquet diagonal ensemble accounting for the out-of-phase term in the response [3].

4.4 Discussion and conclusion

In conclusion, in this chapter we have discussed the relaxation to the diagonal Floquet ensemble in a quantum many-body system in the limit of small amplitude driving. In this limit, we have found a strict relation between the validity of LRT at long times from one side, and energy absorption and boundedness of the spectrum from the other. Indeed, LRT does not describe correctly the relaxation to the Floquet diagonal ensemble of some observables when the energy-per-site spectrum is bounded and the system undergoes a resonant perturbation with small but finite amplitude. For instance, LRT predicts a steady increase of the energy which is not consistent with a bounded energy-per-site spectrum and the related finiteness of the asymptotic Floquet-diagonal value of the energy. Another strictly related example is the operator coupled to the driving field: here LRT predicts a term in the response out-of-phase with the driving, giving rise to steady energy absorption. This contradicts energy relaxation, so this term has to vanish after a transient, consistently with a bounded energy spectrum.

We have checked these predictions numerically for the driven quantum Ising chain and observed a different behaviour for an extensive and a localized driving. In the first case, the energy absorbed per period is extensive and the LRT prediction of steady energy absorption lasts a finite number of periods. This reflects in the behaviour of the observable coupled to the driving: its asymptotic Floquet-diagonal value corresponds only to a part of the LRT prediction, the out-of-phase term responsible for energy absorption is absent. The latter term persists only in the limit of vanishing amplitude of the driving (and vanishing energy absorption): it does not come from the Floquet diagonal ensemble but from off-diagonal terms which, in this limit, become periodic due to the appearance of degeneracies in the quasi-energy spectrum. Remarkably, if the perturbation is non-resonant, and there is no net energy absorption per cycle, the LRT prediction coincides with the relaxation to the diagonal ensemble.

When the perturbation is localized, LRT is valid up to a time extensive in the length L of the system; here the energy absorbed per cycle is non-extensive, and unable to saturate the extensive energy bound. Moreover, there are gaps in the Floquet spectrum closing up in the thermodynamic limit: they give rise to essentially periodic Floquet off-diagonal terms which make the system relax to the LRT prediction before the finite-size revival

---

[3]As a matter of fact, the Floquet diagonal ensemble does not give either the exact in-phase LRT response.

sets up. Physically, in the case of extensive perturbation, the driving gives rise (in a non-extensive number of cycles) to a finite number of excitations per site: the system moves away from its ground state and linearity is lost. When the perturbation is localized, instead, the driving generates a finite amount of excitations per cycle which are free to propagate in an infinite chain, in this way the excitation energy per site stays infinitesimal and the system is kept in the LRT regime.[4]

Since we have explicitly verified our conclusions about energy saturation and LRT only in the case of an integrable model, it is important to discuss their possible generality. We observe that the relaxation of the energy absorbed to a finite (although extensive) value relies only on the continuity of the Floquet spectrum and on the boundedness of the energy-per-site spectrum. Therefore, we expect that our argument is valid for any Fermionic or spin model on a lattice, even if it is not integrable. We see that an upper bound on the energy spectrum is a purely quantum phenomenon valid for electrons in periodic lattices (if coupling to other bands can be neglected) and for models which are low-energy approximations to true systems. Remarkably, they can be realized experimentally in the framework of cold atoms. For instance, cold atom gases at low density in one dimension behave as hard core bosons and their Hamiltonian can be fermionized by means of a Jordan-Wigner transformation, the result is a Fermionic Hamiltonian with a bounded spectrum very similar to the one we have discussed so far [1]. Another important example is the experimental realization of one-dimensional strongly interacting driven Fermi gases [141]. With an appropriate optical lattice these systems can give a realization of the Hubbard model Hamiltonian [142, 143]. It is moreover very important to consider experimentally the case of fermions with a continuum spectrum where effects of energy localization have indeed been observed [136].

The importance of a bounded spectrum for the hindered energy absorption can be exemplified by the case of a driven chain of harmonic oscillators, a system without any upper limit in the energy per site. We couple the central site of this system to a time-periodic electric field $E(t) = E_0 \cos(\omega_0 t)$

$$\hat{H}(t) = \sum_{j=1}^{L} \left[\frac{1}{2M} \hat{P}_j^2 + \frac{K}{2} \left(\hat{X}_j - \hat{X}_{j-1} \right)^2 \right] - \sqrt{L} E(t) \hat{X}_0 \, .$$

The system is integrable and the frequencies of the single modes are $\omega_k = \sqrt{K/M} |\sin(k/2)|$, with $k \in -[\pi, \pi]$ continuous in the thermodynamic limit. The dynamics is easily solved by means of the Fourier transform of coordinates and momenta and the integration of their linear Heisenberg equations of motion. It results that the system is always in the linear response regime

---

[4]The only situation we can devise where a localized driving can coexist with a fast saturation of the energy on the sites near the perturbation is the case of a disordered Hamiltonian with localized excitations.

and, in the thermodynamic limit, whenever the perturbation is resonant with one of the unperturbed frequencies ω_k, there is a steady energy increase. This is valid even if the amplitude of $E(t)$ is extensive with L, consistently with the energy-per-site being unbounded from above. This integrable model is always in the linear response limit, and always in the correspondence limit: the expectations of its observables equal to the corresponding classical quantities. One could ask about the effect of non-integrabilities and nonlinearities: in principle it could be possible that they give rise to a saturation of energy even without a bounded energy spectrum. We are able to consider the effect of non-integrabilites only in the classical limit: we have inquired the dynamics of the classical version of the oscillator model adding to it a cubic coupling term similar to the one considered by Fermi Pasta and Ulam [53, 52] $V_{\mathrm{n.i.}} = \frac{\beta}{3\sqrt{L}} \sum_{j=1}^{L} (X_j - X_{j-1})^3$. What we see is a faster than linear increase of energy: non-linearity causes a faster energy absorption confirming that the saturation effect we observe depends strongly on a bounded energy spectrum. It would be nevertheless interesting to inquire the behaviour of energy absorption in driven classical models with an upper bound in the energy spectrum[5], like the mean field Bose-Hubbard Hamiltonian [144], also in connection with the transition from regularity to chaos.

Another possible example of unhindered energy increase in models without bounds in energy is the driven integrable chain of bosons discussed in Ref [145] in connection with the Luttinger liquid approximation to a system of interacting bosons. The quantum dynamics of this Bosonic driven model can be solved by methods not very different from the ones useful for the Fermionic case we are considering; the resulting equations show parametric instability analogous to the Mathieu oscillator [146], even for very small amplitudes of the driving. At those instabilities the energy seems to increase exponentially: this is a marked deviation from LRT but evidently not a saturation.

About the possibility of observing experimentally the energy saturation we predict, we have already mentioned some models (hard core bosons and Hubbard model) with a bounded energy spectrum, which can be realized in cold atomic experiments. Experimentalists, by using laser fields, are able to engineer artificial periodic potentials (optical lattices) [147] where they can confine up to $N \sim 10^4$ atoms [13, 11] which obey a coherent unitary dynamics for a time, dependent on N, of $\bar{t} \sim 10^2\,\mathrm{s}/N$ [13, 11, 147] [6]. In

---

[5]These models are mean field versions of quantum models (the mean-field counterpart for the Lipkin model is given in Eq. (5.16)), there is indeed no contradiction with our former statement about the bounded spectrum being a purely quantum phenomenon.

[6]In these atomic systems the only channel towards decoherence is spontaneous emission. Thanks to the detuning between the laser field and the relevant atomic internal resonance, the emission rate of incoherent photons is $\Gamma_{\mathrm{eff}} \sim 10^{-2}\,\mathrm{s}^{-1}$ [147]; the estimate of the coherence time $\bar{t}$ is found imposing that the emission probability is 1 ($N\Gamma_{\mathrm{eff}}\bar{t} \sim 1$). The

this way the experimentalists are able to observe in laboratory the long-time coherent dynamics of driven solid-state Hamiltonian like the Fermi or Bose Hubbard. These Hamiltonians are low-energy approximations obtained considering only the lowest energy band of the periodic system, nevertheless the gap with the next band can be engineered to be much higher than all the couplings of the effective Hamiltonian [143]: at least in the Fermi case the low energy Hamiltonian works reasonably also for the driven case, provided the frequency is of the order of the couplings (like in our numerical examples). To give an idea of the order of magnitude of the coherence times in the Hubbard-model experiments, the dynamics of $N \sim 10^3$ atoms can be kept coherent for a time $\sim 100\,\mathrm{ms}$ which, choosing appropriately the inter-well coupling J, can be made $\sim 300 \times 1/J$ [143]. In conclusion, the requirement of thermodynamic limit necessary for a continuous spectrum is fulfilled; moreover the dynamics is coherent for a time long enough to observe relaxation to the Floquet diagonal ensemble. From the experimental point of view, the most promising system is the (Fermionic) Hubbard model, indeed energy saturation has been observed for it in numerical studies based on t-DMRG [20].

---

atoms evolving under coherent dynamics get soon entangled, therefore a measure process over one of them (by means of the spontaneous emission) is enough to break the coherence of all the system.

Chapter 5

Thermalization and the Lipkin model

So far we have explicitly discussed the driven dynamics of the Ising chain: an integrable system which shows no trace of thermal behaviour in the asymptotic periodic regime. The situation is similar to quantum quenches in integrable systems: the observables relax to Floquet-diagonal-ensemble averages which depend on the initial state and show no thermal properties. Indeed, a lot of research has been devoted to understanding the properties that a quantum system has to possess so that its observables relax to thermal equilibrium after a sudden quench. We will review the most important concepts in Sec. 5.1

The topic of the present chapter is how thermalization can emerge upon periodic driving of a fully connected Ising ferromagnet, known as Lipkin model. This model is rather simple to treat: its dynamics can be reduced to that of a single large spin $\widehat{\mathbf{S}}$, with $S = N/2$, where N is the number of spins. When N is large, the dynamics is well approximated by that of a quantum problem with a single degree of freedom and an effective Planck constant $1/N$, which therefore becomes classical in the limit $N \to \infty$. Without driving, the classical dynamics is perfectly regular, due to energy conservation. Upon adding a periodic driving, the properties of the system change considerably: depending on the parameters of the driving, we can observe, in the classical limit, a regular dynamics, a partly chaotic phase space or even full ergodicity and mixing. We will find a strict quantum-classical correspondence: when the classical phase space is ergodic, the quantum system shows quantum chaos and heats up to $T = \infty$, whatever is the initial state. We will show in Sec. 5.5 that this is a consequence of the Floquet states obeying what is known as *Eigenstate Thermalization Hypothesis* (ETH) with $T = \infty$. Moreover, we will see how thermalization is associated to the Floquet states being *extended* in the basis of the unperturbed eigenstates of the Hamiltonian, while they are *localized* when the dynamics is regular and no

thermalization occurs. The periodically kicked version of our model (the so-called "kicked top") has been widely studied in literature in connection to quantum chaos problems [148, 149, 150], but never – as far as we know – from the point of view of the relation among classical ergodicity, quantum thermalization and delocalization of Floquet states.

To set the stage for our discussion, introducing the concepts and tools we will use in our analysis, let us start discussing thermalization and ETH [58, 59].

5.1 Eigenstate Thermalization Hypothesis

The relaxation of a quantum system towards thermal equilibrium is a fundamental question of statistical mechanics, but the interest in this issue has grown impressively in the last years thanks to the possibility of observing this phenomenon experimentally with cold atoms in optical lattices.

Let us begin our discussion with a classical physics framework, where many results are well understood. Classically, thermalization happens in non-linear chaotic systems whenever they are ergodic and mixing [151]. We restrict ourselves, for clarity, to autonomous systems where energy is conserved. In this case, ergodicity means that all the trajectories spread uniformly on the available energy shell, which implies that time averages coincide with averages on the microcanonical ensemble. Indeed, if $\mathbf{X}(t)$ is a generic trajectory and $\mathcal{O}(\mathbf{X})$ an observable, we find

$$\overline{\mathcal{O}(\mathbf{X}(t))} \equiv \lim_{T \to \infty} \frac{1}{T} \int_0^T \mathcal{O}(\mathbf{X}(t)) \mathrm{d}t = \frac{\int_{\mathcal{E}} \mathrm{d}\mathbf{X} \mathcal{O}(\mathbf{X})}{\int_{\mathcal{E}} \mathrm{d}\mathbf{X}} \equiv \mathcal{O}_{\mathrm{MC}}(E) \,, \qquad (5.1)$$

where $\mathcal{E}$ is the microcanonical energy shell, the portion of phase space with energy in the interval $\mathbb{I}_{\Delta E}(E) = [E - \Delta E/2, E + \Delta E/2]$, where ΔE is a non-extensive quantity. We can rephrase the equality of the two averages above, by saying that the 1-dimensional trajectory $\mathbf{X}(t)$ fills the $2N-1$-dimensional energy shell (in a weak sense). We stress that this is true independently of the observable $\mathcal{O}$ considered, which we might rephrase (in a mathematically sloppy way) by writing:

$$\overline{\delta\left[\mathbf{X}(t) - \mathbf{X}\right]} = \frac{\chi_{\mathcal{E}}(\mathbf{X})}{\int_{\mathcal{E}} \mathrm{d}\mathbf{X}} \,, \qquad (5.2)$$

where $\chi_{\mathcal{E}}(\mathbf{X})$ denotes the characteristic function on the microcanonical energy shell. Another essential condition for thermalization is *mixing*: it means that nearby trajectories separate exponentially in time [152]. This implies that, if the initial conditions are not specified exactly and a coarse graining on the phase space is imposed, the observables tend to their thermal equilibrium value without the necessity of time averages.

74

To state the conditions under which ergodicity and mixing occur, we start considering a perfectly integrable Hamiltonian, where there are as many integrals of motion *in involution* [1] as degrees of freedom: The presence of these constraints confines the trajectories on regular invariant tori in phase space [46]; these manifolds have dimensionality smaller than the energy shell, so trajectories are not ergodic [2]. Adding to the Hamiltonian a small-amplitude non-integrable perturbation, only those trajectories starting in a neighborhood of the tori with commensurate frequencies (KAM theorem [47, 48, 49, 45, 46, 50]) become chaotic (this portion of phase space is indeed mixing, because nearby trajectories separate with an exponential rate), but the system as a whole is not ergodic. Indeed the chaotic trajectories are confined to stay in those parts of phase space lying among the still-conserved tori [45, 46]; they explore only a portion of the phase-space volume in the energy shell. Only if the amplitude of the perturbation overcomes a certain threshold, all the phase space becomes chaotic, trajectories explore uniformly the energy shell and the system is ergodic.

Understanding how these results emerge from quantum mechanics has attracted the interest of the researchers since the earliest times [153, 154]. Qualitatively, we can say that quantum mechanics provides a natural coarse graining of phase space, due to the uncertainty principle. Any initial wave function has a finite width in position and momentum; because of mixing it gets spread all over the energy shell and the asymptotic expectation value of the observables coincides with the average on the microcanonical ensemble [59]. To make these considerations more precise, in analogy with the analysis of classical trajectories in phase space sketched above, one can try to study the dynamics of states in the Hilbert space. We can try to see if there is a quantum equivalent of Eq. (5.2), i.e., if the time-averaged density matrix of the system equals the thermal equilibrium density matrix. One soon realizes that this cannot be so: whatever the properties of the classical Hamiltonian, the Schrödinger equation is linear and does not share the properties of ergodicity and mixing which lead to thermalization in classical physics. Indeed, if we expand the instantaneous state of the system in the energy eigenstate basis as $|\psi(t)\rangle = \sum_n C_n \mathrm{e}^{-iE_n t} |\Phi_n\rangle$, we easily realize that the time average of the density matrix is given by the diagonal ensemble

---

[1]Two functions of momenta and coordinates are in involution if their Poisson bracket [45, 46] vanishes. The condition of the integrals of motion being in involution with each other is essential for the invariant surfaces being regular tori [45, 46]. Indeed, in an N-degree-of-freedom autonomous Hamiltonian system there are always $2N$ constants of motion [53], if they are not in involution they can be pathologically multivalued, allowing the trajectories to wander freely over the energy shell.

[2]If there are N degrees of freedom, the energy shell has dimension $2N - 1$ while the invariant tori are N-dimensional manifolds.

(see Chapt. 1)

$$\overline{|\psi(t)\rangle \langle\psi(t)|} = \hat{\rho}_{\mathrm{diag}} \equiv \sum_n |C_n|^2 |\Phi_n\rangle \langle\Phi_n| \ . \qquad (5.3)$$

There is no trace of ergodicity in the Hilbert space: this time average depends strongly on the initial conditions of the system, embedded in the coefficients C_n, and it is in general very different from the density matrix corresponding to the microcanonical ensemble, which might be written as

$$\hat{\rho}_{\mathrm{MC}}(E) = \frac{1}{\mathcal{N}_E} \sum_n^{E_n \in \mathbb{I}_{\Delta E}(E)} |\Phi_n\rangle \langle\Phi_n| \ . \qquad (5.4)$$

We clearly see that the microcanonical density matrix corresponds to having constant $|C_n|^2 = 1/\mathcal{N}_E$ over the whole energy shell, $\mathcal{N}_E = \sum_{E_n \in \mathbb{I}_{\Delta E}}$ being the number of states in that shell. We seem to have reached a paradox: if the observables relax to some steady-state value, the latter has to be given by the average over the diagonal ensemble in Eq. (5.3); if there is thermalization, such a steady-state value must coincide with the microcanonical average $\langle\mathcal{O}\rangle_{\mathrm{MC}}(E) = \mathrm{Tr}\left[\hat{\mathcal{O}}\,\hat{\rho}_{\mathrm{MC}}(E)\right]$ associated to the density matrix in Eq. (5.4).

To solve this apparent paradox, and understand the mechanism behind thermalization, one has to look at the properties of the observables and their expectation values. Indeed, the Heisenberg equations governing the observables dynamics resemble more closely the non-linear classical Hamiltonian equations from which chaos and thermalization arise [68]. What has been found is that, in many cases, thermalization of the observables occurs at the level of their expectation values on each single eigenstate: given an energy eigenstate $|\Phi_n\rangle$ with energy E_n, the expectation value of an observable $\hat{\mathcal{O}}$ on it equals the microcanonical average on the corresponding energy shell:

$$\mathcal{O}_{nn} \equiv \langle\Phi_n|\,\hat{\mathcal{O}}\,|\Phi_n\rangle = \langle\mathcal{O}\rangle_{\mathrm{MC}}(E_n) \ . \qquad (5.5)$$

This assumption is called *Eigenstate Thermalization Hypothesis* (ETH) and implies that, by taking an initial state with overlaps C_n restricted to a narrow energy shell $[E - \Delta E/2, E + \Delta E/2]$, i.e., such that $\sum_{E_n \in \mathbb{I}_{\Delta E}} |C_n|^2 = 1$, the time average of the observable equals its microcanonical average:

$$\overline{\langle\mathcal{O}\rangle_t} = \overline{\langle\psi(t)|\,\hat{\mathcal{O}}\,|\psi(t)\rangle} = \sum_n^{E_n \in \mathbb{I}_{\Delta E}(E)} |C_n|^2\,\mathcal{O}_{nn} \simeq \langle\mathcal{O}\rangle_{\mathrm{MC}}(E) \ . \qquad (5.6)$$

This is the quantum equivalent of the classical expression Eq. (5.1). Moreover, as we have sketched before, because of quantum fluctuations and mixing, we expect that the $\langle\psi(t)|\,\hat{\mathcal{O}}\,|\psi(t)\rangle$ will stay most of the time close to the thermal average, with small fluctuations which vanish in the thermodynamic limit. The heuristic reason for this vanishing of time-fluctuations

is that the wave function gets spread, by mixing, all over the energy shell. Time fluctuations [3] of the expectation around the thermal average originate from the off-diagonal terms $\mathcal{O}_{mn}$ which we show in Eq. (2.7) and reproduce here for reader's convenience

$$(\delta\mathcal{O}_{\text{time}})^2 = \overline{\left[\langle\hat{O}\rangle_t^2 - \overline{\langle\mathcal{O}\rangle_t}^2\right]} = \sum_{n\neq m} |C_n|^2 |\mathcal{O}_{nm}|^2 |C_m|^2 \,.$$

If we assume that the off-diagonal matrix elements $\mathcal{O}_{nm}$ fluctuate little with m and n around their typical value $\mathcal{O}_{mn}^{\text{typ}}$, we can use the ETH assumption to show that they are small. This can be easily done by considering, for each eigenstate $|\Phi_n\rangle$, the expectation value on this state of the quantum fluctuation operator $(\hat{\mathcal{O}} - \mathcal{O}_{nn})^2$. Such expectation, because of ETH, has to be equal to its microcanonical value; it can be argued to be of order 1 if $\hat{\mathcal{O}}$ is a local operator [96] or, at most, order N if $\hat{\mathcal{O}}$ is an extensive operator sum of local objects. At worst we find

$$N \sim \langle\Phi_n|\,(\hat{\mathcal{O}} - \mathcal{O}_{nn})^2\,|\Phi_n\rangle = \sum_{n\neq m} |\mathcal{O}_{mn}|^2 \simeq e^{S(E)}|\mathcal{O}_{mn}^{\text{typ}}|^2 \qquad (5.7)$$

where $S(E) = \log\mathcal{N}_E$ is the entropy on the energy shell, which is linear in the number of degrees of freedom N. Therefore, substituting $|\mathcal{O}_{mn}^{\text{typ}}|^2$ to $|\mathcal{O}_{mn}|^2$ we can give an estimate of the infinite time fluctuations as $\delta\mathcal{O}_{\text{time}} \sim \sqrt{N}e^{-S(E)/2}$. In many-body systems, since the entropy is extensive, this quantity is usually exponentially small in the number of degrees of freedom N; therefore, ETH implies the relaxation of the expectations of the observables to the thermal average.

What we have still to verify is that fluctuations around this average coincide with thermal fluctuations: the general statistical mechanics arguments predict thermal fluctuations scaling like $N^{-1/2}$ with respect to the thermal average [94]. The exponentially small time-fluctuations are indeed not enough, we need to consider also the contribution of quantum fluctuations $\langle[\hat{\mathcal{O}} - \langle\hat{\mathcal{O}}\rangle_t]^2\rangle_t$ which, analytically in the general semiclassical chaotic case [67] and by means of numerical experiments on an ergodic hard-core bosons model [26], have been shown to behave in the right way.

---

[3]Time fluctuations should not be confused with the actual quantum fluctuations which, for each t, give an uncertainty

$$\delta\mathcal{O}_t^2 = \langle[\hat{\mathcal{O}} - \langle\hat{\mathcal{O}}\rangle_t]^2\rangle_t \,.$$

With the usual assumption of non-degeneracy, one can estimate the time-average of such quantum fluctuations to be given by the diagonal average:

$$\overline{\delta\mathcal{O}_t^2} \simeq \sum_n |C_n|^2 \left[[\mathcal{O}_{nn} - \overline{\langle\hat{\mathcal{O}}\rangle_t}]^2 + \sum_m^{\neq n} |\mathcal{O}_{mn}|^2\right] \,.$$

Classical thermalization depends on ergodicity and mixing of the dynamics; in the same way, the validity of ETH is strictly connected to the system showing "quantum chaos". In this regime, the Hamiltonian shows the spectral properties of a random matrix, and its eigenstates also show a random behaviour [155, 156, 149, 59, 157]; the physical observables behave, in the basis of the eigenstates, like pseudo-random matrices [68]. To understand better how the random properties of the eigenstates give rise to thermalization, we focus on the seminal papers on the topic of ETH [58, 59]. Here, the authors consider an integrable Hamiltonian to which an integrability-breaking term strong enough for ergodicity is added. In Ref. [58] this term is a banded random matrix, in Ref. [59] the author considers a gas of free particles to which a strong repulsive core is added. In both cases the perturbed Hamiltonian shows quantum chaos; as a consequence, the new eigenstates are random superpositions of a large number of the old ones taken on the appropriate energy shell: Because of this mixing, each eigenstate "is equivalent" to the microcanonical ensemble of the unperturbed Hamiltonian. Only in many-body systems [58] these random superpositions can involve a huge amount of states and the equivalence with the microcanonical ensemble is possible. We can see this, for instance, in the argument leading to the small time-fluctuations around the microcanonical average. The eigenstates being random superpositions of many objects, each off-diagonal term $\mathcal{O}_{mn}$ behaves like the sum of a huge number of random variables; the law of large numbers implies small fluctuations in m and n and the possibility to replace it with its typical value. A clear example of the random superposition of many states we are discussing is given in Ref. [59]. Here the Berry conjecture is valid: the high-energy eigenstates are random superpositions of products of plane waves with the same energy but different directions of the total momentum. The new eigenstates are indeed delocalized in the basis of the unperturbed ones (the products of plane waves) and show a diffusive behaviour in phase space. Also in Ref. [58] an analogous delocalization phenomenon can be seen.

Delocalization of eigenstates is an important point which appears frequently in recent works where ETH is shown numerically to happen in quantum many-body systems undergoing a sudden quench [31, 55, 30, 56, 158]. Like the classical case we have discussed before, one adds to the Hamiltonian an integrability-breaking perturbation and looks if the system thermalizes after a quench. Also in this case, one tries to understand if there is a threshold in the amplitude of the perturbation beyond which thermalization occurs. It is very interesting to study how the onset of thermalization is related to the properties of delocalization of the eigenstates in the basis of the unperturbed ones [31, 30] or another basis of simple states [55, 158]. There is a large numerical evidence that, whenever the thermalization threshold is overcome, the eigenstates move from localized to extended. For instance, in Ref. [55] the onset of thermalization in an interacting fermionic chain

corresponds to the energy-eigenstates becoming extended in the basis of the momentum eigenstates; in Ref. [30], the same happens for a spin chain in the basis of the quasi-particle eigenstates. This effect is reminiscent of a *many-body localization transition* [159, 30, 160]. Noteworthy, no external disorder is needed for many-body localization to occur: the intrinsic random properties of a quantum chaotic Hamiltonian are enough.

The ETH we have described has been shown to be the mechanism behind quantum thermalization in many situations, by means of analytical [58, 59, 67, 95, 110] and numerical [26, 55, 30, 69, 161, 31, 158, 162] tools; these works refer to non-equilibrium states evolving under static Hamiltonians, in the next section we will see what happens when the Hamiltonian is instead time-periodic.

5.2   Periodic driving: ETH at $T = \infty$.

All the discussion concerning ETH can be generalized to the case of a periodic driving. In this case, we no longer have the constraint of energy conservation; from a classical perspective, if the system is ergodic and mixing and the phase space is bounded, we expect that the trajectories explore uniformly all this space: nothing forces them to be confined to some energy shell. The equivalent in this case of the microcanonical ensemble is therefore a distribution uniform in the phase space, corresponding to the condition of infinite temperature and maximum entropy. As in the autonomous case, observables evaluated over single classical trajectories do not converge to their infinite temperature values, which are recovered only after a time-average, similarly to Eq. (5.1). To see relaxation, therefore, we need to assume a coarse graining in the initial conditions. In the quantum case, as already discussed, such a coarse graining is naturally provided by the quantum fluctuations, so here we indeed expect relaxation to the infinite-temperature values.

Such expectations are consistent with the numerical results of Ref. [70]. By means of exact diagonalization, the authors apply a periodic driving to a system (a disordered spin chain) whose unperturbed eigenstates show a transition, in the basis of the local-spin-operators eigenstates, from localized to ergodic *i.e.* obeying ETH [158]. The driving field couples only to the central site of the system, and provides a stepwise-constant periodic driving: the system evolves alternatively under the unperturbed Hamiltonian and the perturbation. [4] When the system which undergoes the driving is inside the localized phase, the energy absorption saturates well below the $T = \infty$ value, and the Floquet states are localized in the basis of the unperturbed eigenstates. On the contrary, when the authors apply the periodic driving to

---

[4]This is equivalent to considering a perturbation of the "kicking" type: a periodic sequence of delta peaks.

the system in the ergodic phase, they observe that it heats up to $T = \infty$, and connect this fact with the Floquet states being extended in the basis of the unperturbed eigenstates. Indeed, in Ref. [71], it has been shown explicitly that, in the latter case, the Floquet states obey ETH at $T = \infty$. At variance with the quantum quench, here there is no energy conservation, and one sees that each Floquet state is a random superposition of all the eigenstates of the unperturbed Hamiltonian, not restricted to an energy shell; the expectation value of an observable on any Floquet state (or, equivalently, Floquet mode) corresponds to the infinite temperature value:

$$\langle \Psi_\alpha(t)| \, \hat{\mathcal{O}} \, |\Psi_\alpha(t)\rangle = \langle \Phi_\alpha(t)| \, \hat{\mathcal{O}} \, |\Phi_\alpha(t)\rangle = \langle \mathcal{O}\rangle_{T=\infty} \equiv \frac{1}{\mathcal{N}} \, \mathrm{Tr}\left[\hat{\mathcal{O}}\right] \;, \qquad (5.8)$$

where $\mathcal{N}$ is the dimension of the Hilbert space [5]. This $T = \infty$ ETH condition for the Floquet expectation values implies immediately, with an argument similar to that of Eq. (5.6), that the time averages of the observables coincide with their $T = \infty$ value. To show this, simply expand the state of the system in the many-body Floquet basis $|\psi(t)\rangle = \sum_\alpha R_\alpha \mathrm{e}^{-i\overline{\mu}_\alpha t} |\Phi_\alpha(t)\rangle$; if there are no degeneracies (this is often case in quantum chaotic problems) Eq. (5.8) immediately implies

$$\overline{\langle \psi(t)| \, \hat{\mathcal{O}} \, |\psi(t)\rangle} = \langle \mathcal{O}\rangle_{T=\infty} = \frac{1}{\mathcal{N}} \, \mathrm{Tr}\left[\hat{\mathcal{O}}\right] \;. \qquad (5.9)$$

We can see here that, because of ETH, the stroboscopic and the instantaneous time averages give the same result. That is so because, at any time t, the expectations of the observables over the Floquet-diagonal ensemble Eq. (2.14) are equal to the infinite temperature values. Moreover, using an argument similar to the one following Eq. (5.7), we can see that ETH implies small Floquet off-diagonal elements and then small time fluctuations $\delta\mathcal{O}_{\mathrm{time}}$ of the observables which are indeed vanishing in the thermodynamic limit.

In the following, we will illustrate these ideas with the explicit example of the Lipkin model undergoing a periodic driving.

5.3   The Lipkin model: Introduction

We devote this Chapter to studying the periodically driven Lipkin model [163], which is the fully-connected version of the quantum Ising model in transverse field discussed in Chap. 3. In the limit in which the number of spins N tends to infinity, the Lipkin model coincides with the mean field version of the Ising model, and correctly predicts some noteworthy aspects of its equilibrium physics, like the second-order ferromagnet-to-paramagnet quantum phase transition occurring as a function of the transverse field. The coherent quantum dynamics of the Lipkin model under a periodic driving is

---

[5]The infinite temperature density matrix, whatever is the Hamiltonian, is always given by $1/\mathcal{N}$ times the identity.

nevertheless very different from that of the one-dimensional quantum Ising chain: in Chap. 3 we have seen, indeed, that, due to integrability, the system reaches always a steady periodic regime very different from any thermal behaviour. On the contrary, we will see that, in some range of parameters, the periodically-driven Lipkin model obeys ETH and then thermalizes to infinite temperature; this corresponds to a chaotic classical dynamics for $N \rightarrow \infty$. The discussion about the dynamics given in this section follows the presentations of Refs. [164, 165, 166]. We write the Hamiltonian of the model with N sites in the form

$$\widehat{H}(t) = -\frac{2J}{N} \sum_{i,j}^{N} \widehat{S}_i^z \widehat{S}_j^z - 2\Gamma(t) \sum_i^N \widehat{S}_i^x \ . \tag{5.10}$$

where $\widehat{\mathbf{S}}_i$ are 1/2-spins taken in their dimensionless form $\widehat{\mathbf{S}}_i \rightarrow \widehat{\mathbf{S}}_i/\hbar$. In the present Chapter, we set $\hbar = 1$. We define the total spin operator $\widehat{\mathbf{S}} = \sum_i \widehat{\mathbf{S}}_i$; in terms of its components the Hamiltonian can be written as

$$\widehat{H}(t) = -\frac{2J}{N} \widehat{S}_z^2 - 2\Gamma(t)\widehat{S}_x \ . \tag{5.11}$$

If we define $\mathcal{H}_j$ the two-dimensional Hilbert space associated to a 1/2-spin $\widehat{\mathbf{S}}_j$, the total Hilbert space is the tensor product of these spaces $\mathcal{H} = \bigotimes_j \mathcal{H}_j$. Thanks to the theory of composition of angular momenta [167], we can decompose this Hilbert space into the direct sum of Hilbert spaces $\mathcal{H}(S)$, the operator $\widehat{\mathbf{S}}^2$ restricted to each of them is a multiple of the identity with eigenvalue $S(S+1)$. Given an integer or half odd $S \in [0, N/2]$, there are

$$g_N(S) = \binom{N}{\frac{N}{2} + S} - \binom{N}{\frac{N}{2} + S + 1} \tag{5.12}$$

different subspaces $\mathcal{H}(S)$ with this eigenvalue (see Ref. [165] and, for a proof based on the induction principle of this formula, appendix E.1). Because the Hamiltonian commutes at all times with the operator $\widehat{\mathbf{S}}^2$, it is block diagonal in the subspaces $\mathcal{H}(S)$ [167]. Fixing a time t, the Hamiltonian can be diagonalized in each subspace giving $2S + 1$ eigenvalues, the discussion above implies that each of these eigenvalues is $g_N(S)$ times degenerate. Because of the decomposition in independent blocks not mixed by the dynamics, we can study the evolution of the system restricting to one of these subspaces $\mathcal{H}(S)$. Considering here the eigenstates $|S, M\rangle$ of the operator $\widehat{S}_z$ $(-S \le M \le S)$, we expand in this basis the state $|\psi(t)\rangle$ of the system restricted to this subspace

$$|\psi(t)\rangle = \sum_{M=-S}^{S} \psi_M(t)|S, M\rangle \ .$$

Substituting this expansion in the Schrödinger equation $i\partial_t|\psi(t)\rangle = \widehat{H}(t)|\psi(t)\rangle$ and projecting on $\langle S, M|$, we find that the amplitudes $\psi_M(t)$ obey the equation

$$i\frac{\partial}{\partial t}\psi_M = -\frac{2J}{N}M^2\psi_M - \Gamma(t)\sum_{\alpha=\pm 1}\sqrt{S(S+1) - M(M+\alpha)}\,\psi_{M+\alpha}\ . \quad (5.13)$$

This equation, easy to implement numerically, reduces in the limit $N \to \infty$ to a single-particle dynamics. To see this point, we introduce the variable $m = 2M/N$, we define k such that $S = \frac{N}{2}(1-2k)$ and rewrite Eq. (5.13) as

$$
\begin{aligned}
i\left(\frac{1}{N}\right)\frac{\partial}{\partial t}\psi_m(t) &= -\frac{J}{2}m^2\psi_m(t) \\
&\quad - \frac{\Gamma(t)}{2}\sum_{\alpha=\pm 1}\sqrt{(1-2k)^2 - m^2 + \frac{2}{N}(1-\alpha m)}\,\psi_{m+\frac{2}{N}\alpha}(t)\ .
\end{aligned}
$$

We then treat perturbatively the square root, forgetting terms order $1/N$ and higher, and setting $\sqrt{(1-2k)^2 - m^2 + \frac{2}{N}(1-\alpha m)} \to \sqrt{(1-2k)^2 - m^2}$. Both m and k become continuous variables for $N \to \infty$, with $k \in [0, 1/2]$ and $m \in [-(1-2k), (1-2k)]$. On the contrary, we treat the wave-function non-perturbatively, by introducing the translation operator in m, $e^{a\partial_m}$, such that $e^{a\partial_m}\psi_m(t) = \psi_{m+a}(t)$, obtaining:

$$
\begin{aligned}
i\left(\frac{1}{N}\right)\frac{\partial}{\partial t}\psi_m(t) &= -\frac{J}{2}m^2\psi_m(t) \qquad\qquad\qquad\qquad (5.14)\\
&\quad - \Gamma(t)\sqrt{(1-2k)^2 - m^2}\,\cos\left(-i\frac{2}{N}\partial_m\right)\psi_m(t)\ .
\end{aligned}
$$

As anticipated, this is the Schrödinger equation of a single particle in one-dimension, with an effective Planck's constant $\hbar_{\text{eff}} = \frac{1}{N}$: the limit $N \to \infty$ coincides with the semiclassical limit. In Eq. (5.14) m plays the role of a coordinate $\hat{Q}$, while the operator $-\frac{i}{N}\partial_m$ plays the role of a momentum $\hat{P}$: we can see this by evaluating the commutator $\left[m, -\frac{i}{N}\partial_m\right] = i\hbar_{\text{eff}}$. In the limit of large N and small $\hbar_{\text{eff}}$ we can apply the semiclassical WKB approximation [164, 168] and explore the dynamics of wave-packets. We can choose a minimum uncertainty wave-packet, with uncertainties in both P and Q scaling like $1/\sqrt{N}$. One can show [164] that, in the limit of large N, the expectation values of P and Q on the wave-packet (which in this limit become classical values) obey the Hamilton's equations

$$
\begin{cases}
\dot{Q}(t) = \partial_P H(Q,P,t) \\
\dot{P}(t) = -\partial_Q H(Q,P,t)
\end{cases}
\qquad (5.15)
$$

with an Hamiltonian given by the classical version of Eq. (5.14)

$$H(Q,P,t) = -\frac{J}{2}Q^2 - \Gamma(t)\sqrt{(1-2k)^2 - Q^2}\,\cos(2P)\ , \qquad (5.16)$$

and the restriction $Q \in [-(1 - 2k), (1 - 2k)]$. These formulae allow us to discuss the equilibrium properties of the model at fixed Γ in the limit of large N. In this limit, the eigenstates are given by the WKB theory, in particular the ground state is a minimum uncertainty wave packet centred in a minimum of the classical Hamiltonian. [6] For fixed Γ, we see, evaluating the minimum of Eq. (5.15), that the system shows a second order quantum phase transition (QPT) at $\Gamma/J = 1$, with order parameter $Q = \lim_{N\to\infty} \frac{2}{N}\langle \widehat{S}_z \rangle_{\mathrm{GS}}$. Indeed, when $\Gamma/J > 1$ the minimum is in $(Q = 0, P = 0)$ and the system is in the paramagnetic phase. Instead, when $\Gamma/J < 1$ there are two degenerate minima with $P = 0$ but non-vanishing Q

$$ Q_\pm = \pm\sqrt{(1 - 2k)^2 - \left(\frac{\Gamma}{J}\right)^2} \, , \qquad\qquad (5.17) $$

corresponding to a broken-symmetry ferromagnetic phase. As usual in presence of symmetry breaking, although the classical Hamiltonian in Eq. (5.15) is symmetric under the inversion of Q — a symmetry that mirrors the $\mathbb{Z}_2$-invariance of the quantum Hamiltonian in Eq. (5.10) $\mathrm{e}^{-i\pi\widehat{S}_x}\widehat{H}\mathrm{e}^{i\pi\widehat{S}_x} = \widehat{H}$ — the ground state is not symmetric: there are rather two degenerate ground states transformed into each other by the symmetry. [7] The $N \to \infty$ ground state value of the energy is

$$ E_{\mathrm{GS}} = \begin{cases} -\Gamma\sqrt{1 - 2k^2} & \text{for} \quad \Gamma/J < 1 \\ -\frac{\Gamma^2}{2J} - \frac{J}{2}(1 - 2k^2) & \text{for} \quad \Gamma/J > 1 \end{cases} . $$

As we see, the absolute minimum of the energy occurs for $k = 0$, *i.e.* in the non-degenerate subspace with maximum spin $S = N/2$. From now on we will restrict to such a maximum spin subspace. The classical dynamics of the observables is obtained for $N \to \infty$ by solving numerically the Hamilton's equations Eq. (5.15). When Γ is fixed, due to energy conservation, the Hamilton's equations Eq. (5.15) are integrable: the solutions are closed periodic orbits, which in (Q, P) phase space coincide with the curves of fixed energies $H(Q, P) = E$. In Fig. 5.1 we give two examples of phase portraits

---

[6]To see this [164], we can expand Eq. (5.14) up to second order in $1/N$ and then expand the resulting equation in m around a minimum of the classical Hamiltonian (we can do that because we are interested in low-energy behaviour). What we obtain is the Schrödinger equation of an harmonic oscillator; the ground state is a wave-packet centred in the chosen minimum with coordinate and momentum uncertainties scaling like $\sim \sqrt{\hbar_{\mathrm{eff}}} = \sqrt{\frac{1}{N}}$.

[7]As usual, for any finite N the double-degeneracy of the ground state is lifted, since the wave-packets centred in the two minima $Q_\pm$ have an exponentially small overlap $\sim \mathrm{e}^{-N}$. The ground state is the symmetric combination of the two wave-packets, and is separated by an exponentially small gap from the first excited state, which is the anti-symmetric combination of the two. In the limit of $N \to \infty$ there is no more overlap among the wave-packets, which become degenerate eigenstates localized in each minimum: they are not eigenstates of $\mathrm{e}^{i\pi\widehat{S}_x}$, but this operator maps each one into the other.
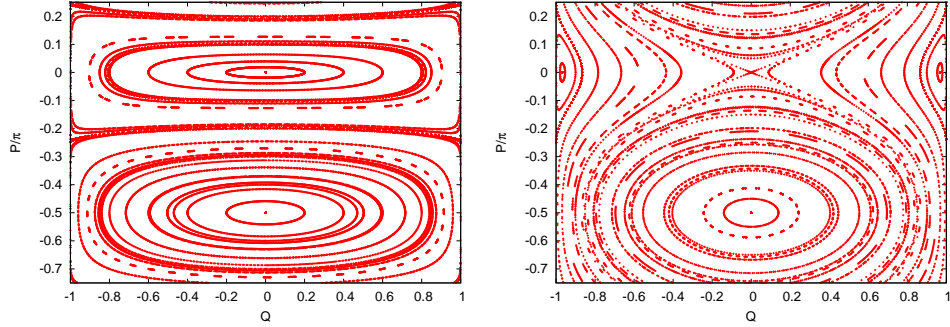
Figure 5.1: (Left panel) Example of phase portrait in the paramagnetic phase ($\Gamma/J = 3$) for the Hamiltonian Eq. (5.15). (Right panel) Phase portrait in the ferromagnetic phase ($\Gamma/J = 0.25$).

for a paramagnetic ($\Gamma/J = 3$) and a ferromagnetic ($\Gamma/J = 0.25$) case. In both cases the phase space is bounded in the Q-coordinate ($Q \in [-1, 1]$) and cyclic in the P coordinate ($P + \pi$ coincides with P). In the paramagnetic case we recognize orbits around the minimum ($Q = 0$, $P = 0$) and the maximum ($Q = 0$, $P = \pi/2$). In the ferromagnetic one there are orbits around the two symmetric minima in ($Q = Q_\pm$, $P = 0$) which are separated from orbits around the maximum at ($Q = 0$, $P = \pi/2$) by a separatrix curve: phase points on this trajectory reach the saddle point of the Hamiltonian ($Q = 0$, $P = 0$) in an infinite time. For numerical implementations, when $\Gamma(t)$ depends on time, it is better to transform Eq. 5.15 into the equations for the three reduced components of the spin $m_\alpha = \langle \widehat{S}_\alpha \rangle_t / S$ with $\alpha = x, y, z$. Using the relations $m_z = Q$, $m_x = \sqrt{1 - Q^2} \cos(2P)$ and $m_y = -\sqrt{1 - Q^2} \sin(2P)$ we find

$$\begin{cases} \dot{m}_x(t) = +2J\, m_y(t)\, m_z(t) \\ \dot{m}_y(t) = -2J\, m_x(t)\, m_z(t) + 2\Gamma(t)\, m_z(t) \\ \dot{m}_z(t) = -2\Gamma(t)\, m_y(t) \end{cases} . \tag{5.18}$$

We see that these equations conserve the modulus squared ($\mathbf{m} \cdot \mathbf{m} = 1$) of the vector $\mathbf{m} = (m_x, m_y, m_z)$, and this fact mirrors the commutation of the quantum Hamiltonian with $\widehat{\mathbf{S}}^2$. Moreover, we notice that these equations are obtained from the Heisenberg equations of motion for the reduced spin operators $\widehat{m}_\alpha = 2\widehat{S}_\alpha / N$ by evaluating their expectation values and neglecting quantum correlations. This is possible in the limit of large N, because the commutator among these operators tends to vanish

$$[\widehat{m}_\alpha, \widehat{m}_\beta] = i\frac{2}{N} \epsilon^{\alpha\beta\gamma} \widehat{m}_\gamma \,, \tag{5.19}$$

where $\epsilon^{\alpha\beta\gamma}$ is the completely antisymmetric tensor. [8]

---

[8]We mention that the classical equations Eq. (5.15) can be obtained also using spin-coherent states [169]: by their use the amplitude $\langle \Psi_f | \hat{U}(t, 0) | \Psi_i \rangle$ (where $\hat{U}(t, 0) =$

Before moving to the analysis of the dynamics in the periodically driven case, we mention that there are many studies on fully-connected driven spin systems, both for the case of a sudden quench of the transverse field [164] and for a slow annealing of the transverse field [171]. In the sudden quench case, the system is taken in the ground state at Γ_i, and the transverse field is suddenly changed from Γ_i to Γ_f; interestingly, a dynamical phase transition if found [164] to occur at $\Gamma_f = \Gamma_c = (\Gamma_i + 1)/2$. Indeed, at Γ_c the phase point associated to the initial ground state energy (which is conserved) lays right on the separatrix of the final Hamiltonian: for $\Gamma_f > \Gamma_c$ it orbits around the maximum with a vanishing time-averaged Q, while for $\Gamma_f < \Gamma_c$ it orbits around one of the two ferromagnetic minima at $(Q_\pm, P = 0)$ and the time-averaged order parameter is non-vanishing. In the case of a slow annealing, the interest focuses on the deviations from adiabaticity, in the context of studies on Quantum Annealing [172, 173, 174], *alias* Adiabatic Quantum Computation [77].

To conclude this section, we observe that the Hamiltonian in Eq. (5.11) reduces to the so-called kicked top model [148] when $\Gamma(t)$ is a time-periodic sequence of delta peaks. Although some of the results we have obtained show similarities with those of the kicked top — the standard "quantum chaos" connections between the regularity of classical dynamics and the characteristics of the Floquet spectral spacing distributions — our point of view will be rather different from that of Ref. [148], because we will take a many-body perspective specifically addressing questions related to the steady state of observables expectations, and the corresponding thermal properties.

$\overleftarrow{\top} \exp\left(-i \int_0^t \widehat{H}(t') \mathrm{d}t'\right)$ is the time-evolution operator) can be written as a Feynman path integral [170]; we obtain the classical equations performing a saddle point integration, legitimate in the limit of large N. For a spin S, coherent states are wave-packets of minimum uncertainty ($\sim \sqrt{1/S}$) in the spin components centred around a certain value of the classical canonical variables P and Q. Introducing the polar coordinates $\phi = -2P$ and $\theta = \arccos Q$, they are obtained by applying to the eigenstate $|S, -S\rangle$ of $\widehat{S}_z$ a rotation of angle θ around the axis $\hat{\mathbf{n}} = \left(\begin{array}{ccc} \sin \phi & -\cos \phi & 0 \end{array}\right)$. The amplitudes of the coherent state $|\theta, \phi\rangle$ in the basis of the eigenstates of the operator $\widehat{S}_z$ are

$$\langle S, M | \theta, \phi \rangle = \sqrt{\binom{2S}{S+M}} \left[\sin\frac{\theta}{2}\right]^{S-M} \left[\cos\frac{\theta}{2}\right]^{S+M} \mathrm{e}^{i(S-M)\phi} .$$

We find convenient also to express this formula directly in terms of the values of the canonical coordinates Q and P where the state is centred

$$\langle S, M | Q, P \rangle = \sqrt{\binom{2S}{S+M}} \left[\frac{1}{2}\sqrt{1-Q^2}\right]^S \left[\sqrt{\frac{1-Q}{1+Q}}\right]^M \mathrm{e}^{-2i(S-M)P} . \qquad (5.20)$$

Equations Eq. (5.15) can be obtained also taking a coherent state $|\theta(t), \phi(t)\rangle$ as variational *Ansatz* and minimizing the resulting action $\mathcal{S} = \int_0^t \langle \theta(t'), \phi(t') | i\partial_{t'} - \widehat{H}(t') |\theta(t'), \phi(t')\rangle \, \mathrm{d}t'$.

5.4 Classical and quantum chaos under periodic driving.

We consider the Lipkin model in Eq. (5.11) undergoing a periodic modulation of the transverse field

$$\Gamma(t) = \Gamma_0 + A \sin(\omega_0 t + \varphi_0) . \qquad (5.21)$$

From now on we will assume $J = 1$. As we have seen, we can restrict ourselves to the subspace $\mathcal{H}(S)$ with $S = N/2$, which is $N+1$-dimensional; the Schrödinger's equation consists of a system of $N+1$ linear differential equations (Eq. (5.13) with $k = 0$), which can be easily integrated numerically on a computer; this is a great simplification, considering that the total Hilbert space is 2^N-dimensional. Thanks to the Floquet theory (see Chap. 2), if we solve the dynamics for the first period of the driving, we can find the evolution at all times. In particular, by diagonalizing the evolution operator over a period $\hat{U}(\tau, 0)$, we can find the $N+1$ Floquet quasi-energies μ_α, [9] and the corresponding Floquet modes $|\Phi_\alpha(t)\rangle$. Moreover, from $\hat{U}(\tau, 0)$ we have easy access to the subsequent stroboscopic dynamics, since $\hat{U}(n\tau, 0) = [\hat{U}(\tau, 0)]^n$. In all the remaining discussion, we take the quasi-energies inside the first Brillouin zone $\mu_\alpha \in [-\omega_0/2, \omega_0/2]$.

We can compare the results of the classical dynamics for $N \to \infty$ with those of a quantum dynamics for N finite but large. The latter comes from the solution of linear differential equations, while the former results from the non-linear Hamilton's Eqs. (5.15). Without driving, as we have seen, these equations are integrable and give rise to a perfectly regular dynamics; in presence of a periodic driving, on the contrary, energy is no longer conserved, and there can be chaos [45]. In the following, we plan to investigate the relationship among classical chaos and the properties of the many-body quantum dynamics given by the Schrödinger equation. For systems with few degrees of freedom, this issue has been widely discussed, giving rise to a plethora of signatures of chaos in the quantum domain [156, 149]. For many-body systems, like the one we are studying, it is more difficult to discuss directly the correspondence with the classical case, but one can use the tools developed in the context of systems with few degrees of freedom to understand if there is integrability or chaos [175, 176, 177]. Here we are rather lucky, because our many-body system, when the number of degrees of freedom is large, can be mapped onto a system with a single degree of freedom: there is a strict analogy to the large-spin kicked top model [148], with the difference that the periodic driving we apply here is smooth.

In Fig. 5.2 we consider different regimes of the dynamics, comparing two qualitative measures of chaos. In the left panels we show some Poincaré

---

[9]We omit the bar over the μ_α because there is no ambiguity here with single-particle quasi-energies

sections of the classical dynamics, while in the right panels we can see the normalized Floquet level spacing distributions for the corresponding quantum cases. The Poincaré section [45] is a plot, in the phase plane (Q, P), of the solution $(Q(t), P(t))$ of Eq. (5.15) taken at stroboscopic times $t = n\tau$ ($\tau = 2\pi/\omega_0$) using different initial conditions. We see in the upper-left panel that driving the system within the paramagnetic phase keeps the dynamics mostly regular; on the contrary (centre and lower-left panel) driving the system inside the ferromagnetic phase gives rise to wide regions of chaotic phase space, even if the driving amplitude is small. The reason is that, when the ferromagnetic Hamiltonian is static, there is a separatrix which is very sensitive to the smallest integrability breaking [45]. If we increase the amplitude of the driving, we move from a partly chaotic phase space (central-left panel) to a fully ergodic dynamics where all the phase space shows chaos (lower-left panel). On the right panels, we show the corresponding Floquet level spacing distributions for $N = 800$. They are the probability distributions of the variables $s_\alpha = \overline{\rho}(\mu_\alpha) \cdot (\mu_{\alpha+1} - \mu_\alpha)$, where $\overline{\rho}(\omega) = \langle \sum_{\alpha=1}^N \delta(\omega - \mu_\alpha) \rangle_{\Delta\mu}$ is the *mean* Floquet density of states [10] (see Ref. [156] for a discussion in the autonomous case). We know that the level spacing distribution $P(s)$ of the eigenvalues of a random matrix Hamiltonian (in the limit of large matrix) assumes a universal form depending only on the symmetry properties of the Hamiltonian under time-reversal [178]. Many works [155, 148] have shown that, when the classical dynamics is ergodic, the levels (eigen-energies in the autonomous case, Floquet quasi-energies in the driven one) corresponding to states in the same symmetry-class (if the Hamiltonian has some symmetry) show a spacing statistics similar to that of a random matrix with appropriate time-reversal symmetry. In our case, the Floquet levels fall in two symmetry classes, according with the corresponding Floquet state being an eigenstate of eigenvalue $+1$ or -1 of the operator $\mathrm{e}^{i\pi\widehat{S}_x}$ under which the Hamiltonian is symmetric [148]. We evaluate the spacing distribution for each class and then average the distributions. When the dynamics is regular (upper-right panel) we see that $P(s)$ is well described by a Poisson distribution $P_P(s) = \mathrm{e}^{-s}$, a result in agreement with the predictions of Ref. [179]; the agreement becomes better for larger N. On the contrary, in the ergodic case (lower-right panel), up to fluctuations vanishing for $N \to \infty$, $P(s)$ is well described by an "orthogonal" $\beta = 1$ Wigner-Dyson distribution $P_{\mathrm{WD}}(s) = \frac{\pi}{2} s \exp\left(-\frac{\pi}{4}s^2\right)$ [149, 178]. This distribution describes the level spacings of both a Gaussian Orthogonal Ensemble (GOE) random matrix Hamiltonian, and a Circular Orthogonal Ensemble (COE) random Floquet operator, even under time-reversal. This result is interesting in connection

---

[10]This is the Floquet density of states $\rho(\omega) = \sum_{\alpha=1}^N \delta(\omega - \mu_\alpha)$ smoothed in ω by a coarse graining over a scale $\Delta\mu$, such that $\omega_0/N < \Delta\mu \ll \omega_0$. This is a mesoscopic scale, much smaller than the width of the Floquet Brillouin zone but nevertheless larger that the average distance between Floquet levels; in this way all traces of singular deltas corresponding to individual levels and level clustering are obliterated.
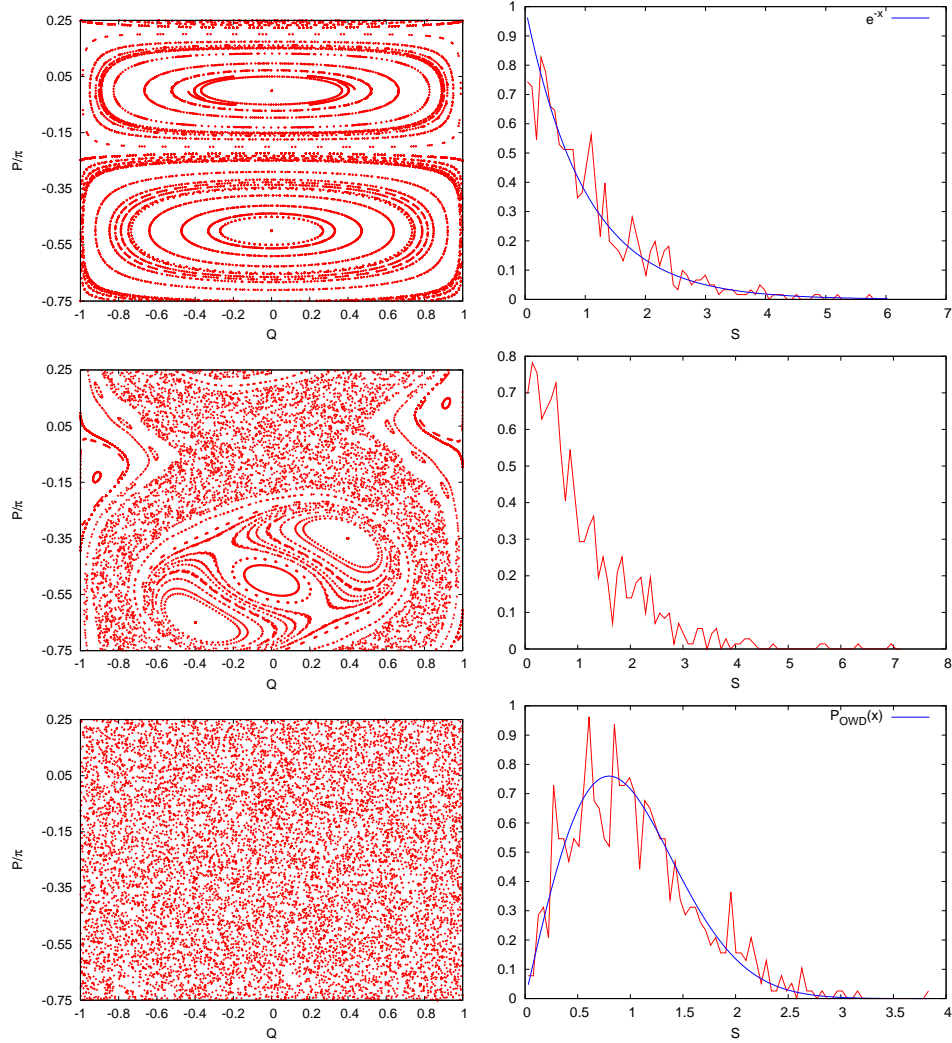
Figure 5.2: On the left we plot the Poincaré sections and on the right the corresponding Floquet level spacing statistics $P(s)$ for different parameters of the driving in Eq. (5.21). In all the plots we choose $\omega_0 = 2$, $\varphi_0 = 0$. In the upper panel the driving is restricted to the paramagnetic phase ($\Gamma_0 = 3$, $A = 0.5$), the classical dynamics is regular and the $P(s)$ is Poissonian. In the lower panel the driving is restricted to the ferromagnetic case ($\Gamma_0 = 0.25$, $A = 0.45$), the classical dynamics is ergodic and the $P(s)$ is Wigner-Dyson. In the middle panel ($\Gamma_0 = 0.25$, $A = 0.05$), the phase space is mixed, regular and chaotic, and the $P(s)$ is intermediate among the two mentioned above.

with the convergence towards a periodic steady regime: if the Floquet levels behave like the eigenvalues of a random matrix, they become a continuum in the limit $N \to \infty$. In the partially chaotic case, the distribution is intermediate among the two introduced before, and is well fitted by the predictions of Ref. [180]. These results on the relationship between regularity properties of classical dynamics and level spacing statistics are very similar to those found for the closely related kicked top model [148].

We will see in the next section how the random properties of the quasi-energies reflect in the behaviour of the Floquet states. Indeed, the quasi-energies μ_α and the Floquet states $|\Psi_\alpha(0)\rangle$ are, respectively, the eigenvalues and eigenstates of the Hermitian matrix $\hat{H}_F$ defined by $\hat{U}(\tau, 0) \equiv e^{-i\tau \hat{H}_F}$. The Wigner-Dyson distribution of the Floquet level spacings tells us that $\hat{H}_F$ is a full random matrix whose eigenstates are superpositions of all the eigenstates of the Hamiltonian $\hat{H}(0)$. The expectation of an observable over each Floquet-state, therefore, is equivalent to a uniform average of the corresponding expectations over the energy eigenstates: This equals the $T = \infty$ value, as we will see better in the next section.

5.5 Asymptotic regime, thermalization and delocalization in energy space

In this section we discuss how the quantum chaos shown by the Floquet quasi-energies $P(s)$ reflects in the evolution of the observables and the properties of the Floquet states. We start by comparing the numerical results for the quantum dynamics of two paradigmatic cases: 1) driving inside the paramagnetic phase, whose classical limit is regular (upper panel of Fig. 5.2) and 2) driving inside the ferromagnetic phase, whose classical limit is ergodic (lower panel of Fig. 5.2). We are in principle interested in the thermodynamic limit $N \to \infty$: indeed, only for $N \to \infty$ the convergence of the observables to a steady periodic regime is possible. Of course this limit is unattainable numerically: we will consider finite-size systems and we will discuss how the fluctuations scaling with N. To compare different values of N, we consider intensive observables, like the energy per site $e(t) = \langle \psi(t)| \widehat{H}(t) |\psi(t)\rangle /N$ and the longitudinal magnetization per site $m_z(t) = 2 \langle \psi(t)| \widehat{S}_z |\psi(t)\rangle /N$, which is the order parameter of the static quantum phase transition. To understand the convergence to a steady regime and the thermal behaviour of these observables, we consider their infinite stroboscopic-time averages and fluctuations. More explicitly, follow-

ing Eqs. (2.18) and (2.19), we have

$$\overline{e(k\tau)} \;=\; \lim_{n\to\infty}\frac{1}{n}\sum_{k=1}^{n}e(k\tau) = \sum_{\alpha}|R_\alpha|^2 e_{\alpha\alpha}(0) \qquad (5.22)$$

$$(\delta e_{\text{strobo}})^2 \;=\; \overline{e^2(k\tau)} - \left(\overline{e(k\tau)}\right)^2 = \sum_{\alpha\neq\beta}|R_\alpha|^2 e_{\alpha\beta}(0)|R_\beta|^2, \quad (5.23)$$

where we define $e_{\alpha\beta}(0) = \langle\Phi_\alpha(0)|\,\hat{H}(0)\,|\Phi_\beta(0)\rangle/N$. (Similar equations can be written for $m_z(t)$.) Here we substitute $\rho_{\alpha\beta}(0)$ with $R_\alpha^* R_\beta$, because we take a pure initial state $|\psi_0\rangle$ with overlaps $R_\alpha = \langle\Phi_\alpha(0)\,|\psi_0\rangle$. We still have the freedom to choose the initial state $|\psi_0\rangle$. To make meaningful comparisons between different values of N, we have to choose an initial state changing in a definite way with N. For instance, we can choose coherent states Eq. (5.20) centred in a fixed point in phase space or, in the ferromagnetic case, the symmetry-broken ground state; in both cases we have a wave-packet with a fixed centre and width scaling like $1/\sqrt{N}$. An alternative possibility is to choose one eigenstate of the operator $\hat{m}_z = 2\widehat{S}_z/N$, i.e. taking $|\psi_0\rangle = |m\rangle = \left|S=\frac{N}{2},\,M=\frac{N}{2}m\right\rangle$, which also changes in a definite way with N.

In the upper panel of Fig. 5.3 we plot some instances of the stroboscopic energy-per-site evolution $e(n\tau)$ for the ergodic (left panel) and regular (right panel) case, together with the corresponding stroboscopic time fluctuations δe_{strobo} (in the inset). In both cases, $e(n\tau)$ fluctuates around $\overline{e(k\tau)}$ (with very small fluctuations, essentially invisible in the chosen scale, in the regular case) but there is an important difference: in the latter case this average depends strongly on the initial state considered, while in the former it is almost independent of the initial state [11] and coincides with the infinite-temperature value of the operator $\hat{H}(0)/N$, of course restricted to the subspace of maximum spin $S = N/2$ which we are considering. Moreover, the stroboscopic time fluctuations δe_{strobo} tend to vanish in the thermodynamic limit: the scaling with $N^{-1/2}$ is very clear for the ergodic case; in the regular case the scaling is less clear but the fluctuations are much smaller. In Fig. 5.3 we consider, for the classically ergodic case (left panel), two different initial states: the symmetry-broken ferromagnetic ground state of the initial Hamiltonian and an eigenstate $|m\rangle$ of $2\widehat{S}_z/N$. In all cases, whatever initial state we take (coherent states, eigenstates of other components of the spin), we can see always the energy fluctuating around the $T = \infty$ value and (if the initial state changes with N in a definite way) the stroboscopic-time fluctuations scale as $N^{-1/2}$. An instance of this remarkable independence of $e(n\tau)$ from the initial state can be seen in the lower panel of Fig. 5.3, where we show $\overline{e(k\tau)}$ versus m when we take as initial state $|m\rangle$; we can see the strong dependence on m in the regular case and the small fluctuations

---

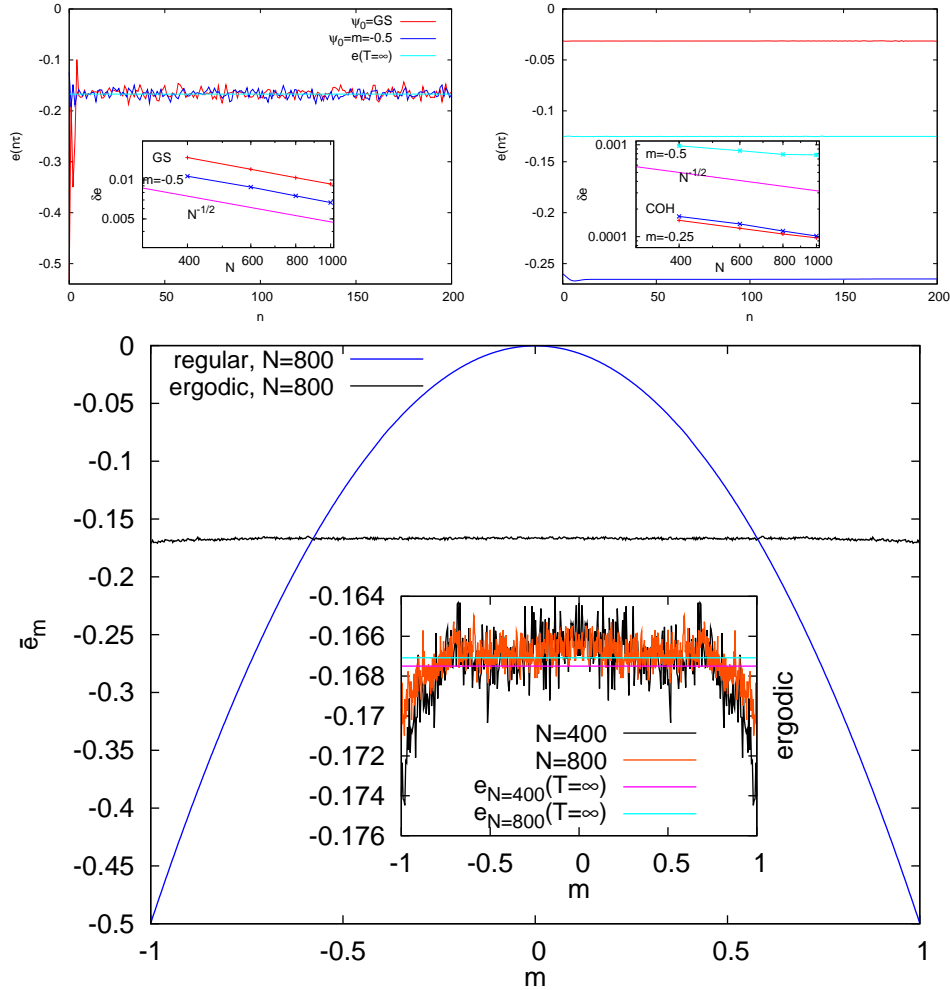[11]There are small differences of order $1/N$ which tend to vanish in the thermodynamic limit.

Figure 5.3: On the upper left panel we see the stroboscopic evolution of energy in the ergodic case for two different initial states, the symmetry-broken ground state and an eigenstate $|m\rangle$ of $2\widehat{S}_z/N$, in both cases the energy converges towards its $T = \infty$ value and fluctuations δe_{strobo} (inset) decay like $N^{-1/2}$. On the upper right panel we show $e(n\tau)$ for the classically regular case; the initial states are two different eigenstates of $2\widehat{S}_z/N$ and a coherent state centred in $P = -0.7485$ and $Q = 0.3236$; here the stroboscopic average $\overline{e(k\tau)}$ attained asymptotically depends on the initial state and fluctuations are much smaller but still decaying with N. On the lower panel we see $\overline{e(k\tau)}$ versus m taking as initial state an eigenstate $|m\rangle$ of $2\widehat{S}_z/N$, in the regular and ergodic case. We observe strong dependence on m in the regular case and the small fluctuations around the $T = \infty$ value in the ergodic case. Parameters are the same as in Fig. 5.2.

around the $T = \infty$ value (getting smaller for larger N) in the ergodic case. Entirely similar results can be found for the other intensive quantities, like $m_z(n\tau)$.

5.5.1 Thermalization and ETH in the ergodic case

Rather than considering particular initial states $|\psi_0\rangle$, we can show in full generality that, in the classically ergodic case, all the possible initial states give rise to thermalization at $T = \infty$ because the Floquet states obey the ETH at infinite temperature. We illustrate this on the left panel of Fig. 5.4 where we consider the energy per site and show its expectation value on the Floquet modes $e_{\alpha\alpha} \equiv \frac{1}{N} \langle \Phi_\alpha(0)| \hat{H}(0) |\Phi_\alpha(0)\rangle$ versus the quasi-energy μ_α. We can see that, in the ergodic case, $e_{\alpha\alpha}$ is indeed independent of the Floquet mode (up to small fluctuations of order $N^{-1/2}$) and equal to the $T = \infty$ expectation value: the Floquet modes obey Eq. (5.8). Indeed we can see that thermalization happens by means of convergence to the Floquet diagonal ensemble which, thanks to Eq. (5.9), coincides with the thermal expectation value at $T = \infty$, whatever is the initial state considered. In the regular case the situation is much different: $e_{\alpha\alpha}$ (also shown in Fig. 5.4) fluctuate strongly between a Floquet mode and the other and we never see thermalization. In the right panel of the same figure we can see how the fluctuations in α of those expectations $\delta(e_{\alpha\alpha}) = \sqrt{\langle e_{\alpha\alpha}^2\rangle - \langle e_{\alpha\alpha}\rangle^2}$ (with $\langle e_{\alpha\alpha}^n\rangle = \frac{1}{N+1} \sum_{\alpha=1}^{N+1} e_{\alpha\alpha}^n$) stay almost constant in the regular case; in the ergodic one instead they are much smaller and decay as $N^{-1/2}$: as we expected, in this case thermalization is more exact when we increase the number of sites [12].

Moreover, to show that time-fluctuations are small for all possible initial states and understand convergence to stationariety in both the regular and the ergodic case, we need to consider the value of the off-diagonal matrix elements in the Floquet basis: $|e_{\alpha\beta}| = \frac{1}{N} \left| \langle \Phi_\alpha(0)| \hat{H}(0) |\Phi_\beta(0)\rangle \right|$. We plot $\langle|e_{\alpha\beta}|\rangle$ – the average in α and β of $|e_{\alpha\beta}|$ – versus N in the left panel of Fig. 5.5; the corresponding fluctuation $\delta|e_{\alpha\beta}|$ is shown in the right panel. In the ergodic case the situation is quite clear: $\langle|e_{\alpha\beta}|\rangle$ is some order of magnitude smaller than the (almost) constantly equal to $e(T = \infty)$ value of the diagonal elements $e_{\alpha\alpha}$, and scales like $N^{-1/2}$; the same scaling is shown by $\delta|e_{\alpha\beta}|$. This implies that the stroboscopic time fluctuations around the $T = \infty$ value of the energy scale like $N^{-1/2}$, whatever is the initial state, as we can observe in the upper left panel of Fig. 5.3. So, for the Lipkin model, time fluctuations show the same scaling as those of the microcanonical ensemble: Here, time fluctuations and quantum fluctuations are of the same order of magnitude

---

[12]We note incidentally that the average over the Floquet modes of the expectation $\langle e_{\alpha\alpha}\rangle = \frac{1}{N+1} \sum_\alpha e_{\alpha\alpha}$ gives right the infinite temperature value of the energy; indeed it is just the trace of the operator $\hat{H}(0)/N$.
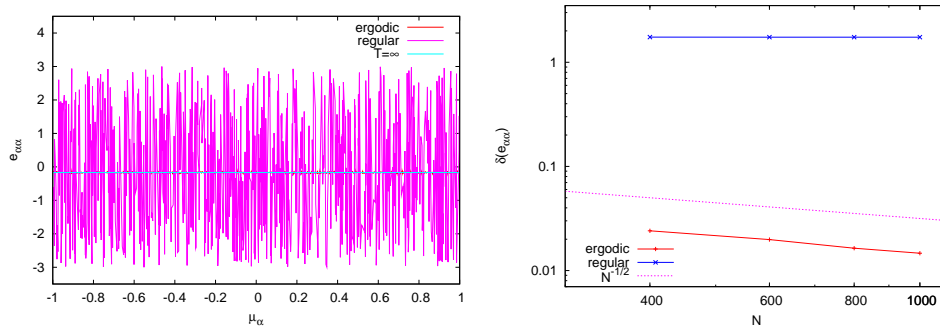
Figure 5.4: In the left panel we show $e_{\alpha\alpha}$ (the expectation value of the unperturbed energy per site over the Floquet mode $|\Phi_\alpha(0)\rangle$) versus μ_α, in both the ergodic and the regular case, for $N = 800$. We see that in the ergodic case it is almost constantly equal to the $T = \infty$ value, in agreement with ETH at $T = \infty$. On the contrary, $e_{\alpha\alpha}$ fluctuates wildly in the regular case. Fluctuations in the ergodic case tend to vanish for large N as $N^{-1/2}$ as shown in the right panel; here we can see also that fluctuations persist for large N in the regular case.

and both contribute to the thermal fluctuations. In the regular case both the average and the fluctuations are smaller than in the regular one: $\langle|e_{\alpha\beta}|\rangle$ scales faster, like N^{-1} and $\delta(|e_{\alpha\beta}|)$ scales still as $N^{-1/2}$. This implies that stroboscopic time fluctuations are much smaller in absolute value than in the ergodic case, in agreement with the upper right panel of Fig. 5.3, also in this case it seems that fluctuations are suppressed for large N. Nevertheless, since the Floquet diagonal elements $e_{\alpha\alpha}$ fluctuate wildly with α, the value $\overline{e(k\tau)}$ to which $e(n\tau)$ relaxes depends strongly on the initial conditions.

5.5.2 ETH and delocalization in energy space

As we have just discussed, thermalization depends strongly on the properties of the Floquet states and the averages of the observables on them. In this Section, we will explore how the relation among thermalization and delocalization of the Floquet states (see Sec. 5.1) manifests in our model. Because each Floquet state is equivalent, in the ergodic case, to the infinite temperature average (see Sec. 5.2), we can expect that each of them is a superposition of all the unperturbed eigenstates with random phases. In this way ETH is valid: the expectation value of an observable over each Floquet state equals its normalized trace Eq. (5.8) because interference among the random phases makes the contribution of the off-diagonal elements small. Indeed, this is just the behaviour of an eigenstate of a random matrix, in agreement with the random matrix behaviour of the Floquet spectrum in the ergodic case (see Fig. 5.2).
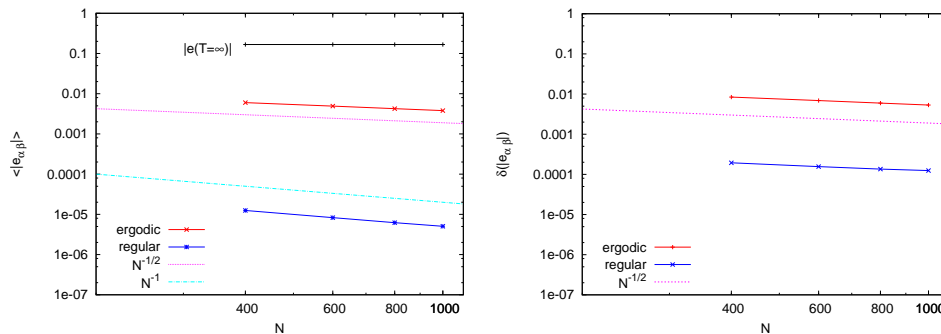
Figure 5.5: (Left panel) Average of the off-diagonal Floquet matrix elements of the energy versus N in the ergodic and regular case, they are compared with the $T = \infty$ value of the same quantity. (Right panel) fluctuations of the same matrix elements versus N.

We can give a quantitative measure of the delocalization of a state in some basis by means of the inverse participation ratio (IPR) [30, 149, 181]. Considering a basis $\mathcal{B} \equiv \{|n\rangle\}_{n=1,\dots,\mathcal{N}}$ of an Hilbert space of dimension $\mathcal{N}$, we can take a state $|\psi\rangle$ in this space and expand it as $|\psi\rangle = \sum_n \psi_n |n\rangle$ (where $\psi_n = \langle n| \psi\rangle$). The IPR of the state with respect the basis $\mathcal{B}$ is defined as [13]

$$\mathcal{I}_{\mathcal{B}}(\psi) = \sum_{n=1}^{\mathcal{N}} |\psi_n|^4 \, .$$

The inverse IPR (participation ratio) physically expresses the number of elements of the basis $\mathcal{B}$ having a significant overlap with the state $|\psi\rangle$. Indeed, if we consider a state $|\phi\rangle$ which is a normalized superposition with uniform square amplitudes of $\mathcal{N}_{\text{eff}}$ elements of the basis

$$|\phi\rangle = \frac{1}{\sqrt{\mathcal{N}_{\text{eff}}}} \sum_{j=1}^{\mathcal{N}_{\text{eff}}} \mathrm{e}^{-i\varphi_j} |n_j\rangle \, ,$$

the IPR is just $\mathcal{I}_{\mathcal{B}}(\phi) = 1/\mathcal{N}_{\text{eff}}$. In case of a generic state $|\psi\rangle$, its inverse gives a measure of the number of states in the basis giving a significant contribution to $|\psi\rangle$. Therefore, a maximally delocalized state will have $\mathcal{I}_{\mathcal{B}}(\psi) = 1/\mathcal{N}$, while each of the states of the basis will have $\mathcal{I}_{\mathcal{B}}(\psi) = 1$, with all the intermediate situations. We see indeed that it is a very useful measure of delocalization, widely employed in the literature on Anderson localization [181], and particularly relevant when the relation among thermalization and delocalization is discussed [55, 30, 31, 70].

---

[13]We can see the IPR as the average value of the square amplitude $|\psi_n|^2$ over the probability distribution induced by the $|\psi_n|^2$.

Here we consider the basis $\mathcal{E} = \{|E_n(0)\rangle\}_{n=1,\ldots,N+1}$ of the eigenstates of the Hamiltonian $\hat{H}(0)$ in the spin sector $S = N/2$; we discuss the localization properties of the Floquet states $|\Psi_\alpha(0)\rangle$ in this basis. For each of them the interesting IPR is

$$\mathcal{I}_\mathcal{E}(\alpha) = \sum_{n=1}^{N+1} |\langle E_n(0)| \Psi_\alpha(0)\rangle|^4.$$

In the left panel of Fig. 5.6 we plot this object averaged over α

$$\langle \mathcal{I}_\mathcal{E}\rangle_\alpha = \frac{1}{N+1} \sum_{\alpha=1}^{N+1} \mathcal{I}_\mathcal{E}(\alpha)$$

versus N for both the regular and the ergodic case. We can see that in the regular case it is approximately constant and equal to ~ 1, while in the ergodic one it scales as N^{-1}. Therefore, as we expected, in the ergodic case the Floquet states are delocalized in the basis of the eigenstates, while they are localized in the regular one [14]. Moreover, as we can see in the right panel of Fig. 5.6, this fact is true for all the Floquet states: fluctuations in $\mathcal{I}_\mathcal{E}(\alpha)$ are small. We notice how the Floquet states being extended on the whole basis of the unperturbed eigenstates is strictly related to thermalization to $T = \infty$ and to the Floquet level spacing statistics $P(s)$ being GOE/COE, that of a full (not banded) random matrix. Remarkably, we can see by inspection the localization properties of the Floquet states in the basis $\mathcal{E}$; we show this in Fig. 5.7, where we plot the square amplitudes $|\langle E_n(0) |\Psi_\alpha(0)\rangle|^2$ versus e_n for a Floquet state $|\Psi_\alpha(0)\rangle$ in the ergodic case (left panel) and the ergodic one (right panel). We can see how the former is extended and the latter is localized, consistently with the evidences coming from the IPR. (The plot refers to a single Floquet state, but the behaviour shown is typical for all Floquet states.) This plot reminds us of the left panel of Fig. 2 in Ref. [70].

One interesting issue has to do with how the convergence to the steady state periodic regime in the quantum case is related to the persistent fluctuations in the classical limit $N \to \infty$. The contrast is very striking, especially for the ergodic case: here the clear and simple quantum thermalization coexists with the irregular fluctuations shown by the classical ergodic and mixing system. Indeed, as we have pointed out, this happens always in the quantum behaviour of a classical ergodic and mixing system [59]: it can be seen as an instance of the quantum fluctuations providing the coarse graining

---

[14]In the ergodic case, the unperturbed Hamiltonian is a ferromagnetic one and all the eigenstates with energy below the broken-symmetry edge [165] ($e^* = -\Gamma_0$) are in doublets which are degenerate up to an exponentially small gap of order $\sim e^{-N}$. In performing these computations we have chosen in each doublet the exact eigenstates, the even and the odd one under the transformation $\mathrm{e}^{i\pi\hat{S}_x}$ which is a symmetry of the Hamiltonian.
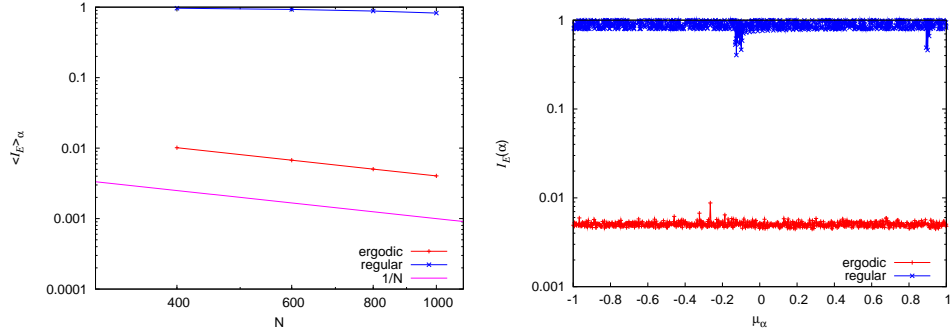
Figure 5.6: (Left panel) Scaling with N of $\langle \mathcal{I}_{\mathcal{E}} \rangle_\alpha$ for the regular and ergodic case. (Right panel) $\mathcal{I}_{\mathcal{E}}(\alpha)$ versus μ_α in both cases for $N = 800$.
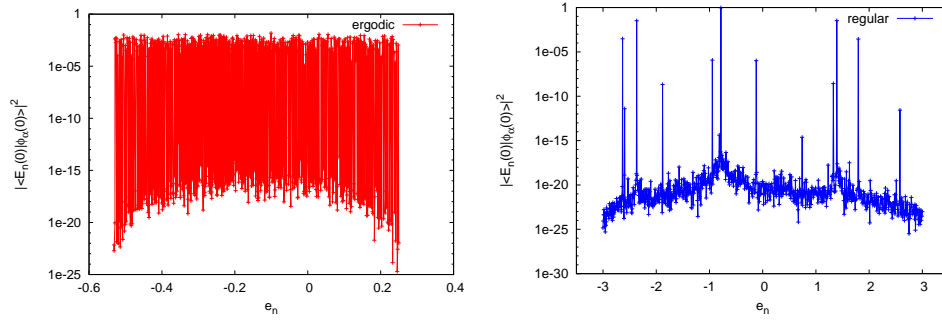

Figure 5.7: Square amplitude of a Floquet state $|\Psi_\alpha(0)\rangle$ in the basis $\mathcal{E}$ for the ergodic case (left panel) and the regular one (right panel). We can see how the former is extended while the latter is localized. The parameters are the same as in the lower and the upper panel of Fig. 5.2 and $N = 800$. In both cases we have taken $\mu_\alpha = -1.34$, but it is not important because, in each case, all the Floquet states behave in the same way for what concerns localization.

necessary for convergence to the thermal regime. To understand better this point we will discuss it in some detail for our case. If N is finite, taking as initial state $|\psi_0\rangle$ a minimum uncertainty wave-packet centred somewhere, the observables coincide with their classical limit for a time logarithmic in N, after which we can see thermalization. Indeed, a minimum uncertainty wave-packet comprises points in the phase space inside a circle of radius $\sqrt{\hbar_{\text{eff}}} \sim 1/\sqrt{N}$. Since the classical dynamics is ergodic, the Lyapunov exponent [152, 164] λ is positive whatever are the initial conditions and trajectories starting from points in the considered circle separate from each other exponentially in time as $e^{\lambda t}$. In a short time, the width of the packet is as large as the whole phase space and the resulting expectation of the observables is very different from the classical counterpart; the time at which this happens is the so-called Ehrenfest time [182, 183, 164] $t^* \sim \frac{1}{2\lambda} \ln N$. Using coherent state wave-packets (Eq. (5.20)), we can see numerically that quantum expectations diverge from the corresponding classical values after $\omega_0 t^*/2\pi \sim 10$ periods of the driving, for $N = 1000$; if we take $N = 10^{23}$ (which might be physically considered as "the thermodynamic limit") our argument gives that the divergence happens after ~ 80 periods. The mathematical limit $N \to \infty$ is indeed very singular: it corresponds actually to the limit $\hbar \to 0$ in semiclassical quantum mechanics [156] When the dynamics is regular, instead, classical and quantum dynamics diverge after a polynomial time $\sim N^\alpha$, this agrees with a less clear scaling of the fluctuations with N in this case.

As a last point, we discuss the behaviour of the order parameter $m_z(t)$ shown in Fig. 5.8. When the dynamics is ergodic, it vanishes after a transient reaching its $T = \infty$ value consistently with ETH. This happens although the driving is restricted to the ferromagnetic phase. If we take as $|\psi_0\rangle$ the symmetry-broken ferromagnetic ground state $|\text{GS}\rangle$, and increase the amplitude of the driving, we see a crossover from a finite to a vanishing value of the stroboscopic average $\overline{m_z(k\tau)}$ [15]. This is similar to the dynamical-phase-transition findings of Ref. [164] and we can give a classical phase space interpretation of this phenomenon. When the driving amplitude A is small, the initial ground state is such that the system stays within a region of regular dynamics and $\overline{m_z(k\tau)}$ differs from 0. By increasing the driving amplitude A, the initial ground state (and the subsequent evolution) fall in a chaotic region and $\overline{m_z(k\tau)}$ vanishes.

---

[15]This crossover seems to behave like a transition: the order parameter vanishes after A overcomes a certain threshold A_c. Nevertheless, the very jagged dependence on A just before A_c makes very difficult to understand if it is really a transition and what is the order. Further studies and larger values of N are in order.
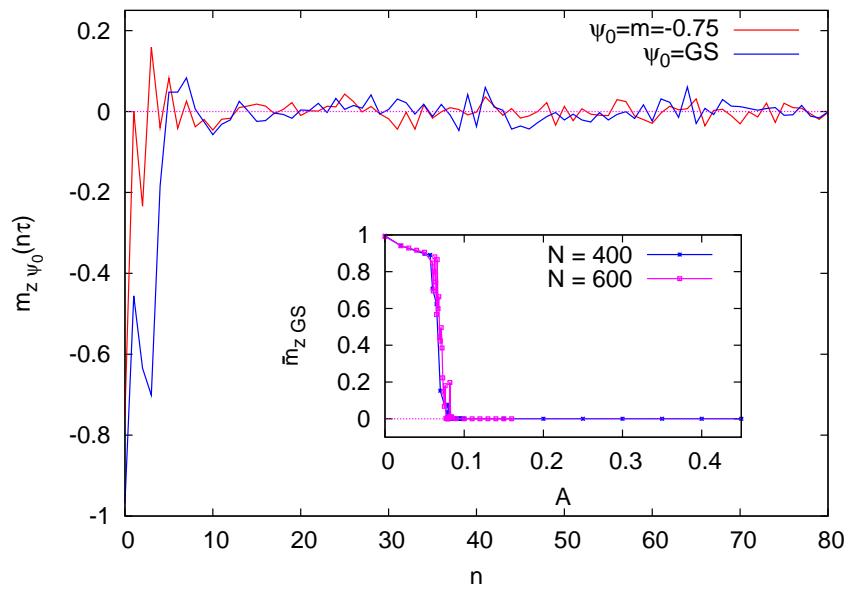
Figure 5.8: (Main figure) The order parameter relaxing to 0 (its $T = \infty$ value) in the ergodic case for different initial conditions in agreement with the Floquet states obeying ETH (the plot is for $N = 800$). (Inset) The infinite stroboscopic-time average of the same object for different values of the driving amplitude; we can see a crossover from a non-vanishing value to 0 reminding us a dynamical phase transition.

5.5.3 Mixed chaotic-regular cases and crossover from regularity to ergodicity.

Up to now we have discussed in detail only two extreme cases, those of completely regular and totally ergodic classical phase space. It is interesting to consider intermediate situations, especially to understand how, in the quantum regime, we move from ergodicity to regularity when we change the parameters of the driving. The most important question is if this process becomes a transition in the thermodynamic limit or is still a smooth crossover. Classically, when the number of degrees of freedom is finite, KAM theorem [46, 45] predicts a smooth increase of the portion of phase space which is chaotic, when the amplitude of the non-integrable term is increased. Above the the so-called KAM threshold, all the phase space becomes ergodic. In the thermodynamic limit, in some cases the threshold remains at a finite value [144, 54] of the non-integrability parameter, in others it moves to a vanishing value [184, 185]. In the quantum case, numerical studies have considered only systems with a small number of particles [31, 161, 30, 28], therefore the situation in the thermodynamic limit is not clear. Moreover, it appears that there can be delocalization without thermalization [31], so the demonstration of the existence of a many body localization transition [160] in some models does not settle the question.

We are going to show that, in our model, we move from regularity to ergodicity with a smooth crossover, which does not become a sharp transition in the thermodynamic limit. This is a manifestation of the quantum-classical correspondence: KAM theorem applies to the classical limit (which has few degrees of freedom): classically the system does not move immediately to ergodicity, but in a range of parameters it shows mixed phase space. We provide an instance of that by means of the case shown in the center left panel of Fig. 5.2; we start our discussion considering the quantum behaviour of the system in this specific case [16].

In the upper left panel of Fig. 5.9 we plot some instances of the stroboscopic evolution of the energy $e(n\tau)$, for different initial states $|\psi_0\rangle$. We consider coherent states (Eq. (5.20)) centred in the chaotic region (COH1 and COH2), a coherent state centred in the regular region (COH3) and an eigenstate $|m\rangle$ of $\hat{m}_z = 2\widehat{S}_z/N$. We can see that, as in the regular case, the asymptotic value depends strongly on the initial state. This is not true for an important class of states: we obtain the same asymptotic value of the observables for all initial states $|\psi_0\rangle$ which are coherent states centred in the chaotic region (like cases COH1 and COH2 in Fig. 5.9) [17]. This is consistent with the qualitative picture of the initial wave-packet being spread by the

---

[16] The quantum behaviour of a strictly related model (the kicked top) when the classical phase space is mixed has been considered in Ref. [150], but from a different point of view.

[17] There are small differences from a state to another which tend nevertheless to vanish for large N.
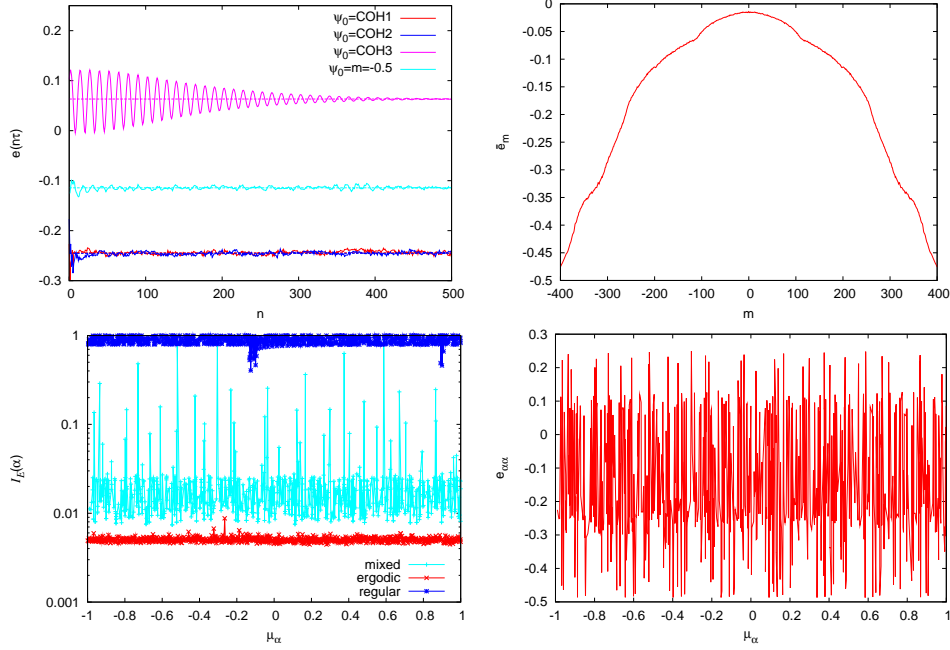
Figure 5.9: Quantum behaviour of a mixed classical-chaotic case (central panel of Fig. 5.2). (Upper left panel) Some instances of evolution of the energy per site $e(n\tau)$ for different initial states $|\psi_0\rangle$. We consider two coherent states in the chaotic region of the phase space (COH1 centred in $P = 0.52$ and $Q = 0.48$, COH2 in $P = -0.42$ and $Q = -0.15$), one coherent state in the regular region (COH3 centred in $P = -1.31$ and $Q = 0.43$) and an eigenstate $|m\rangle$ of $\widehat{m}_z = 2\widehat{S}_z/N$ with eigenvalue $m = -0.5$. (Upper right panel) Time-average $\overline{e_m(k\tau)}$ for initial state $|m\rangle$ versus m, we see the strong dependence on m. (Lower left panel) IPR $\mathcal{I}_{\mathcal{E}}(\alpha)$ versus μ_α for the mixed case we are considering, the regular and the ergodic one. (Lower right panel) Expectation of the energy over a Floquet mode $e_{\alpha\alpha}$ versus μ_α. All the data are for $N = 800$.

mixing dynamics all-over the chaotic region; nevertheless, this asymptotic regime is not thermal. Indeed, we have verified that, although it is possible to define an effective temperature for the asymptotic average of the energy $\overline{e(k\tau)}$, this is impossible for the corresponding average $\overline{m_x(k\tau)}$ of another observable, the local transverse magnetization ($\hat{m}_x = 2\widehat{S}_x/N$). Outside this class of privileged wave-packets, there is a strong dependence of the asymptotic energy on the initial state; we show an instance of this in the right upper panel of Fig 5.9, where we plot $\overline{e(k\tau)}$ versus m, the quantum number of the initial state $|\psi_0\rangle = |m\rangle$, eigenstate of $\hat{m}_z = 2\widehat{S}_z/N$. Also this class of initial states gives rise to a non-thermal asymptotic regime; $\overline{e(k\tau)}$ and $\overline{m_x(k\tau)}$ are described by different finite effective temperatures. This is consistent with the expectation that, there being no energy conservation, the only possible thermal regime is the one at $T = \infty$. In the limit of large N, also in the mixing case, observables do converge to the asymptotic average for different initial states: we have verified that the average $\langle|e_{\alpha\beta}|\rangle$ of the Floquet off-diagonal elements scales to 0 with N and the time fluctuations δe_{strobo} decrease [18] for larger N. The same is valid also for the other observables: interestingly the scaling exponent of $\langle|e_{\alpha\beta}|\rangle$ (~ -0.83) is between -1 (valid for the regular case) and $-1/2$ (valid for the ergodic one). In the lower left panel we plot the IPR $\mathcal{I}_{\mathcal{E}}(\alpha)$ versus μ_α, comparing it with the regular and the ergodic cases considered also in Fig. 5.6. We can see that the mixed case shows much larger fluctuations in μ_α, moreover the values of the IPR are intermediate between the regular and the ergodic ones. Here Floquet states are less extended than in the ergodic case: some are more localized, other more delocalized, with marked differences from one state to the next. The absence of maximal delocalization is related to the Floquet states not obeying ETH, consistently with the absence of thermalization we have discussed above. Finally, the lower right panel of Fig. 5.9 shows the diagonal matrix elements $e_{\alpha\alpha}$ over a Floquet mode $|\Phi_\alpha(0)\rangle$ versus μ_α: they are far from being constant, as in the ergodic case, and show marked fluctuations from a Floquet mode to another. The situation is not different in spirit from the regular case, but in the latter case fluctuations are even larger.

We can find the features we have seen in this classically mixed ergodic-regular case also in the crossover between full regularity and ergodicity. We could plot something like a phase diagram in the space whose coordinates are the parameters of the driving A, ω_0 and Γ_0. There are regions of classically regular, ergodic and mixed dynamics and the properties of the quantum counterpart change correspondingly. For sake of a clearer explanation, we choose to fix the frequency of the driving to $\omega_0 = 2.0$ and its amplitude to $A = 0.45$; we take a classically ergodic case ($\Gamma_0 = 0.25$) and a classically

---

[18]At least for the values of N we have considered, fluctuations do not decrease with a clear scaling for all the considered initial states.
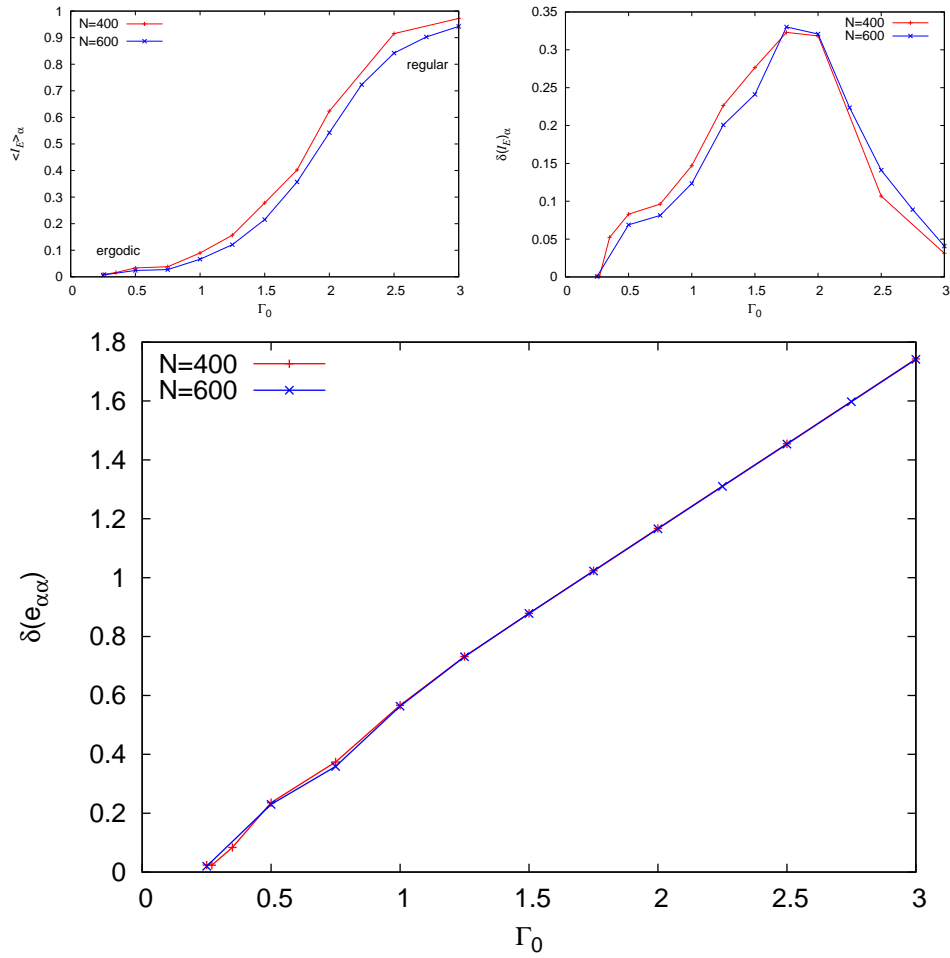
Figure 5.10: (Upper panels) Average IPR (left) and its fluctuations (right) as we move from $\Gamma_0 = 0.25$ (ergodic) to $\Gamma_0 = 3.0$ (regular), at fixed $A = 0.45$ and $\omega_0 = 2.0$. (Lower panel) The same plot for the fluctuations of the diagonal matrix elements $e_{\alpha\alpha}$. All the plots are for $\omega_0 = 2.0$, $A = 0.45$.

regular one ($\Gamma_0 = 3.0$) and see what happens at the intermediate values of Γ_0. In this way we select a segment in the phase diagram; but what happens along this line is representative of what we would see choosing any other path connecting regularity to ergodicity. The first thing we notice in the upper left panel of Fig. 5.10 is that the average IPR $\langle \mathcal{I}_\mathcal{E} \rangle_\alpha$ increases when we change Γ_0 and move from the ergodic to the regular case; this marks a crossover from two extreme condition: delocalization of all the Floquet states and localization of all of them. We can see that the curve is less steep at the extrema of the interval of variation: here $\langle \mathcal{I}_\mathcal{E} \rangle_\alpha$ has an almost constant value because the system is near to being completely ergodic or localized. In the upper right panel of Fig. 5.10 we plot the fluctuations of the IPR

$$\delta(\mathcal{I}_\mathcal{E})_\alpha = \sqrt{\langle [\mathcal{I}_\mathcal{E}(\alpha) - \langle \mathcal{I}_\mathcal{E} \rangle_\alpha]^2 \rangle_\alpha}.$$

We see that, in the completely ergodic and regular cases, they are small: here the Floquet states are uniformly extended or localized. In the intermediate situations the fluctuations are huge: as in the special case considered above, Floquet states are partially delocalized with marked difference among one and another. We can see the relation existing between this delocalization crossover and the validity of the ETH in the lower panel of Fig. 5.10. Here we plot the fluctuations in α $\delta(e_{\alpha\alpha})$ of the Floquet-diagonal matrix elements of the energy-per-site. We see how the fluctuations are small when the Floquet states are maximally delocalized; when Γ_0 increases, classical ergodicity stops, $\langle \mathcal{I}_\mathcal{E} \rangle_\alpha$ starts to increase and also diagonal energy fluctuations $\delta(e_{\alpha\alpha})$ do the same: the Floquet states are no more all equivalent to the $T = \infty$ density matrix. We see that the curve has a uniform slope: energy expectations are more susceptible to the breaking of ergodicity than the IPRs.

This gradual crossover from ergodicity to regularity persists if we consider larger values of N, and does not become a transition: it mirrors the corresponding crossover in the behaviour of the system in the classical limit attained when $N \to \infty$. From the classical point of view, decreasing Γ_0 from the value where all the phase space is regular, the surface of the chaotic portion of phase space increases gradually (thanks to the KAM theorem) until all the phase space is ergodic. From a quantitative point of view, this could be seen by plotting a finite-time numerical estimate of the maximal Lyapunov exponent [144, 152] which vanishes in the regular phase and increases gradually when we move towards the ergodic one in a way similar to what is shown in the lower panel of Fig. 5.10.

5.6 Conclusions

In conclusion, we have shown that, by applying a periodic driving to the Lipkin model, we obtain thermalization of the observables to $T = \infty$, pro-

vided that the driving parameters are such that the classical dynamics is ergodic. This is a noteworthy result for a fully-connected model which, without a driving (like other models with long-range interactions [186]) is far from being ergodic, as we have discussed in Sec. 5.3. Moreover, whenever there is thermalization, its mechanism is given by the Floquet states of the system obeying Eigenstate Thermalization Hypothesis at $T = \infty$. This phenomenon is associated with the underlying classical dynamics being ergodic and mixing and the Floquet levels and states showing signatures of quantum chaos. In particular, the Floquet states are extended in the basis of the unperturbed eigenstates of the Hamiltonian. The link between thermalization and delocalization is very strict: whenever the Floquet states are localized, the system does not thermalize and the observables tend to an asymptotic periodic condition which strongly depends, however, on the initial state. The same conclusions are valid if we consider other forms of driving, like the periodically kicked field along $\widehat{S}_x$ used in Ref. [150].

Remarkably, our conclusions can be verified experimentally. Although seemingly quite artificial, the driven Lipkin model can be shown to be equivalent to a driven two-mode Bose-Hubbard model [150] which can be realized experimentally via modulation of the inter-well barrier height in a double-well BEC realization [187].

Chapter 6

Conclusions and perspectives

In conclusion, in this Thesis we have discussed the dynamics of many body systems under a periodic driving. We have found a strict analogy between this case and that of a quantum quench where the observables can relax to the diagonal ensemble. In the periodically driven case, observables can relax to the Floquet diagonal ensemble attaining asymptotically a steady periodic regime with the same period of the driving; this happens whenever the Floquet spectrum enjoys certain continuity properties. These properties are similar to those of the spectrum of the final Hamiltonian leading to relaxation after a quantum quench. Indeed, we have argued that relaxation to the Floquet diagonal ensemble can happen in all those systems showing relaxation after a quantum quench, for which there are many examples in literature. Our phenomenon seems, therefore, to be pretty general.

We have seen explicitly relaxation to the Floquet-diagonal ensemble for an integrable system, the quantum Ising chain in a periodically-driven transverse field. We have discussed the dependence of the asymptotic value of the energy in connection with the periodic crossing of the critical value of the field. We have shown that, for all the local observables, the Floquet-diagonal ensemble is equivalent to a GGE ensemble; this is connected with the integrability of the model. Discussing the full probability distribution of the work, we have seen that its asymptotic value is different from the prediction of the GGE ensemble, which therefore misses important quantum correlations.

Then we have moved to compare the results of the Floquet-diagonal ensemble with those of Linear Response Theory (LRT) for a driving with small but finite amplitude. We have argued that, whenever the energy-per-site spectrum is bounded and the driving frequency is resonant, this approximation fails in predicting the long-time behaviour of the absorbed energy and of the term in the response connected to the energy absorption. The quantum Ising chain has given us the opportunity to compare the exact evolution with the analytical predictions of LRT. We have discussed both

the cases of extensive and localized driving, in the former case the LRT-predicted steady energy absorption stops after a time independent of L, in the latter this time is linear in L. Remarkably, when the driving is extensive, LRT works for the long-time behaviour of the term in the response not connected to the energy absorption. We have connected the different behaviours for extensive and localized driving with the dynamics of the absorbed excitations. Moreover, we have found that terms in LRT not described by the Floquet-diagonal ensemble come from Floquet off-diagonal terms which become periodic in the LRT limit thanks to gaps closing in the Floquet spectrum.

Another example of relaxation to the Floquet-diagonal ensemble has been provided by the Lipkin model undergoing a periodic driving; here we have noted the strict relation between classical ergodicity, quantum chaos of Floquet levels and states, and the Eigenstate Thermalization Hypothesis (ETH). In the ergodic case, the Floquet states obey ETH leading to observables attaining asymptotically the $T = \infty$ value, whatever is the initial state. This is intimately connected to the Floquet states being chaotic and delocalized in the basis of the unperturbed eigenstates of the Hamiltonian. Indeed, averages over the Floquet-diagonal ensemble are equal to thermal averages at $T = \infty$, therefore the Floquet-diagonal averages equal those at $T = \infty$. When the classical dynamics is regular, instead, Floquet states are localized in the basis of the original eigenstates and the observables relax to a Floquet-diagonal value depending on the initial state. Remarkably, in both cases the off-diagonal elements of the observables in the Floquet basis are small and fluctuations around the Floquet-diagonal value tend to vanish for large number of sites.

Concerning perspectives of future work, there are two points we would like to mention.

One is the behaviour of the entanglement entropy of a driven system. In the case of a quantum quench of one-dimensional systems, relaxation to the diagonal ensemble has been shown to be strictly related to the propagation of the generated excitations [105]; this makes the system entangled and leads to an increase of the so-called entanglement entropy [73, 188], which is an important entanglement measure [131]. We would like to see if a similar picture is valid for the entanglement entropy in case of driven systems, especially in connection with the Ising chain problem [73] and driving around the quantum critical point. For the fully-connected Lipkin model, the picture of propagating excitations fails; nevertheless it would be very interesting to compare the behaviour of the entanglement entropy of this model [189] in the two cases of classically ergodic and regular dynamics.

A second question concerns the dynamics of driven models with integrability-breaking terms. Considering, for instance, the driven Ising chain, we can see that, in many physical realizations, this model is only meaningful to describe the low-energy dynamics of the system. Driving the system provides

106

energy to it and non-integrable terms become relevant, so it is interesting to consider their effect on the properties of the asymptotically periodic regime. Pretending to do that in an exact way would allow us to consider only very small systems, very far from the thermodynamic limit, as we can see in many examples in the literature [26, 55, 30, 69, 161, 31, 70]; the situation is a bit better if t-DMRG is employed [28, 19, 20, 38]. A possibility is to use approximate methods, like a time-dependent mean field treatment, working with Jordan-Wigner fermions. In this way we would be able to consider larger systems, although in an approximate way; as usual our focus would be on the threshold of ergodicity, its relation with delocalization and if the crossover to regular behaviour turns into a sharp transition in the thermodynamic limit. An alternative possibility would be to discuss the dynamics of the driven Hubbard model by means of a Gutzwiller Ansatz [190].

f

Acknowledgements

it will be resumed some day. It is even sadder to leave all the people whose friendship has helped me to overcome the worst moments of these difficult years, it is impossible to mention everyone, but a special mention is deserved by my dear friends of the CUT (Centro Universitario Teatrale), the crew in the SISSA canteen and library, my friends and colleagues Anna, Davide, Nicola, Luo Ye and Giacomo and Prof. Michele Fabrizio whose bright understanding equals his humanity. In conclusion, I thank you, reader, for the patience which has led you to read what has been written in this Thesis.

Appendix A

Coherent destruction of tunneling

We consider the dynamics of small-k non-adiabatic modes, which should be excited even at low frequencies unless effects of Coherent destruction of tunneling [120, 194, 97] intervene. To see how this happens, we consider strongly non-adiabatic modes $k \ll \omega_0$: using that $\Delta_k = \sin k \approx k$ and $\cos k \simeq 1 - k^2/2$, we can approximate the Hamiltonian in Eq. (3.2) to 2nd order in k

$$H_{k\ll1}(t) \simeq \begin{pmatrix} \frac{k^2}{2} + \cos(\omega_0 t) & -ik \\ ik & -\frac{k^2}{2} - \cos(\omega_0 t) \end{pmatrix}. \qquad \text{(A.1)}$$

Now we change reference frame, via the transformation

$$|\psi_k(t)\rangle = V(t) \left|\widetilde{\psi}_k(t)\right\rangle \quad \text{with} \quad V(t) = \mathrm{e}^{-i\sin(\omega_0 t)\sigma^z/\omega_0}. \qquad \text{(A.2)}$$

In the new reference frame the evolution is given by the Schrödinger equation with the Hamiltonian

$$\widetilde{H}_{k\ll1}(t) \simeq \sigma^z \frac{k^2}{2} + k\sigma^y \exp\left(2i\frac{\sin(\omega_0 t)}{\omega_0}\sigma^z\right). \qquad \text{(A.3)}$$

To first order in perturbation theory (using as perturbation the Hamiltonian in Eq. (A.3)) we obtain that the evolution operator over a period is

$$
\begin{aligned}
\widetilde{U}_{k\ll1}(\tau,0) &\simeq \mathbf{1} - i \int_0^\tau \widetilde{H}_{k\ll1}(t)\,\mathrm{d}t \\
&= \mathbf{1} - i \begin{pmatrix} \dfrac{k^2}{2} & -ikJ_0\left(\dfrac{2}{\omega_0}\right) \\ ikJ_0\left(\dfrac{2}{\omega_0}\right) & -\dfrac{k^2}{2} \end{pmatrix} \tau.
\end{aligned}
$$

$$\text{(A.4)}$$

The application of first order perturbation theory is justified because we have assumed $k \ll \omega_0$. We can see that, whenever $J_0 \left(\dfrac{2}{\omega_0} \right)$, the out-of-diagonal terms vanish and exciting the mode considered becomes impossible to first order in k. This phenomenon is the so-called Coherent destruction of tunneling, diagonalizing Eq. (A.4), we can see how this fact reflects in the structure of the Floquet states and gives rise to the dips in energy absorption seen in Fig. 3.3-b. More details about this question can be found in the Supplementary material of Ref. [66].

Appendix B

Details on the dynamics of the Quantum Ising chain

We consider the case of a generic non-uniform Hamiltonian. After the Jordan-Wigner transformation

$$
\begin{aligned}
\hat{\sigma}_j^x &= 1 - 2c_j^\dagger c_j \\
\hat{\sigma}_j^z &= \tau_j \left(c_j^\dagger + c_j \right) \\
\hat{\sigma}_j^y &= i\tau_j \left(c_j^\dagger - c_j \right) ,
\end{aligned}
\tag{B.1}
$$

the Hamiltonian Eq. (3.1) of the system acquires a quadratic fermion form. If we consider anti-periodic boundary conditions like in Section 3.1 we have

$$
\begin{aligned}
\hat{H}(t) &= -\sum_{j=1}^{L-1} \left[J_j(\hat{c}_j^\dagger \hat{c}_{j+1} + H.c.) + (\hat{c}_j^\dagger \hat{c}_{j+1}^\dagger + H.c.) \right] + \sum_{j=1}^{L} h_j(t)(2\hat{c}_j^\dagger \hat{c}_j - 1) \\
&+ J \left[(\hat{c}_L^\dagger \hat{c}_1 + H.c.) + (\hat{c}_L^\dagger \hat{c}_1^\dagger + H.c.) \right] .
\end{aligned}
\tag{B.2}
$$

If we define an appropriate $2L \times 2L$ matrix $\mathbb{H}(t)$, a Nambu column vector of Fermionic operators

$$
\widehat{\boldsymbol{\Psi}} = \begin{pmatrix} \hat{c}_1 \\ \vdots \\ \hat{c}_L \\ \hat{c}_1^\dagger \\ \vdots \\ \hat{c}_L^\dagger \end{pmatrix} = \begin{pmatrix} \hat{\mathbf{c}} \\ \hat{\mathbf{c}}^\dagger \end{pmatrix}
\tag{B.3}
$$

and the row-vector $\widehat{\boldsymbol{\Psi}}^\dagger$ which is its Hermitian conjugate, we can give to the Hamiltonian a shape like that of Eq. (3.2)

$$
\hat{H}(t) = \widehat{\boldsymbol{\Psi}}^\dagger \cdot \mathbb{H}(t) \cdot \widehat{\boldsymbol{\Psi}} = \begin{pmatrix} \hat{\mathbf{c}}^\dagger & \hat{\mathbf{c}} \end{pmatrix} \begin{pmatrix} \mathbf{A}(t) & \mathbf{B} \\ -\mathbf{B} & -\mathbf{A}(t) \end{pmatrix} \begin{pmatrix} \hat{\mathbf{c}} \\ \hat{\mathbf{c}}^\dagger \end{pmatrix} .
\tag{B.4}
$$

Here, the block structure of $\mathbb{H}(t)$ is a consequence of particle-hole symmetry, the blocks $\mathbf{A}(t)$ and $\mathbf{B}$ are $L \times L$ are real matrices; their elements are all vanishing but those given by

$$\begin{cases} A_{j,j} = h_j \\ A_{j,j+1} = A_{j+1,j} = -\dfrac{J_j^+}{2} = -\dfrac{J_j}{2} \end{cases} \quad \begin{cases} B_{j,j} = 0 \\ B_{j,j+1} = -B_{j+1,j} = -\dfrac{J_j^-}{2} = -\dfrac{J_j}{2} \end{cases} \quad \text{(B.5)}$$

Anti-periodic boundary conditions give us the supplementary conditions

$$\begin{aligned} A_{L,1} &= A_{1,L} = \frac{J_L}{2} \,, \\ B_{L,1} &= -B_{1,L} = \frac{J_L}{2} \,. \end{aligned} \quad \text{(B.6)}$$

At every instant of time, we can reduce the Hamiltonian in a quadratic diagonal Fermion form by applying a unitary transformation on the Nambu spinors

$$\widehat{\boldsymbol{\Phi}}_t = \mathbb{U}_t^\dagger \widehat{\boldsymbol{\Psi}} = \begin{pmatrix} \mathbf{U}_t^\dagger & \mathbf{V}_t^\dagger \\ \mathbf{V}_t^T & \mathbf{U}_t^T \end{pmatrix} \begin{pmatrix} \hat{\mathbf{c}} \\ \hat{\mathbf{c}}^\dagger \end{pmatrix} . \quad \text{(B.7)}$$

$\mathbb{U}_t$ diagonalizes the matrix $\mathbb{H}(t)$ which, thanks to the particle-hole symmetry of the Hamiltonian, is divided in $L \times L$ blocks related to each other (see Eq. (B.4)). This property reflects in the block form of the operator $\mathbb{U}_t^\dagger$. We can write the diagonalization relation explicitly:

$$\hat{H}(t) = \widehat{\boldsymbol{\Psi}}^\dagger \cdot \mathbb{H}(t) \cdot \widehat{\boldsymbol{\Psi}} = \widehat{\boldsymbol{\Phi}}_t^\dagger \cdot \mathbb{U}_t^\dagger \cdot \mathbb{H} \cdot \mathbb{U}_t \cdot \widehat{\boldsymbol{\Phi}}_t = \widehat{\boldsymbol{\Phi}}_t^\dagger \cdot \mathbb{E}_D(t) \cdot \widehat{\boldsymbol{\Phi}}_t \,.$$

Here $\mathbb{E}_D(t) = \text{diag}\left(\epsilon_\mu(t), -\epsilon_\mu(t)\right)$ is a $2L \times 2L$ diagonal matrix. If, in analogy with Eq. (B.3), we define L Fermionic operators $\gamma_{t\,\mu}$ such that

$$\widehat{\boldsymbol{\Phi}}_t = \begin{pmatrix} \hat{\boldsymbol{\gamma}}_t \\ \hat{\boldsymbol{\gamma}}_t^\dagger \end{pmatrix} \quad \text{(B.8)}$$

we can write the Hamiltonian as

$$\hat{H} = \sum_{\mu=1}^L \epsilon_\mu(t) \left(\hat{\gamma}_{t\,\mu}^\dagger \hat{\gamma}_{t\,\mu} - \hat{\gamma}_{t\,\mu} \hat{\gamma}_{t\,\mu}^\dagger \right) .$$

We can see how the Hamiltonian has been mapped to a problem of free fermions: $\epsilon_\mu(t)$ are the corresponding single-particle excitation energies at time t. The ground state at time t is defined as the state which is annihilated by all the operators $\gamma_{t\,\mu}$ associated to the single-particle excitations

$$\hat{\gamma}_{t\,\mu} |\text{GS}\rangle_t = 0 \quad \forall \mu \,. \quad \text{(B.9)}$$

Making the Ansatz that the many-body ground state has a Gaussian form and enforcing the condition above, it is not difficult to see [122] that it is exactly a Gaussian state given by

$$|\text{GS}\rangle_{\text{t}} = \mathcal{N}_t \, e^{\frac{1}{2}(\hat{\mathbf{c}}^\dagger)^T \cdot \mathbf{Z}_t \cdot (\hat{\mathbf{c}}^\dagger)} \, |0\rangle \quad \text{where}$$

$$|\mathcal{N}_t| \equiv \sqrt{|\det[\mathbf{U}_t]|} \quad \text{and} \quad \mathbf{Z}_t \equiv -(\mathbf{U}_t^\dagger)^{-1} \cdot \mathbf{V}_t^\dagger \qquad (\text{B.10})$$

($\mathbf{U}_t$ and $\mathbf{V}_t$ are $L \times L$ matrices introduced in Eq. (B.7)). By means of a unitary transformation, we can reduce the matrix $\mathbf{Z}_t$ in standard canonical form: we can find some complex coefficients $\lambda_{t\,p}$ and some time-dependent Fermionic operators $\hat{d}_{t\,p}$, $\hat{d}_{t\,\bar{p}}$ such that the many-body state acquires manifestly a BCS form

$$|\text{GS}\rangle_{\text{t}} = \mathcal{N}_{\text{t}} \prod_{p=1}^{L/2} \left(1 + \lambda_{\text{t}\,p} \hat{d}_{\text{t}\,p}^\dagger \hat{d}_{\text{t}\,\bar{p}}^\dagger \right) |0\rangle \,. \qquad (\text{B.11})$$

We can see that it resembles the translationally-invariant ground state Eq. (3.5). We would like to stress that the basis $\{|0\rangle, \hat{d}_{t\,p}^\dagger \hat{d}_{t\,\bar{p}}^\dagger |0\rangle\}_{p=1,\dots,L/2}$ in which the state is factorized is *time dependent*. Moreover, in general, the Hamiltonian is block-diagonal in a different time-dependent basis. For that, as we will see soon, the dynamics cannot be reduced to uncoupled 2×2 subspaces. The uniform case is very special: because of translational invariance the state and the Hamiltonian are block-diagonal in the same fixed basis.

About the dynamics, we can find it by writing the Heisenberg evolution equations for the operators $\hat{c}_{i\,H}(t)$ in Heisenberg representation. In analogy with Eqs. (B.7) and using the $\hat{\gamma}_0$ defined in Eq. (B.8), we define the unitary $2L \times 2L$ matrix $\mathbb{U}(t)$ so that

$$\begin{pmatrix} \hat{\mathbf{c}}_H(t) \\ \hat{\mathbf{c}}_H^\dagger(t) \end{pmatrix} = \mathbb{U}(t) \widehat{\boldsymbol{\Phi}}_0 = \begin{pmatrix} \mathbf{U}(t) & \mathbf{V}^*(t) \\ \mathbf{V}(t) & \mathbf{U}^*(t) \end{pmatrix} \begin{pmatrix} \hat{\gamma}_0 \\ \hat{\gamma}_0^\dagger \end{pmatrix} \,. \qquad (\text{B.12})$$

We can see that $\mathbb{U}(t)$ reduces to its static counterpart Eq. (B.7) at $t = 0$: as we will see more explicitly this is equivalent to enforcing the ground state as the initial condition of the dynamics. The Heisenberg equations of motion for $\hat{c}_{i\,H}(t)$ plus Eq. (B.12) give us a system of $2L \times 2L$ (Bogoliubov-de Gennes) first order differential equations Eq. (3.24). Thanks to the block structure of $\mathbb{U}(t)$ (see Eq. B.12) we can see that it is enough to solve a system of $2L \times L$ equations

$$i\hbar \frac{d}{dt} \begin{pmatrix} \mathbf{U}(t) \\ \mathbf{V}(t) \end{pmatrix} = 2\mathbb{H}(t) \cdot \begin{pmatrix} \mathbf{U}(t) \\ \mathbf{V}(t) \end{pmatrix} \,; \qquad (\text{B.13})$$

where, according to the Ansatz Eq. (B.12), the initial conditions are $\mathbf{U}(t = 0) = \mathbf{U}_0$ and $\mathbf{V}(t = 0) = \mathbf{V}_0$ where $\mathbf{U}_0$ and $\mathbf{V}_0$ diagonalize the Hamiltonian

114

at initial time (see Eq. (B.7)). The many-body state of the system at time t has a Gaussian form very similar to the ground state Eq. (B.11)

$$|\Psi(t)\rangle = \sqrt{|\det[\mathbf{U}(t)]|}\, e^{\frac{1}{2}(\hat{\mathbf{c}}^{\dagger})^{\mathrm{T}} \cdot \mathbf{Z}(t) \cdot (\hat{\mathbf{c}}^{\dagger})} |0\rangle \quad \text{where} \quad \mathbf{Z}(t) \equiv -(\mathbf{U}^{\dagger}(t))^{-1} \cdot \mathbf{V}^{\dagger}(t)\,;$$
(B.14)

from Eq. (B.12) we can see that the $t=0$ initial condition is given right by the ground state. Moreover, by means of Eq. (B.13) it is possible (although lengthy) to show explicitly that this state obeys Schrödinger Equation with Hamiltonian (B.2).

We can evaluate at all times the quantum expectation value of every many-body operator. Because the state is always Gaussian, the Wick's theorem applies and any expectation value can be reduced to the evaluation of the single-particle Green functions $G_{ij}(t) = \langle \hat{c}_i^{\dagger} \hat{c}_j \rangle_t$ and $F_{ij}(t) = \langle \hat{c}_i \hat{c}_j \rangle_t$. Using the Heisenberg representation, Eq. (B.12) and the property Eq. (B.9) of the initial ground state we find

$$\begin{aligned} G_{ij}(t) &= \left[\mathbf{V}(t) \cdot \mathbf{V}^{\dagger}(t) \right]_{ij} \\ F_{ij}(t) &= \left[\mathbf{U}(t) \cdot \mathbf{V}^{\dagger}(t) \right]_{ij}. \end{aligned}$$
(B.15)

For instance, the expectation value of the energy Eq. (B.4) is

$$E(t) = \mathrm{Tr}\left[\mathbf{V}^{\dagger}(t) \cdot \mathbf{A}(t) \cdot \mathbf{V}(t) - \mathbf{U}^{\dagger}(t) \cdot \mathbf{A}(t) \cdot \mathbf{U}(t) + 2\mathbf{U}^{\dagger}(t) \cdot \mathbf{B} \cdot \mathbf{V}(t) \right].$$
(B.16)

In conclusion, although the Hilbert space of this problem has dimension 2^L, we can reduce the dynamics to L Schrödinger-like equations in a fictitious $2L$-dimensional Hilbert space (Eq. (B.13)). We can easily implement them numerically and use them to evaluate all the expectation values of the observables thanks to Eq. (B.15). As discussed in Subsec. 3.3.1, these evolution equations cannot be further reduced in the form of independent 2×2 blocks.

To conclude, we give to the reader the form of the Floquet off-diagonal part of the Green functions we have introduced in Subsec. 3.3.3

$$F_{ij}^{\mathrm{off-diag}}(t) = \sum_{\alpha \neq \beta\, \nu} \left[R_{\alpha i}^* U_{P\nu\alpha}(t) V_{P\nu\beta}^*(t) R_{\beta j} + S_{\beta i}^* V_{P\nu\beta}(t) U_{P\nu\alpha}^*(t) S_{\alpha j} \right] e^{i(\mu_\alpha - \mu_\beta)t/\hbar}$$

$$+ \left[\mathbf{R}^{\dagger} \cdot e^{i\boldsymbol{\mu}t/\hbar} \cdot \mathbf{U}_{\mathbf{P}}^{\dagger}(t) \cdot \mathbf{V}_{\mathbf{P}}^*(t) \cdot e^{i\boldsymbol{\mu}t/\hbar} \cdot \mathbf{S} + \mathbf{S}^{\dagger} \cdot e^{-i\boldsymbol{\mu}t/\hbar} \cdot \mathbf{V}_{\mathbf{P}}^{\mathbf{T}}(t) \cdot \mathbf{V}_{\mathbf{P}}^*(t) \cdot e^{-i\boldsymbol{\mu}t/\hbar} \cdot \mathbf{R} \right]_{ij};$$

$$G_{ij}^{\mathrm{off-diag}}(t) = \sum_{\alpha \neq \beta\, \nu} \left[R_{\alpha i}^* V_{P\nu\alpha}(t) V_{P\nu\beta}^*(t) R_{\beta j} + S_{\beta i}^* U_{P\nu\beta}(t) U_{P\nu\alpha}^*(t) S_{\alpha j} \right] e^{i(\mu_\alpha - \mu_\beta)t/\hbar}$$

$$+ \left[\mathbf{S}^{\dagger} \cdot e^{-i\boldsymbol{\mu}t/\hbar} \cdot \mathbf{U}_{\mathbf{P}}^{\mathbf{T}}(t) \cdot \mathbf{V}_{\mathbf{P}}(t) \cdot e^{-i\boldsymbol{\mu}t/\hbar} \cdot \mathbf{R} + \mathbf{R}^{\dagger} \cdot e^{i\boldsymbol{\mu}t/\hbar} \cdot \mathbf{V}_{\mathbf{P}}^{\dagger}(t) \cdot \mathbf{U}_{\mathbf{P}}^*(t) \cdot e^{i\boldsymbol{\mu}t/\hbar} \cdot \mathbf{S} \right]_{ij}.$$
(B.17)

Appendix C

Asymptotic behaviour and small W "universality" of the work statistics in a periodically driven Ising chain.

C.1 Asymptotic periodic regime of the stroboscopic cumulant generating function.

In this appendix we show how the stroboscopic cumulant generating function tends towards the stationary value given in Eq. (3.50). Our first step is to expand the logarithm in Eq. (C.3) when the argument is near 1. To that purpose, we need to show that the second addend inside the logarithm is < 1. We know that $\sin^2(n\mu_k\tau) \leq 1$ and $(1 - \mathrm{e}^{-2sE_k(0)}) \leq 1$; moreover we notice that

$$2\frac{q_k}{1+q_k} = 2\left|r_k^+\right|^2 \left|r_k^+\right|^2 = 2x^2\left(1 - x^2\right) \tag{C.1}$$

Where we have defined $x \equiv \left|r_k^+\right|$. Maximizing over x we can easily see that

$$2\frac{q_k}{1+q_k} \leq 1\,.$$

In conclusion, we see that the second term is ≤ 1; therefore the ensuing expansion holds for all k only if $s < \infty$, otherwise it holds for all k only when there is no Floquet quasi-resonance. Nevertheless, we see in Fig. 3.7 that the formula Eq. (3.43) for the asymptotic dynamical fidelity is valid also outside this regime, so we are confident that the same thing is here. Defining

$$\xi_k = \xi_k(s) \equiv 2\frac{q_k}{1+q_k}\left(1 - \mathrm{e}^{-2sE_k(0)}\right)\,, \tag{C.2}$$

we can recast Eq. (C.3) as

$$\frac{\mathcal{G}_{n\tau}(s)}{L} = -\sum_{m=1}^{\infty} \int_0^\pi \frac{\mathrm{d}k}{2\pi} \frac{\xi_k^m}{m} \sin^{2m}(\mu_k n\tau) , \tag{C.3}$$

where we have exchanged the integral and the summation thanks to the dominated convergence theorem. At this point we have to expand the sine term in the form

$$\sin^{2m}(\mu_k n\tau) = \frac{(-1)^m}{4^m} \sum_{j=0}^{2m} \binom{2m}{j} (-1)^j e^{2i(m-j)\mu_k n\tau} \tag{C.4}$$

and perform the integral in k in each of the terms of the summation in m. The summation in j, for each m, has a finite number of terms, so there is no problem in exchanging the integral and this sum. The terms where $j \neq m$ contain rapid oscillating factors and vanish in the limit $n \to \infty$ thanks to the Riemann-Lebesgue lemma and the regularity of the factors ξ_k^m; hence, in this limit, we can write

$$\lim_{n\to\infty} \frac{\mathcal{G}_{n\tau}(s)}{L} = -\int_0^\pi \frac{\mathrm{d}k}{2\pi} \sum_{m=1}^{\infty} \frac{1}{4^m} \binom{2m}{m} \frac{\xi_k^m}{m} . \tag{C.5}$$

Thanks to Ref. [119], we can write this expansion in a closed form; defining $f(\xi) \equiv \sum_{m=1}^{\infty} \frac{1}{4^m} \binom{2m}{m} \frac{\xi^m}{m}$ we have

$$\frac{\mathrm{d}}{\mathrm{d}\xi} f(\xi) = \frac{1}{\xi} \left(2\sqrt{\xi} \frac{\mathrm{d}}{\mathrm{d}\xi} \arcsin\left(\sqrt{\xi}\right) - 1 \right) , \tag{C.6}$$

which can be integrated to give

$$\begin{aligned}
f(\xi) &= \int_0^\xi \frac{1}{\xi'} \left[\frac{1}{\sqrt{1-\xi'}} - 1 \right] \mathrm{d}\xi' = \int_0^{\arcsin\sqrt{\xi}} \tan\left(\frac{\eta}{2}\right) \mathrm{d}\eta \\
&= -2 \Big[\log\left(\cos\eta'\right) \Big]_0^{\frac{1}{2}\arcsin\sqrt{\xi}} = -\log\left[\frac{1}{2}\left(1 + \sqrt{1-\xi}\right) \right] .
\end{aligned} \tag{C.7}$$

Here we have performed the substitutions $\xi = \sin^2(\eta)$ and $\eta' = \eta/2$. In conclusion, we have

$$\frac{\mathcal{G}_\infty(s)}{L} \equiv \lim_{n\to\infty} \frac{\mathcal{G}_{n\tau}(s)}{L} = \int_0^\pi \frac{\mathrm{d}k}{2\pi} \log\left[\frac{1 + \sqrt{1-\xi_k(s)}}{2} \right] \tag{C.8}$$

where $\xi_k(s)$ is given in Eq. (C.2).

C.2 Universal edge singularity in the asymptotic distribution function

To prove Eq. (3.54), we start from the expansion of the cumulant generating function Eq. (C.3) expanding $\xi_k(s)^m$ with the Newton binomial

$$\xi_k(s)^m = \left[2\frac{q_k}{1+q_k}\right]^m \sum_{l=0}^{m} \binom{m}{l}(-1)^l e^{-2lsE_k(0)}\,.$$

Thanks to the finiteness of one sum and the dominated convergence theorem we obtain

$$\frac{\mathcal{G}_{n\tau}(s)}{L} = -\sum_{m=1}^{\infty}\sum_{l=0}^{m}\frac{1}{m}\binom{m}{l}(-1)^l \int_0^{\pi}\frac{\mathrm{d}k}{2\pi}\left[2\frac{q_k}{1+q_k}\right]^m e^{-2\,lsE_k(0)}\sin^{2m}\left(\mu_k n\tau\right)\,.$$
(C.9)

If s is large ($s \gg 1/|h_i - 1|$) and $l \neq 0$, we can use the *saddle point approximation* in the integrals in k. To do that, we exploit the fact that the energy $E_k(0)$ has a stationary point (actually a minimum) for $k = 0$ when the initial state is *not at the critical point*. Indeed, when the initial field is different from the critical value ($h_i \neq 1$), we can expand the energy around $k = 0$ up to second order in k

$$E_k(0) = |h_i - 1| + \frac{h_i}{2\,|h_i - 1|}k^2\,.$$
(C.10)

If s is large enough such that $sE_k(0) \gg 1$, we can restrict this expansion to second order and the integrals are easy to perform because they are Gaussian. There is nevertheless an important caveat concerning the factors $\sin^{2m}\left(\mu_k n\tau\right)$ in the asymptotic limit $n\tau \to \infty$ on which we are focusing now. Once more, because of the Riemann-Lebesgue lemma, the oscillating terms in their expansion Eq. (C.4) vanish and only the term with $j = m$ survives. We have, therefore

$$\int_0^{\pi}\frac{\mathrm{d}k}{2\pi}\left[2\frac{q_k}{1+q_k}\right]^m e^{-2\,lsE_k(0)}\sin^{2m}\left(\mu_k n\tau\right)$$

$$\simeq \left[2\frac{q_0}{1+q_0}\right]^m e^{-2\,ls|h_i-1|}\int_0^{\infty}\frac{\mathrm{d}k}{2\pi}e^{-h_i\,lsk^2/(2|h_i-1|)}\sin^{2m}\left(\mu_k n\tau\right)$$

$$\xrightarrow{n\to\infty}\frac{1}{2}\left[2\frac{q_0}{1+q_0}\right]^m\frac{1}{4^m}\binom{2m}{m}\sqrt{\frac{|h_i-1|}{2\pi h_i\,ls}}e^{-2\,ls|h_i-1|}\,.$$
(C.11)

At this point we have to substitute this equation in the formula of the cumulant generating function Eq. (C.9). To that purpose, we need first to isolate the terms with $l = 0$; those terms in the limit $n \to \infty$ can be summed

118

up with a method strictly analogous to the one sketched in the foregoing section and give rise to

$$-\sum_{m=1}^{\infty}\frac{1}{m}\int_0^{\pi}\frac{\mathrm{d}k}{2\pi}\left[2\frac{q_k}{1+q_k}\right]^m\sin^{2m}(\mu_k n\tau)\xrightarrow{n\to\infty}\frac{\mathcal{G}_\infty(s\to\infty)}{L}$$
$$=\int_0^{\pi}\frac{\mathrm{d}k}{2\pi}\log\left[\frac{1}{2}\left(1+\sqrt{1-2\frac{q_k}{1+q_k}}\right)\right] \tag{C.12}$$

which is the asymptotic cumulant generating function in the limit of $s\to\infty$. Always in the limit $n\to\infty$, the other terms are given by

$$-\frac{1}{2}\sum_{m=1}^{\infty}\sum_{l=1}^{m}\frac{1}{m}\binom{m}{l}(-1)^l\left[\frac{q_0}{2(1+q_0)}\right]^m\binom{2m}{m}\sqrt{\frac{|h_{\mathrm{i}}-1|}{2\pi h_{\mathrm{i}}ls}}e^{-2\,ls|h_{\mathrm{i}}-1|}\,.$$

When s is large, we can only keep the contributions with $l=1$; the ones with larger l are exponentially small with respect to these; exploiting Ref. [119] to write the summation over m in closed form, we have therefore

$$\frac{1}{2}\sum_{m=1}^{\infty}\left[\frac{2q_0}{1+q_0}\right]^m\frac{1}{4^m}\binom{2m}{m}\sqrt{\frac{|h_{\mathrm{i}}-1|}{2\pi h_{\mathrm{i}}s}}e^{-2s|h_{\mathrm{i}}-1|}$$
$$=\frac{1}{2}\left(\frac{1}{\sqrt{1-4\left|r_0^+\right|^2\left|r_0^-\right|^2}}-1\right)\sqrt{\frac{|h_{\mathrm{i}}-1|}{2\pi h_{\mathrm{i}}s}}e^{-2s|h_{\mathrm{i}}-1|}\,. \tag{C.13}$$

In conclusion, by defining

$$a\equiv\frac{1}{2}\left(\frac{1}{\sqrt{1-4\left|r_0^+\right|^2\left|r_0^-\right|^2}}-1\right)\sqrt{\frac{|h_{\mathrm{i}}-1|}{2\pi h_{\mathrm{i}}}}$$

we can write the cumulant generating function in the limit of large s in the form

$$\frac{\mathcal{G}_\infty(s)}{L}\simeq\frac{\mathcal{G}_\infty(s\to\infty)}{L}+\frac{a}{\sqrt{s}}e^{-2s|h_{\mathrm{i}}-1|}\,. \tag{C.14}$$

Looking at the formulae (3.41) and (C.3), we can see that $\frac{\mathcal{G}_\infty(s\to\infty)}{L}=-g_\infty$. Exploiting the fact that s is large, moreover, we can give an approximate formula for the asymptotic moment generating function $G_\infty(-is)=e^{\mathcal{G}_\infty(s)}$

$$G_\infty(-is)\simeq e^{-Lg_\infty}\left(1+\frac{La}{\sqrt{s}}e^{-2s|h_{\mathrm{i}}-1|}\right)\,. \tag{C.15}$$

This object (see Eq. (3.44)) is the Laplace transform of the work distribution function

$$G_\infty(-is)=\int_0^{\infty}P_\infty(W)e^{-sW}\mathrm{d}W\,.$$

Exploiting this formula, it is not difficult to show (using the properties of the Gamma function) that the distribution function associated to Eq. (C.15) is

$$P_\infty(W) \simeq e^{-Lg_\infty} \left(\delta(W) + \frac{La\theta\left(W - 2\left|h_\mathrm{i} - 1\right|\right)}{\sqrt{\pi}\left(W - 2\left|h_\mathrm{i} - 1\right|\right)^{1/2}} \right) . \qquad (\mathrm{C.16})$$

So our theory predicts an edge singularity in the asymptotic work distribution function at a precise value of W which is totally independent on the details of the periodic protocol (and even of the frequency). They only enter into the factor a through the factors $\left|r_0^+\right|^2$ and $\left|r_0^-\right|^2$. The only condition for the validity of this approximate formula is that the driving field does not start with the critical point value: there the quadratic expansion (C.10) fails and the stationary phase approximation we have used cannot be applied.

Appendix D

Results and derivations concerning Chapter 4

D.1 Appearance of the out-of-phase term in the linear response as a singularity

In this appendix we examine the singularities of the LRT susceptibility in the light of the standard textbook approach, which includes an adiabatic switching-on factor for $t \in (-\infty, 0]$. Consider a periodic perturbing field which is turned on at $-\infty$ as:

$$v(t) = v_{\text{switch}}(t) + v_{\text{per}}(t) = v_0 \sin(\omega_0 t) \left[e^{\eta t} \theta(-t) + \theta(t) \right] , \qquad \text{(D.1)}$$

where $\eta \to 0$ at the end of the calculation, and define $\delta \langle A \rangle_t \equiv \langle A \rangle_t - \langle A \rangle_{\text{eq}}$. Since we will consider only the linear terms in v, we can calculate the two terms separately and add the results. The switching-on part $v_{\text{switch}}(t) = v_0 \theta(-t) e^{\eta t} \sin(\omega_0 t)$ leads, for $t \geq 0$ and $\eta \to 0$, to:

$$\delta \langle A \rangle_t^{\text{switch}} = v_0 \fint_{-\infty}^{+\infty} \frac{\mathrm{d}\omega}{2\pi i} \left(\frac{\chi''(\omega)}{\omega + \omega_0} - \frac{\chi''(\omega)}{\omega - \omega_0} \right) e^{-i\omega t} - v_0 \chi''(\omega_0) \cos(\omega_0 t) ,$$
$$\text{(D.2)}$$

where we made use of the standard approach for dealing with poles in terms of Cauchy principal-value integrals and Dirac's deltas:

$$\lim_{\eta \to 0} \int_{-\infty}^{+\infty} \mathrm{d}\omega \, \frac{f(\omega)}{\omega - \omega_0 + i\eta} = \fint_{-\infty}^{+\infty} \mathrm{d}\omega \, \frac{f(\omega)}{\omega - \omega_0} - i\pi f(\omega_0) .$$

It is clear that the first integral will have to cancel, for large t, the second term, because, physically, $\delta \langle A \rangle_t^{\text{switch}}$ represents the relaxation towards equilibrium after the field was turned on in $(-\infty, 0]$. Before proceeding with the (simple) mathematical justification of this statement, let us comment that the Cauchy principal value integral appearing in Eq. (D.2) is exactly the

same, with an opposite sign, as that appearing in the expression for $\delta\langle A\rangle_t^{\mathrm{per}}$ derived in Section 4.1, since

$$\fint_{-\infty}^{+\infty}\frac{\mathrm{d}\omega}{2\pi i}\left(\frac{\chi''(\omega)}{\omega+\omega_0}-\frac{\chi''(\omega)}{\omega-\omega_0}\right)\mathrm{e}^{-i\omega t}=2\omega_0\fint_0^{+\infty}\frac{\mathrm{d}\omega}{\pi}\frac{\chi''(\omega)}{\omega^2-\omega_0^2}\sin\left(\omega t\right).$$
(D.3)

Therefore, if we sum the two terms we obtain the total response to $v(t)$ as:

$$\delta\langle A\rangle_t=v_0\left[\chi'(\omega_0)\sin\left(\omega_0 t\right)-\chi''(\omega_0)\cos\left(\omega_0 t\right)\right]\ ,$$
(D.4)

as indeed expected.

We now show that:

$$v_0\fint_{-\infty}^{+\infty}\frac{\mathrm{d}\omega}{2\pi i}\left(\frac{\chi''(\omega)}{\omega+\omega_0}-\frac{\chi''(\omega)}{\omega-\omega_0}\right)\mathrm{e}^{-i\omega t}=v_0\chi''(\omega_0)\cos\left(\omega_0 t\right)+F^{\mathrm{relax}}(\omega_0,t)\ ,$$
(D.5)

where $F^{\mathrm{relax}}(\omega_0,t)$ is a function which relaxes to 0 for $t\to\infty$. First, we see from Eq. (4.5) that $\chi''(\omega)$ is non-vanishing only when ω matches a resonance frequency of the system. We assume we are dealing with a system whose resonance spectrum is a smooth continuum, in which case $\chi''(\omega)$ is a regular function. The function $\chi''(\omega)$ is odd in ω, so if ω_0 falls inside the resonance spectrum $\chi''(-\omega_0)=-\chi''(\omega_0)\neq0$; if it falls outside $\chi''(\pm\omega_0)=0$. In both cases we can formally split the first term in the integrand (the second term can be treated in the same way)

$$\frac{\chi''(\omega)}{\omega+\omega_0}\mathrm{e}^{-i\omega t}=\frac{\chi''(\omega)-\chi''(-\omega_0)}{\omega+\omega_0}\mathrm{e}^{-i\omega t}+\frac{\chi''(-\omega_0)}{\omega+\omega_0}\mathrm{e}^{-i\omega t}\ .$$
(D.6)

The first term is always regular, even for $\omega\to-\omega_0$, and it leads to an integral that vanishes for large t (Riemann-Lebesgue lemma). Whenever $\chi''(\pm\omega_0)\neq0$, the second term is singular in $-\omega_0$ and contributes to the integral with the piece

$$\chi''(-\omega_0)\fint_{-\infty}^{+\infty}\frac{\mathrm{d}\omega}{2\pi i}\frac{\mathrm{e}^{-i\omega t}}{\omega+\omega_0}\ .$$
(D.7)

Because of the singularity, this integral does not vanish in the long-time limit, as we are going to show evaluating it with the usual complex plane techniques. Assuming $t>0$, we can close the integration contour, both at infinity and around the singularity, in the lower half complex semi-plane, as shown in Figure D.1. Using standard techniques, one concludes that the principal-value integral we need is given by (minus) the contribution around the singularity $(-i\pi\mathrm{e}^{i\omega_0 t}/(2\pi i))$, hence:

$$\chi''(-\omega_0)\fint_{-\infty}^{+\infty}\frac{\mathrm{d}\omega}{2\pi i}\frac{\mathrm{e}^{-i\omega t}}{\omega+\omega_0}=-\frac{\chi''\left(-\omega_0\right)}{2}e^{i\omega_0 t}\ .$$
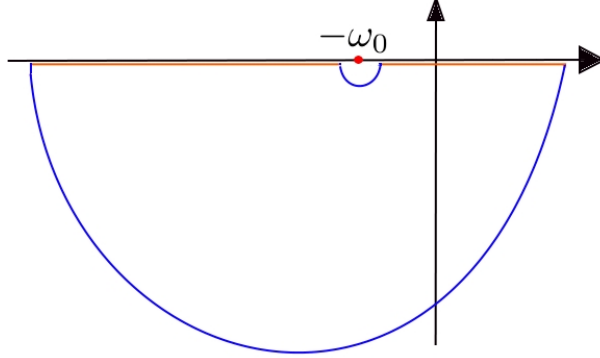(D.8)

Figure D.1: The integration contour used to evaluate the principal value integral in Eq. (D.7).

By repeating this argument for the term with the pole at ω_0 and exploiting the fact that $\chi''(\omega)$ is odd in ω, one finally arrives at Eq. (D.5), where F^{relax} is explicitly given by:

$$F^{\text{relax}}(\omega_0, t) = v_0 \int_{-\infty}^{\infty} \frac{d\omega}{\pi} \frac{[\chi''(\omega) - \chi''(\omega_0)]}{\omega - \omega_0} \sin(\omega t) . \qquad (D.9)$$

Notice, finally, that $F^{\text{relax}}(\omega_0, t) = -F^{\text{trans}}(\omega_0, t)$, where $F^{\text{trans}}(\omega_0, t)$ is the transient term appearing in Eqs. (4.11)-(4.10), and $\delta\langle A\rangle_t^{\text{switch}} = F^{\text{relax}}(\omega_0, t)$.

D.2 Response for a uniform driving

In this appendix we evaluate the zero-temperature transverse magnetisation density for a Ising chain within linear response theory. The response function we need to calculate is (with $\hbar = 1$):

$$\chi(t) = -i\theta(t) \langle \Psi_{\text{GS}}| \left[\hat{m}(t), \hat{M}\right] |\Psi_{\text{GS}}\rangle = -i\theta(t)\frac{1}{L} \sum_{k>0}^{\text{ABC}} \left\langle \psi_0^k \right| [\hat{m}_k(t), \hat{m}_k] \left| \psi_0^k \right\rangle ,$$

$$(D.10)$$

where $\hat{m}_k(t) = 2 \left(\hat{c}_{-k}(t)\hat{c}^\dagger_{-k}(t) - \hat{c}^\dagger_k(t)\hat{c}_k(t)\right)$ is a Heisenberg's operator evolving with $\hat{H}_0$, (Eq. 3.2 with $h = 1$), $\hat{m}_k = \hat{m}_k(0)$, and we have exploited the fact that the different k-subspaces are perfectly decoupled. The ground state $|\Psi_{\text{GS}}\rangle$ of $\hat{H}_0$ is given by Eq. (3.5) in which $u_k^0 = \cos(\theta_k/2)$ and $v_k^0 = i\sin(\theta_k/2)$ with $\tan\theta_k = (\sin k)/(1 - \cos k)$. To find $\hat{m}_k(t)$ we need $\hat{c}_k(t)$, which obeys a Heisenberg's equation of motion with Hamiltonian $\hat{H}_0$ and initial value $\hat{c}_k(0) = \hat{c}_k$. It is simple to derive that $\hat{c}_k(t) = p_k(t)\hat{c}_k + q_k(t)\hat{c}^\dagger_{-k}$ with $p_k(t) = \cos(\epsilon_k^0 t) - i\cos(\theta_k)\sin(\epsilon_k^0 t)$, $q_k(t) = -\sin(\theta_k)\sin(\epsilon_k^0 t)$, and

123

$\epsilon_k^0 = 2\sin(k/2)$. With these ingredients it is a matter of simple algebra to derive the following expression for $\chi(t)$:

$$\chi(t) = -\theta(t)\frac{8}{L}\sum_{k>0}^{\text{ABC}}\cos^2\left(\frac{k}{2}\right)\sin(2\epsilon_k^0 t) \ , \tag{D.11}$$

which in turn immediately gives, by Fourier transforming:

$$\chi(z) = -\frac{4}{L}\sum_{k>0}^{\text{ABC}}\cos^2\left(\frac{k}{2}\right)\left[\frac{1}{2\epsilon_k^0 - z} + \frac{1}{2\epsilon_k^0 + z}\right] \ . \tag{D.12}$$

The spectral function $\chi''(\omega)$ can be directly extracted from this expression:

$$\chi''(\omega > 0) = -\frac{4\pi}{L}\sum_{k>0}^{\text{ABC}}\cos^2\left(\frac{k}{2}\right)\delta\left(\omega - 2\epsilon_k^0\right) \overset{L\to\infty}{\longrightarrow} -\theta(4-\omega)\sqrt{1 - \left(\frac{\omega}{4}\right)^2} \ , \tag{D.13}$$

where we have taken the thermodynamic limit $\left(\frac{1}{L}\sum_{k>0}^{\text{ABC}} \to \int_0^\pi \frac{dk}{2\pi}\right)$ which transforms the discrete sum of Dirac's delta functions into a smooth function.

D.3   Response for a driving restricted to $l < L$

In this section we discuss the local susceptibility χ_{j0}. The local magnetisation operators are defined as $\hat{m}_j \equiv \sigma_j^x$, and the response function we are interested in can be written as

$$\chi_{j0}(t) \equiv -\frac{i}{\hbar}\theta(t)\langle\Psi_{\text{GS}}|\left[\hat{m}_j(t),\,\hat{m}_0\right]|\Psi_{\text{GS}}\rangle \ . \tag{D.14}$$

As mentioned in Subsection 4.3.2, the crucial information is contained in $\chi''_{j0}(\omega)$ which reads:

$$\chi''_{j0}(\omega) = -\frac{\pi}{\hbar}\sum_{n\neq 0}\left[(m_j)^*_{n0}(m_0)_{n0}\,\delta\left(\omega - \omega_{n0}\right) - (m_j)_{n0}(m_0)^*_{n0}\,\delta\left(\omega - \omega_{0n}\right)\right] \ , \tag{D.15}$$

where the sum extends over the eigenstates (0 labels the ground state); the matrix elements $(m_j)_{mn}$ and the frequencies ω_{mn} are defined as in Eq. (4.4). As $\chi''_{j0}(\omega)$ is odd in ω, we need to consider only $\omega \geq 0$. Using the Jordan-Wigner transformation we can write

$$(m_j)_{n0} = \langle n|\,\hat{m}_j\,|\Psi_{\text{GS}}\rangle = -\frac{2}{L}\sum_{k,\,k'}\langle n|\,\hat{c}_k^\dagger\hat{c}_{k'}\,|\Psi_{\text{GS}}\rangle\,e^{i(k'-k)j} \tag{D.16}$$

where the Fermionic operators $\hat{c}_k$ are defined in appendix B. The operators $\hat{\gamma}_k$ diagonalizing the quadratic Hamiltonian Eq. (3.2) at time 0 can be obtained from the $\hat{c}_k$ with a Bogoliubov transformation $\hat{c}_k = u_k^0\hat{\gamma}_k + v_k^0\hat{\gamma}_{-k}^\dagger$,

$\hat{c}^\dagger_{-k} = -v^{0*}_k \hat{\gamma}_k + u^0_k \hat{\gamma}^\dagger_{-k}$. If we substitute in Eq. D.16 we see that the only non-vanishing matrix element is among the ground state and excited states whose form is $\hat{\gamma}^\dagger_{\widetilde{k}'} \hat{\gamma}^\dagger_{\widetilde{k}} |\Psi_{\mathrm{GS}}\rangle$. Applying Wick's theorem we can write

$$(m_j)_{n0} = -\frac{2}{L} \sum_{k,\, k'} \langle n| \hat{c}^\dagger_k \hat{c}_{k'} |\Psi_{\mathrm{GS}}\rangle \, \mathrm{e}^{i(k'-k)j} = -\frac{2}{L} \left(-u^0_{\widetilde{k}'} v^0_{\widetilde{k}} + u^0_{\widetilde{k}} v^0_{\widetilde{k}'} \right) \mathrm{e}^{-i(\widetilde{k}+\widetilde{k}')j},$$
(D.17)

where we have exploited that $v^0_{-k} = -v^0_k$ and $u^0_{-k} = u^0_k$. Substituting this expression in Eq. (D.15), and using that for the relevant excited states $\omega_{n0} = \epsilon_{\widetilde{k}} + \epsilon_{\widetilde{k}'}$ we can write

$$\chi''_{j0}(\omega \geq 0) = -\frac{\pi}{\hbar} \frac{4}{L^2} \sum_{\widetilde{k} > \widetilde{k}'} \left| u^0_{\widetilde{k}} v^0_{\widetilde{k}'} - u^0_{\widetilde{k}'} v^0_{\widetilde{k}} \right|^2 \mathrm{e}^{-i(\widetilde{k}+\widetilde{k}')j} \delta(\omega - \epsilon^0_{\widetilde{k}} - \epsilon^0_{\widetilde{k}'}) , \quad (D.18)$$

where the condition $\widetilde{k} > \widetilde{k}'$ has been enforced to avoid double counting of the excited states $|n\rangle$. The object inside the sum is symmetric upon exchange of $\widetilde{k}$ and $\widetilde{k}'$. Using this, restricting the sum to the positive $\widetilde{k}$ and $\widetilde{k}'$ and going to the thermodynamic limit we get:

$$\chi''_{j0}(\omega \geq 0) = -\frac{4}{\pi\hbar} \int_0^\pi \mathrm{d}k \int_0^\pi \mathrm{d}k' \left\{ \left| u^0_k v^0_{k'} \right|^2 \cos(kj) \cos(k'j) \right.$$
$$\left. - u^0_{k'} v^0_k u^0_k v^0_{k'} \sin(kj) \sin(k'j) \right\} \delta(\omega - \epsilon^0_k - \epsilon^0_{k'}) .$$

Using the expressions for u^0_k and v^0_k in Section 3.1 and changing variable to $\epsilon = 2\sin(k/2)$, we can rewrite this as:

$$\chi''_{j0}(\omega \geq 0) = -\frac{1}{\pi\hbar} \int_{\max(0,\omega-2)}^{\min(\omega,2)} \mathrm{d}\epsilon \left[\sqrt{\frac{(2-\epsilon)(2+\epsilon-\omega)}{(2+\epsilon)(2+\omega-\epsilon)}} \cos(k_\epsilon j) \cos(k_{\omega-\epsilon} j) \right.$$
$$\left. + \sin(k_\epsilon j) \sin(k_{\omega-\epsilon} j) \right], \quad (D.19)$$

where we have defined the function $k_\epsilon \equiv 2\arcsin(\epsilon/2)$.

The linear response function needed in the text is obtained from χ_{j0} via the expression:

$$\chi_l(t) = -\frac{i}{\hbar} \theta(t) \langle \Psi_{\mathrm{GS}} | \left[\hat{M}_l(t), \hat{M}_l \right] |\Psi_{\mathrm{GS}}\rangle = l \sum_{j=-l+1}^{l-1} \chi_{j0}(t). \quad (D.20)$$

Observe that cancellations in the sum over j, due to the highly oscillating contributions $\chi_{j0}(t)$, make χ_l proportional to l rather than to l^2.

Appendix E

Results and derivations concerning Chapter 5

E.1 Demonstration of the formula Eq. (5.12)

We claim that, when there are N interacting spins, the subspaces with total spin $S \leq N/2$ are in number

$$g_N(S) = \begin{pmatrix} N \\ \dfrac{N}{2} + S \end{pmatrix} - \begin{pmatrix} N \\ \dfrac{N}{2} + S + 1 \end{pmatrix}. \tag{E.1}$$

This formula can be proved by iteration. To that purpose we need to demonstrate a recursion formula

$$\begin{cases} g_{N+1}\left(S + \frac{1}{2}\right) = g_N(S+1) + g_N(S) & \text{if} \quad 1 < S < N/2 \\ g_{N+1}\left(\frac{N+1}{2}\right) = g_N\left(\frac{N}{2}\right) = 1 \\ g_{N+1}\left(0\right) = g_N\left(\frac{1}{2}\right) \end{cases} \tag{E.2}$$

Indeed, when there are N spins with total spin $N/2$, we can decompose the Hilbert space as a direct sum

$$\frac{N}{2} \oplus \underbrace{\left[\left(\frac{N}{2} - 1\right) \otimes \cdots \oplus \left(\frac{N}{2} - 1\right)\right]}_{g\left(\frac{N}{2}-1\right) \text{ times}} \oplus \underbrace{\left[\left(\frac{N}{2} - 2\right) \otimes \cdots \oplus \left(\frac{N}{2} - 2\right)\right]}_{g\left(\frac{N}{2}-2\right) \text{ times}} \oplus \cdots \oplus \underbrace{\left[\frac{1}{2} \oplus \cdots \oplus \frac{1}{2}\right]}_{g(1/2) \quad \text{times}}.$$

$$\tag{E.3}$$

If we add one more spin, we have to perform the tensor product of this space with a subspace of spin $1/2$; we find

$$\frac{1}{2} \otimes \left[\cdots \underbrace{(S+1 \oplus \cdots \oplus S+1)}_{g_N(S+1) \text{ times}} \oplus \underbrace{(S \oplus \cdots \oplus S)}_{g_N(S) \text{ times}} \oplus \cdots \right] \qquad \text{(E.4)}$$

$$= \cdots \oplus \underbrace{\left(\left(S+\frac{3}{2} \right) \oplus \cdots \oplus \left(S+\frac{3}{2} \right) \right)}_{g_N(S+1) \text{ times}} \oplus \underbrace{\left(\left(S+\frac{1}{2} \right) \oplus \cdots \oplus \left(S+\frac{1}{2} \right) \right)}_{g_N(S+1)+g_N(S) \text{ times}}$$

$$\oplus \underbrace{\left(\left(S-\frac{1}{2} \right) \oplus \cdots \oplus \left(S-\frac{1}{2} \right) \right)}_{g_N(S) \text{ times}} \oplus \cdots .$$

Therefore, $g_N(S)$ subspaces of spin $S+1/2$ arise from the subspaces of spin S, other $g_N(S+1)$ arise from those of spin $S+1$ and the first line of Eq. (E.2) follows; the other two lines are deduced in the same way.

It is not difficult to check that the formula Eq. (E.1) obeys the recursion relation (E.2) [1] ; so if we are able to show that Eq. (E.1) holds for $N = 1$ we conclude our demonstration by induction. That is quite easy: when $N = 1$, the only allowed value of the spin is $1/2$ and it is easy to see that $g_1(1/2) = 1$.

---

[1]Substituting Eq. (E.1) in Eq. (E.2), we can see that both members are given by the expression

$$2 \frac{(S+1)(N+1)!}{\left(\frac{N}{2} - S \right)! \left(\frac{N}{2} + S + 2 \right)!} .$$

Bibliography

[1] I. Bloch, J. Dalibard, and W. Zwerger. Many-body physics with ultracold lattices. *Rev. Mod. Phys.*, 80:885–964, 2008.

[2] C. Orzel, A. K. Tuchman, M. L. Fenselau, M. Yasuda, and M. A. Kasevich. Squeezed states in a bose-einstein condensate. *Science*, 291:2386, 2001.

[3] S. Inouye, M. R. Andrews, J. Stenger, H.-J. Miesner, D. M. Stamper-Kurn, and W. Ketterle. Observation of feshbach resonances in a bose-einstein condensate. *Nature*, 392:151, 1998.

[4] Markus Greiner, Olaf Mandel, Tilman Esslinger, Theodor W. Hansch, and Immanuel Bloch. Quantum phase transition from a superfluid to a mott insulator in a gas of ultracold atoms. *Nature (London)*, 415:39, 2002.

[5] C. Regal and D. S. Jin. *Experimental realization of BCS-BEC crossover physics with a Fermi gas of atoms.* PhD thesis, University of Colorado, Boulder, 2006.

[6] Markus Greiner, Olaf Mandel, Theodor W. Hansch, and Immanuel Bloch. Collapse and revival of the matter wave field of a bose-einstein condensate. *Nature (London)*, 419:51, 2002.

[7] Toshiya Kinoshita, Trevor Wenger, and David S. Weiss. A quantum newton's cradle. *Nature (London)*, 440:900, 2006.

[8] L. E. Sadler and J. M. Higbie and S. R. Leslie and M. Vengalattore and D. M. Stamper-Kurn. Spontaneous symmetry breaking in a quenched ferromagnetic spinor bose-einstein condensate. *Nature (London)*, 443:312, 2006.

[9] Anatoli Polkovnikov, Krishnendu Sengupta, Alessandro Silva, and Mukund Vengalattore. Nonequilibrium dynamics of closed interacting quantum systems. *Rev. Mod. Phys.*, 83:863, 2011.

[10] S. Hofferberth, I. Lesanovsky, T. Schumm, A. Imambekov, V. Gritsev, E. Demler, and J. Schmiedmayer. Probing quantum and thermal noise in an interacting many-body system. *Nature Physics*, 4:489, 2008.

[11] H. Lignier, C. Sias, D. Ciampini, Y. P. Singh, A. Zenesini, O. Morsch, and E. Arimondo. Dynamical control of matter-wave tunneling in periodic potentials. *Phys. Rev. Lett.*, 99:220403, 2007.

[12] Andrè Eckardt, Martin Holthaus, Hans Lignier, Alessandro Zenesini, Donatella Ciampini, Oliver Morsch, and Ennio Arimondo. Exploring dynamic localization with bose-einstein condensate. *Phys. Rev. A*, 79:013611, 2009.

[13] C. Sias, H. Lignier, Y.P. Singh, A. Zenesini, D. Ciampini, O. Morsch, and E. Arimondo. Observation of photon assisted tunneling in optical lattices. *Phys. Rev. Lett.*, 100:040404, 2008.

[14] N. Gemelke, E. Sarajlic, Y. Bidel, S. Hong, and S. Chu. Parametric amplification of matter waves in periodically traslated optical lattices. *Phys. Rev. Lett.*, 95:170404, 2005.

[15] Alessandro Zenesini, Hans Lignier, Donatella Ciampini, Oliver Morsch, and Ennio Arimondo. Parametric amplification of matter waves in periodically traslated optical lattices. *Phys. Rev. Lett.*, 102:100403, 2009.

[16] N. Strohmaier and D. Greif and R. Jördens and L. Tarruell and H. Moritz and T. Esslinger and R. Sensarma and D. Pekker and E. Altman and E. Demler . Observation of elastic doublon decay in the fermi-hubbard model. *Phys. Rev. Lett.*, 104:080401, 2010.

[17] André Eckardt, Tharanga Jinasundera, Christoph Weiss, and Martin Holthaus. Analog of photon-assisted tunneling in a bose-einstein condensate. *Phys. Rev. Lett.*, 95:200401, 2005.

[18] André Eckardt, Christoph Weiss, and Martin Holthaus. Superfluid-insulator transition in periodically driven optical lattice. *Phys. Rev. Lett.*, 95:260404, 2005.

[19] C. Kollath, A. Iucci, T. Giamarchi, W. Hofstetter, and U. Schollwöck. Spectroscopy of ultracold atoms by periodic lattice modulations. *Phys. Rev. Lett.*, 97:050402, 2006.

[20] C. Kollath, A. Iucci, I. McCulloch, and T. Giamarchi. Modulation spectroscopy with ultracold fermions in optical lattices. *Phys. Rev. A*, 74:041604(R), 2006.

[21] Victor Mukherjee and Amit Dutta. Effects of interference in the dynamics of spin-1/2 transverse XY Chain driven periodically through quantum critical points . *JSTAT*, page P05005, 2009.

[22] Arnab Das. Exotic freezing of response in a quantum many body system. *Phys. Rev. B*, 82:172402, 2010.

[23] Sirshendu Bhattacharyya, Arnab Das, and Subinay Dasgupta. Transverse ising chain under periodic instantaneous quenches: Dynamical many-body freezing and emergence of slow solitary oscillations. *Phys. Rev. B*, 86:054410, 2012.

[24] Dario Poletti and Corinna Kollath. Slow quench dynamics of periodically driven quantum gases. *Phys. Rev. A*, 84:013615, 2011.

[25] Thilo Stöferle, Henning Moritz, Christian Schori, Michael Kohl, and Tilman Esslinger. Transition from a Strongly Interacting 1D Superfluid to a Mott Insulator. *Phys. Rev. Lett*, 92:130403, 2004.

[26] M. Rigol, V. Dunjko, and M. Olshanii. Thermalization and its mechanism for generic isolated quantum systems. *Nature*, 452:854–858, 2008.

[27] Marcos Rigol, Vanja Dunjko, Vladimir Yurovsky, and Maxim Olshanii. Relaxation in a completely integrable many-body quantum system: An *ab initio* study of the dynamics of the highly excited states of 1d lattice hard-core bosons. *Phys. Rev. Lett.*, 98:050405, 2007.

[28] C. Kollath, A. M. Läuchli, and E. Altman. Quench dynamics and nonequilibrium phase diagram of the bose-hubbard model. *Phys. Rev. Lett.*, 98:180601, 2007.

[29] S. R. Manmana, S. Wessel, R. M. Noack, and A. Muramatsu. Strongly correlated fermions after a quantum quench. *Phys. Rev. Lett.*, 98:210405, 2007.

[30] Elena Canovi, Davide Rossini, Rosario Fazio, Giuseppe E. Santoro, and Alessandro Silva. Quantum quenches, thermalization, and many-body localization. *Phys. Rev. B*, 83:094431, 2011.

[31] Clemens Neuenhahn and Florian Marquardt. Thermalization of interacting fermions and delocalization in fock space. *Phys. Rev. E*, 85:060101(R), 2012.

[32] Marcus Kollar and Martin Eckstein. Relaxation of a one-dimensional mott insulator after an interaction quench. *Phys. Rev. A*, 78:013626, 2008.

[33] Martin Eckstein and Marcus Kollar. Nonthermal steady states after an interaction quench in the falicov-kimball model. *Phys. Rev. Lett.*, 100:120404, 2008.

[34] M. A. Cazalilla. Effect of suddenly turning on interactions in the luttinger model. *PRL*, 97:156403, 2006.

[35] A. Iucci and M. A. Cazalilla. Quantum quench dynamics of some exactly solvable models in one dimension. *PRA*, 80:063619, 2009.

[36] Pasquale Calabrese, Fabian H. L. Essler, and Maurizio Fagotti. Quantum quench in the transverse field Ising chain: I. Time evolution of order parameter correlators. *J. Stat. Mech.*, page P07016, 2012.

[37] Pasquale Calabrese, Fabian H. L. Essler, and Maurizio Fagotti. Quantum quenches in the transverse field Ising chain: II. Stationary state properties. *J. Stat. Mech.*, page P07022, 2012.

[38] M. Cramer, A. Flesch, I. P. McCulloch, U. Schollwock, and J. Eisert. Exploring local quantum many-body relaxation by atoms in optical superlattices. *Phys. Rev. Lett.*, 101:063001, 2008.

[39] T. Barthel and U. Schollwöck. Dephasing and the steady state in quantum many-particle systems. *Phys. Rev. Lett.*, 100:100601, 2008.

[40] E. T. Jaynes. Information theory and statistical mechanics. ii. *Phys. Rev.*, 108:171–190, 1957.

[41] Simone Ziraldo and Giuseppe E. Santoro. Relaxation and thermalization after a quantum quench: Why localization is important. *Phys. Rev. B*, 87:064201, Feb 2013.

[42] Davide Fioretto and Giuseppe Mussardo. Quantum Quenches in Integrable Field Theories. *New Journal of Physics*, 12:055015, 2010.

[43] J.-S. Caux and J. Mossel. Remarks on the notion of quantum integrability. *JSTAT*, page P02023, 2011.

[44] S. K. Ma. *Modern Theory of Critical Phenomena*. Perseus, 2000.

[45] M. V. Berry. Regular and irregular motion. In S. Jonna, editor, *Topics in Nonlinear Mechanics*, volume 46, pages 16–120. Am.Inst.Ph., 1978.

[46] V. I. Arnol'd. *Mathematical Methods of Classical Mechanics*. Springer, 1989.

[47] A. N. Kolmogorov. On Conservation of Conditionally Periodic Motions for a Small Change in Hamilton's Function. *Dokl. Akad. Nauk SSSR*, 98:527–530, 1954.

[48] V. I. Arnol'd. Proof of a Theorem of A. N. Kolmogorov on the Preservation of Conditionally Periodic Motions under a Small Perturbation of the Hamiltonian. *Uspehi Mat. Nauk*, 18:13–40, 1963.

[49] J. Moser. On Invariant Curves of Area-Preserving Mappings of an Annulus. *Nachr. Akad. Wiss. Göttingen Math.-Phys. Kl*, II:1–20, 1962.

[50] Grayson H. Walker and Joseph Ford. Asymptotic Instability and Ergodic Behavior for Conservative Nonlinear Oscillator Systems. *Phys. Rev.*, 188:416, 1969.

[51] Kerson Huang. *Introduction to Statistical Physics.* Taylor&Francis (London, New York), 2001.

[52] E. Fermi, J. Pasta, and S. Ulam. Studies of non linear problems. Los Alamos Report No. LA-1940, 1955.

[53] Joseph Ford. The Fermi-Pasta-Ulam problem: paradox turns discovery. *Physics Reports*, 5:271–310, 1992.

[54] Roberto Livi, Marco Pettini, Stefano Ruffo, Massimo Sparpaglione, and Angelo Vulpiani. Equipartition threshold in nonlinear large hamiltonian systems: The fermi-pasta-ulam model. *Phys. Rev. A*, 31:1039, 1985.

[55] Lea F. Santos and Marcos Rigol. Localization and the effects of symmetries in the thermalization properties of one-dimensional quantum systems. *Phys. Rev. E*, page 031130, 2010.

[56] Elena Canovi, Davide Rossini, Rosario Fazio, Giuseppe E. Santoro, and Alessandro Silva. Many-body localization and thermalization in the full probability distribution function of observables. *New Journal of Physics*, 14:095020, 2012.

[57] G. Biroli, C. Kollath, and A. Läuchli. Effect of rare fluctuations on the thermalization of isolated quantum systems. *Phys. Rev. Lett.*, 105:250401, 2010.

[58] J. M. Deutsch. Quantum statistical mechanics in a closed system. *Phys. Rev. A*, 43:2046–2049, 1991.

[59] Mark Srednicki. Chaos and quantum thermalization. *Phys. Rev. E*, 50:888–901, 1994.

[60] Simone Ziraldo, Alessandro Silva, and Giuseppe E. Santoro. Relaxation dynamics of disordered spin chains: Localization and the existence of a stationary state. *Phys. Rev. Lett.*, 109:247205, Dec 2012.

[61] Subir Sachdev. *Quantum Phase Transitions (Second Edition)*. Cambridge University Press, 2011.

[62] Jacek Dziarmaga. Dynamics of a quantum phase transition and relaxation to a steady state. *Advances of Physics*, 59:1063, 2010.

[63] T. Dittrich, P. Hänggi, G.-L. Ingold, B. Kramer, G. Schön, and W. Zwerger. *Quantum Transport and Dissipation*. Wiley-VCH Weinheim, 1998.

[64] J. H. Shirley. Solution of Schrödinger equation with a hamiltonian periodic in time. *Phys. Rev.*, 138:B979, 1965.

[65] J. Hausinger and M. Grifoni. Dissipative two-level system under strong ac driving: A combination of floquet and van vleck perturbation theory. *Phys. Rev. A*, 81:022117, 2010.

[66] A. Russomanno, A. Silva, and G. E. Santoro. Periodic steady regime and interference in a periodically driven quantum system. *Phys. Rev. Lett*, 109:257201, 2012.

[67] Mark Srednicki. Thermal fluctuations in quantized chaotic systems. *J. Phys. A*, 29:L75–L79, 1996.

[68] Asher Peres. Ergodicity and mixing in quantum theory. i. *Phys. Rev. A*, 30:504, 1984.

[69] Marcos Rigol and Lea F. Santos. Quantum chaos and thermalization in gapped systems. *Phys. Rev. A*, page 011604(R), 2010.

[70] Pedro Ponte, Anushya Chandran, Z. Papić, and Dmitry A. Abanin. Periodically driven ergodic and many-body localized quantum systems. arXiv cond-mat/1403.6480v1, 2014.

[71] Hyungwon Kim, Tatsuhiko N. Ikeda, and David A. Huse. Testing whether all eigenstates obey the Eigenstate Thermalization Hypothesis. arXiv cond-mat.stat-mech/1408.0535v2, 2014.

[72] Anna Maraga, Pietro Smacchia, Michele Fabrizio, and Alessandro Silva. Nonadiabatic stationary behavior in a driven low-dimensional gapped system. *PRB*, 90:041111(R), 2014.

[73] P. Calabrese and J. Cardy. Evolution of entanglement entropy in one-dimensional systems. *J. Stat. Mech.*, page 0504:P04010, 2005.

[74] G. De Chiara, S. Montangero, P. Calabrese, and R. Fazio. Entanglement Entropy dynamics in Heisenberg chains. *J. Stat. Mech.*, page 0603:L03001, 2006.

[75] L. Stella, Giuseppe E. Santoro, and Erio Tosatti. Optimization by quantum annealing: Lessons from simple cases. *Phys. Rev. B*, 72:014303, 2005.

[76] Roman Martoňák, Giuseppe E. Santoro, and Erio Tosatti. Quantum annealing of the traveling-salesman problem. *Phys. Rev. E*, 70:057701, 2004.

[77] E. Farhi, J. Goldstone, S. Gutmann, J. Lapan, A. Lundgren, and D. Preda. A quantum adiabatic evolution algorithm applied to random instances of an NP-Complete problem. *Science*, 292:472, 2001.

[78] P. Calabrese and J. Cardy. Time Dependence of Correlation Functions Following a Quantum Quench. *Phys. Rev. Lett.*, 96:136801, 2006.

[79] Takuya Kitagawa, Adilet Imambekov, Jörg Schmiedmayer, and Eugene Demler. The dynamics and prethermalization of one-dimensional quantum systems probed through the full distributions of quantum noise. *New Journal of Physics*, 13:073018, 2011.

[80] M. Gring, M. Kuhnert, T. Langen, T. Kitagawa, B. Rauer, M. Schreitl, I. Mazets, D. Adu Smith E. Demler, and J. Schmiedmayer. Relaxation and Prethermalization in an Isolated Quantum System. *Science*, 337:1318–1322, 2012.

[81] Peter Talkner, Eric Lutz, and Peter Hänggi. Fluctuation theorems: Work is not an observable. *Phys. Rev. E*, 75:050102(R), 2007.

[82] C. Jarzynski. Nonequilibrium equality for free energy differences. *Phys. Rev. Lett.*, 78:2690, 1997.

[83] Michele Campisi, Peter Hanggi, , and Peter Talkner. Quantum fluctuation relations: Foundations and applications. *Rev. Mod. Phys.*, 83:771, 2011.

[84] A. Silva. Statistics of the work done on a quantum critical system by quenching a control parameter. *PRL*, 101:120603, 2008.

[85] G. Bunin, L. D'Alessio, Y. Kafri, and A. Polkovnikov. Universal energy fluctuations in thermally isolated driven systems. *Nat. Phys.*, 7:913, 2011.

[86] Pietro Smacchia and Alessandro Silva. Work distribution and edge singularities for generic time-dependent protocols in extended systems. *PRE*, 88:042109, 2013.

[87] A. Gambassi and A. Silva. Large deviations and universality in quantum quenches. *PRL*, 109:250602, 2012.

[88] Andrea Gambassi and Alessandro Silva. Statistics of the Work in Quantum Quenches, Universality and the Critical Casimir Effect. arXiv 1106.2671v1, 2011.

[89] S. Sotiriadis, A. Gambassi, and A. Silva. Statistics of the work done by splitting a one-dimensional quasi-condensate. *PRE*, 87:052129, 2013.

[90] Shraddha Sharma, Angelo Russomanno, Giuseppe E. Santoro, and Amit Dutta. Loschmidt echo and dynamical fidelity in periodically driven quantum systems. *EPL*, 106:67003, 2014.

[91] A. Russomanno, A. Silva, and G. E. Santoro. Linear response as a singular limit for a periodically driven closed quantum system. *J. Stat. Mech.*, page P09012, 2013.

[92] S. Bochner and K. Chandrasekharan. *Fourier Transforms*. Princeton University Press, 1949.

[93] L.D̃. Landau and E.M̃. Lifshitz. *Quantum Mechanics*. Pergamon, Oxford, 1976.

[94] L.D̃. Landau and E.M̃. Lifshitz. *Statistical Physics, Part 1, Course of Theoretical Physics, Vol. 5*. Butterworth-Heinemann, New York, 1980.

[95] Mark Srednicki. The approach to thermal equilibrium in quantized chaotic systems. *J. Phys. A*, 32:1463, 1999.

[96] Anatoli Polkovnikov. Quantum ergodicity: fundamentals and applications, 2013. Available at: http://physics.bu.edu/ asp/teaching/PY_747.pdf.

[97] M. Grifoni and P. Hänggi. Driven quantum tunneling. *Phys. Rep.*, 304:229–354, 1998.

[98] A. Russomanno, S. Pugnetti, V. Brosco, and R. Fazio. Floquet theory of Cooper pair pumping. *Phys. Rev. B*, 83:214508, 2011.

[99] Giulio Casati and Luca Molinari. "Quantum Chaos" with Time-Periodic Hamiltonians. *Prog. Theor. Phys. Suppl.*, 98:287, 1989.

[100] G. Grosso and G.P̃astori Parravicini. *Solid State Physics*. Academic, San Diego, 2000.

[101] Sir Nevi11 Mott. The mobility edge since 1967. *J. Phys. C*, 20:3075, 1987.

[102] Dominique Delande1 and Giuliano Orso. Mobility Edge for Cold Atoms in Laser Speckle Potentials. *Phys. Rev. Lett.*, 113:060601, 2014.

[103] K. Yajima. Resonances for the ac stark effect. *Commun. Mat. Phys.*, 87:331, 1982.

[104] H. P. Breuer and M. Holthaus. Adiabatic processes in the ionization of highly excited hydrogen atoms. *Z. Phys. C*, 11:1, 1989.

[105] M. Cramer, C. M. Dawson, J. Eisert, and T. J. Osborne. Exact relaxation in a class of nonequilibrium quantum lattice systems. *Phys. Rev. Lett.*, 100:030602, 2008.

[106] M. Cramer and J. Eisert. A quantum central limit theorem for non-equilibrium systems: exact local relaxation of correlated states. *New J. Phys.*, 12:055020, 2010.

[107] S. Trotzky, Y-A. Chen, A. Flesch, I. P. Mc Culloch, U. Schollwöck, J. Eisert, and I. Bloch. Probing the relaxation towards equilibrium in an isolated strongly correlated one-dimensional bose gas. *Nature Physics*, 8:325, 2012.

[108] Marin Bukov, Luca DAlessio, and Anatoli Polkovnikov1. Universal high-frequency behavior of periodically driven systems: from dynamical stabilization to floquet engineering. arXiv cond-mat.quant-gas/1407.4803v2, 2014.

[109] A. Polkovnikov, personal communication.

[110] Mark Srednicki. Does quantum chaos explain quantum statistical mechanics? 1995.

[111] Davide Rossini, Alessandro Silva, Giuseppe Mussardo, and Giuseppe E. Santoro. Effective Thermal Dynamics Following a Quantum Quench in a Spin Chain. *Phys. Rev. Lett.*, 102:127204, 2009.

[112] E. Lieb, T. Schultz, and D. Mattis. Two soluble models of an antiferromagnetic chain. *Annals of Physics*, 16:407–466, 1961.

[113] A. L. Fetter, J. D. Walecka. *Quantum Theory of Many-Particle Systems*. McGraw-Hill, New York, 1971.

[114] R. W. Cherng and L. S. Levitov. Entropy and correlation functions of a driven quantum spin chain. *Phys. Rev. A*, 73:043614, 2006.

[115] Charles P. Slichter. *Principles of Magnetic Resonance*. Springer-Verlag, 1996.

[116] A. Messiah. *Quantum mechanics*, volume 2. North-Holland, Amsterdam, 1962.

[117] W. H. Zurek, U. Dorner, and P. Zoller. Dynamics of a quantum phase transition. *Phys. Rev. Lett.*, 95:105701, 2005.

[118] C. Zener. Non-adiabatic crossing of energy levels. *Proc. Royal Soc. A*, 137:696, 1932.

[119] Milton Abramowitz, Irene A. Stegun (eds.). *Handbook of Mathematical Functions.* Dover, 1972.

[120] F. Grossmann, T. Dittrich, P. Jung, and P. Hänggi. Coherent destruction of tunneling. *Phys. Rev. Lett.*, 67:516–519, Jul 1991.

[121] P. Calabrese and J. Cardy. Quantum Quenches in Extended Systems. *J. Stat. Mech.*, page 0706:P06008, 2007.

[122] C. Bloch and A. Messiah. Canonical form of an antisymmetric tensor and its application to the theory of superconductivity. *Nucl. Phys.*, 39:95, 1962.

[123] Tommaso Caneva, Rosario Fazio, and Giuseppe E. Santoro. Adiabatic quantum dynamics of a random Ising chain across its quantum critical point. *Phys. Rev. B*, 76:144427, 2007.

[124] G. E. Crooks. Nonequilibrium measurements of free energy differences for microscopically reversible markovian systems. *J. Stat. Phys.*, 90:1481, 1998.

[125] Hal Tasaki. Jarzynski relations for quantum systems and some applications. arXiv cond-mat/0009244v2, 2000.

[126] Peter Talkner, Peter Hänggi, and Manuel Morillo. Microcanonical quantum fluctuation theorems. *Phys. Rev. E*, 77:051131, 2008.

[127] P. W. Anderson. Absence of diffusion in certain random lattices. *Phys. Rev.*, 109:1492, 1958.

[128] R. Artuso. Kicked Harper model. *Scholarpedia*, 6(10):10462, 2011.

[129] Marco Cozzini, Radu Ionicioiu, , and Paolo Zanardi. Quantum fidelity and quantum phase transitions in matrix product states. *Physical Review B*, 76:104420, 2007.

[130] H.T. Quan, Z. Song, X. F. Liu, P. Zanardi, and C. P. Sun. Decay of Loschmidt Echo Enhanced by Quantum Criticality. *Physical Review Letters*, 96:140604, 2006.

[131] L. Amico, R. Fazio, A. Osterloh, and V. Vedral. Entanglement in many-body systems. *Rev. Mod. Phys.*, 80:517, 2008.

[132] M. Nielsen and I. L. Chuang. *Quantum Computation and Quantum Information.* Cambridge University Press, 2000.

[133] D. Forster. *Hydrodynamic Fluctuations, Broken Symmetry and Correlation Functions.* W.A. Benjamin, Inc., 1975.

[134] G. F. Giuliani and G. Vignale. *Quantum Theory of the Electron Liquid.* Cambridge University Press, 2005.

[135] N. G. van Kampen. The case against linear response theory. *Phys. Norv.*, 5:279–284, 1971.

[136] Y. Gefen and D. J. Thouless. Zener transitions and energy dissipation in small driven systems. *Phys. Rev. Lett.*, 59:1752–1755, Oct 1987.

[137] F.M. Izrailev G. Casati, B.V. Chirikov and J. Ford. In G. Casati and J. Ford, editors, *Stochastic Behaviour in classical and Quantum Hamiltonian Systems*, volume 93 of *Lecture Notes in Physics.* Springer N. Y., 1979.

[138] S. Fishman, D.R. Grempel, and R.E. Prange. Chaos, Quantum Recurrences, and Anderson Localization. *Phys. Rev. Lett.*, 49:509, 1982.

[139] A. J. Daley, C. Kollath, U. Schollwöck, and G. Vidal. Time-dependent density-matrix renormalization-group using adaptive effective hilbert spaces. *JSTAT*, page P04005, 2004.

[140] S. R. White and A. E. Feiguin. Real-time evolution using the density matrix renormalization group. *Phys. Rev. Lett.*, 93:076401, 2004.

[141] Henning Moritz, Thilo Stoferle, Kenneth Gunter, Michael Kohl, and Tilman Esslinger. Connement induced molecules in a 1d fermi gas. *Phys. Rev. Lett.*, 94:210401, 2005.

[142] W. Hofstetter, Cirac, Zoller, Demler, and M. D. Lukin. High-Temperature Superuidity of Fermionic Atoms in Optical Lattices. *Phys. Rev. Lett.*, 89:220407, 2002.

[143] D. Jaksch, C. Bruder I. C. Cirac, C. W. Gardiner, and P. Zoller. Cold bosonic atoms in optical lattices. *Phys. Rev. Lett.*, 81:3108, 1998.

[144] Amy C. Cassidy, Douglas Mason, Vanja Dunjko, and Maxim Olshanii. Threshold for chaos and thermalization in the one-dimensional mean-field bose-hubbard model. *Phys. Rev. Lett.*, 102:025302, 2009.

[145] Susanne Pielawa. Interference of parametrically driven one-dimensional ultracold gases. *Phys. Rev. A*, 83:013628, 2011.

[146] L. D. Landau and E. M. Lifshits. *Mechanics*, volume 1 of *Course of theoretical physics*. Pergamon Press, third edition, 1976.

[147] D. Jaksch and P. Zoller. The cold atom hubbard toolbox. *Annals of Physics*, 315:52–79, 2005.

[148] F. Haake, M. Kuś, and R. Scharf. Classical and quantum chaos for a kicked top. *Z. Phys. B*, 65:381–395, 1986.

[149] Fritz Haake. *Quantum Signatures of Chaos (2nd ed)*. Springer, 2001.

[150] Christine Khripkov, Doron Cohen, and Amichay Vardi. Coherence dynamics of kicked bose-hubbard dimers: Interferometric signatures of chaos. *Physical Review E*, 87:012910, 2013.

[151] Joel L. Lebowitz and Oliver Penrose. Modern ergodic theory. *Physics Today*, 26:23, 1973.

[152] Edward Ott. *Chaos in dynamical systems (2nd Ed.)*. Cambridge University Press, 2002.

[153] J. von Neumann. Beweis des ergodensatzes und des <i>h</i>-theorems in der neuen mechanik. *Zeitschrift für Physik A*, 57(1):30–70, 1929.

[154] J. von Neumann. Proof of the Ergodic Theorem and the H-Theorem in Quantum Mechanics. *European Phys. J. H*, 35:201–237, 2010.

[155] O. Bohigas, M. J. Giannoni, and C. Schmit. Characterization of chaotic quantum spectra and universality of level fluctuation laws. *Phys. Rev. Lett.*, 52:1, 1984.

[156] M. V. Berry. Semiclassical mechanics of regular and irregular motion. In R. Stora G. Ioos, R. H. G. Helleman, editor, *Les Houches, Session XXXVI, 1981 — Chaotic Behaviour of Deterministic Systems*, pages 174–271. North-Holland Publishing Company, 1983.

[157] G. Casati, I. Guarnieri, F. Izrailev, and R. Scharf. Scaling Behavior of Localization in Quantum Chaos. *Phys. Rev. Lett.*, 64:5, 1990.

[158] Arijeet Pal and David A. Huse. Many-body localization phase transition. *Phys. Rev. B*, 82:174411, 2010.

[159] Boris L. Altshuler, Yuval Gefen, Alex Kamenev, and Leonid S. Levitov. Quasiparticle lifetime in a finite system: A nonperturbative approach. *Phys. Rev. Lett.*, 78:2803, 1997.

[160] D. M Basko, I .L. Aleiner, and B.L. Altshuler. Metal-insulator transition in a weakly interacting many-electron system with localized single-particle states. *Annals of Physics*, 321:1126, 2006.

[161] Marcos Rigol. Breakdown of thermalization in finite one-dimensional systems. *Phys. Rev. Lett.*, 103:100403, 2009.

[162] Mihai Horoi, B. Alex Brown, and Vladimir Zelevinsky. Chaos vs Thermalization in the Nuclear Shell Model. *Phys. Rev. Lett.*, 74:5194, 1995.

[163] H.J. Lipkin, N. Meshkov, and A.J. Glick. Validity of many-body approximation methods for a solvable model. *Nuclear Physics*, 62:188, Feb 1965.

[164] Bruno Sciolla and Giulio Biroli. Dynamical transitions and quantum quenches in mean-field models. *JSTAT*, page P11003, 2011.

[165] Giacomo Mazza and Michele Fabrizio. Dynamical quantum phase transitions and broken-symmetry edges in the many-body eigenvalue spectrum. *Phys. Rev. B*, 86:184303, Nov 2012.

[166] Victor Bapst and Guilhem Semerjian. On quantum mean field models and their quantum annealing. *JSTAT*, page P06007, 2012.

[167] J. J. Sakurai. *Modern Quantum Mechanics*. Benjamin, Menlo Park, Calif., 1985.

[168] L. D. Landau and E. M. Lifshits. *Quantum mechanics - non-relativistic theory*, volume 3 of *Course of theoretical physics*. Pergamon Press, third edition, 1977.

[169] F. T. Arecchi, Eric Courtens, Robert Gilmore, and Harry Thomas. Atomic coherent states in quantum optics. *Phys. Rev. A*, 6:2211–2237, Dec 1972.

[170] Eduardo Fradkin. *Field Theories of Condensed Matter Physics*. Cambridge University Press, 2013.

[171] Tommaso Caneva, Rosario Fazio, and Giuseppe E. Santoro. Adiabatic quantum dynamics of the Lipkin-Meshkov-Glick model. *Phys. Rev. B*, 78:104426, 2008.

[172] T. Kadowaki and H. Nishimori. Quantum annealing in the transverse Ising model. *Phys. Rev. E*, 58:5355, 1998.

[173] J. Brooke, D. Bitko, T. F. Rosenbaum, and G. Aeppli. Quantum annealing of a disordered magnet. *Science*, 284:779, 1999.

[174] Giuseppe E. Santoro, R. Martoňák, E. Tosatti, and R. Car. Theory of quantum annealing of an Ising spin glass. *Science*, 295:2427, 2002.

[175] D. POILBLANC, T. ZIMAN, J. BELLISSARD, F. MILA, and G. MONTAMBAUX. Poisson vs. goe statistics in integrable and non-integrable quantum hamiltonians. *Europhys. Lett.*, 22:537–542, 1993.

[176] B. Georgeot and D. L. Shepelyansky. Breit-Wigner width and Inverse Participation Ratio in Finite Interacting Fermi Systems. *Phys. Rev. Lett.*, 79:4365, 1997.

[177] Ph. Jacquod and D. L. Shepelyansky. Emergence of Quantum Chaos in Finite Interacting Fermi Systems. *Phys. Rev. Lett.*, 79:1837, 1997.

[178] Madan Lal Mehta. *Random Matrices.* Academic Press, 2004.

[179] Michael Tabor. *Chaos and integrability in nonlinear dynamics: an introduction.* John Wiley & sons, 1999.

[180] M. V. Berry and M. Robnik. Closed orbits and the regular bound spectrum. *J. Phys. A*, 17:2413–2421, 1984.

[181] J. T. Edwards and D. J. Thouless. Numerical studies of localization in disordered systems. *J. Phys. C*, page 807, 1972.

[182] Paul Ehrenfest. Bemerkung uber die angenäherte gültigkeit der klassichen machanik innerhalb der quanatenmechanik. *Z. Physik*, 45:455–457, 1927.

[183] George M. Zaslavsky. Stochasticity in quantum systems. *Physics Reports*, 80:157250, 1981.

[184] F. M. Izrailev and B. V. Chirikov. Statistical properties of a nonlinear string. *Soviet Physics-Doklady*, 11:30, 1966.

[185] Marco Pettini and Monica Cerruti-Sola. Strong stochasticity threshold in nonlinear large hamiltonian systems: Effect on mixing times. *Phys. Rev. A*, 44:975, 1991.

[186] A. Campa, T. Dauxois, D. Fanelli, and S. Ruffo. *Physics of Long-Range Interacting Systems.* Oxford University Press, 2014.

[187] Michael Albiez, Rudolf Gati, Jonas Folling, Stefan Hunsmann, Matteo Cristiani, and Markus K. Oberthaler. Direct observation of tunneling and nonlinear self-trapping in a single bosonic josephson junction. *Physical Review Letters*, 95:010402, 2005.

[188] Latorre J. I., Rico E., and Vidal G. Ground state entanglement in quantum spin chains. *Quantum Inf. Comput.*, 4:048, 2004.

[189] José I. Latorre, Román Orús, Enrique Rico, and Julien Vidal. Ground state entanglement in quantum spin chains. *Phys. Rev. A*, 71:064101, 2005.

[190] Marco Schiró and Michele Fabrizio. Time-dependent mean field theory for quench dynamics in correlated electron systems. *Phys. Rev. Lett.*, 105:076401, 2010.

[191] John Donne. *Donne's Devotions.* Cambridge University Press, 1923.

[192] Lucio Russo. *The Forgotten Revolution: How Science Was Born in 300 BC and Why It Had to Be Reborn.* Berlin, Springer, 2004.

[193] Galileo Galilei. *Dialogues Concerning Two New Sciences.* Dover, 1954 (original italian edition, Elzevir 1638).

[194] Yosuke Kayanuma. Role of phase coherence in the transition dynamics of a periodically driven two-level system. *Phys. Rev. A*, 50:843, 1994.